Identifying Protein Interaction Partners of the Pitx2c N-terminus during Embryogenesis

Shian Yea Wong

Department of Human Genetics

McGill University, Montreal, Quebec, Canada

November, 2013

A thesis submitted to the Faculty of Graduate and Postdoctoral Studies in partial fulfillment of the requirements of the degree of Master of Science.

Table of Contents

Abstract

The vertebrate body is patterned asymmetrically along the left-right axis. Left-right patterning is required to establish correct asymmetric organ formation and positioning, and ultimately it is essential for normal physiological functioning. Misregulation in this process can lead to severe physiological defects in multiple organs, including the heart and gut.

Pitx2c is a paired-like homeodomain transcription factor and is crucial for translating left-right signals into asymmetric morphogenesis. It is asymmetrically expressed in the left lateral plate mesoderm and continues to be expressed on the left side of organ primordia that are destined to become asymmetrically formed or positioned organs. Previous work studying Pitx2c has demonstrated its evolutionarily conserved role in left-right patterning. While the homeodomain is important for Pitx2c's function, our lab identified a putative interaction domain in the N-terminus of Pitx2c that is required for its function in left-right patterning.

To further characterize the role of Pitx2c, I used a yeast two-hybrid screen to identify candidate protein interaction partners of its N-terminus. Thirty-two candidates were identified from the screen. Candidates that were isolated at least twice were prioritized for further analysis. After eliminating non-coding clones, false positive interactions, and confirming interactions of the candidate putative interaction domains with the Pitx2c N-terminus in yeast, six candidates remained: Anti-silencing function 1 homolog B (*S. cerevisiae*; *Asf1b*), Eukaryotic translation initiation factor 3, subunit A (*Eif3a*), Eukaryotic translation initiation factor 3, subunit M (*Eif3m*), Niemann-Pick C type 2 (*Npc2*), Serine/arginine-rich splicing

factor 2 (*Srsf2*), and Serine/arginine-rich splicing factor 15 (*Srsf15*). mRNA Expression patterns of these six Pitx2c candidate protein interaction partners was analyzed by whole mount *in situ* hybridization and compared to *Pitx2c* expression patterns. All candidates were expressed symmetrically in the embryo, including tissues where *Pitx2c* is asymmetrically expressed. In the chick embryo, *Npc2* and *Srsf2* were expressed in a tissue-specific manner from HH stage 10 to HH stage 26, while *Eif3a* and *Eif3m* were broadly expressed throughout the embryo from HH stage 10 and only became enriched in particular tissues at HH stage 24 to HH stage 26. All candidates were coexpressed with *Pitx2c* in the looped heart tube. Only *Srsf2* was coexpressed with *Pitx2c* in the lateral plate mesoderm. The known functions of these candidates are consistent with the known role of Pitx2c in transcriptional regulation and suggests new roles for Pitx2c in mRNA processing and translational regulation during left-right patterning.

Résumé

Le corps des vertébrés est structuré asymétriquement le long de l'axe gauche-droit. La latéralité est requise afin d'établir la formation des organes ainsi que leur positionnement qui, ultimement, sont essentielles pour un fonctionnement physiologique normal des vertébrés. Lors de ce processus, une mauvaise régulation peut causer des troubles physiologiques sévères dans plusieurs organes incluant le cœur et l'intestin.

Le facteur de transcription homéodomaine Pitx2c joue un rôle essentiel lors de la traduction des signaux gauche-droit en morphogénèse asymétrique des organes. Pitx2c est exprimé de façon asymétrique dans le mésoderme de la plaque latérale gauche et continu d'être exprimé du côté gauche des futurs organes asymétriques. Quelques études ont démontré que Pitx2c a un rôle qui est conservé lors de l'évolution dans la latéralité. Le rôle de l'homéodomaine est important pour la fonction de Pitx2c et nous avons démontré dans notre laboratoire qu'un domaine d'interaction de la partie N-terminale de Pitx2c est aussi important pour sa fonction lors de la latéralité.

Afin de caractériser d'avantage le rôle de Pitx2c, j'ai utilisé la méthode de double hybride afin d'identifier des protéines candidates d'interaction avec la partie N-terminale de Pitx2c. Trente-deux candidats ont été sélectionnés. De ce nombre, les faux positifs ainsi que les candidats qui représentent région la non-codante d'une protéine ont été supprimés ce qui a permis de réduire la liste à six candidats : Anti-silencing function 1 homolog B (*S. cerevisiae; Asf1b*), Eukaryotic translation initiation factor 3, subunit A (*Eif3a*), Eukaryotic translation

initiation factor 3, subunit M (*Eif3m*), Niemann-Pick C type 2 (*Npc2*), Serine/arginine-rich splicing factor 2 (*Srsf2*), ainsi que Serine/arginine-rich splicing factor 15 (*Srsf15*).

Les patrons d'expression des six protéines candidates potentielles d'interaction avec Pitx2c ont été examinés par hybridation *in situ* et ont été comparé avec le patron d'expression de *Pitx2c*. Chez tous les candidats, l'expression asymétrique dans les embryons de poulet a été observée incluant dans les tissus où *Pitx2c* est aussi exprimé asymétriquement. *Npc2* et *Srsf2* sont exprimés de façon spécifique dans certains tissus à partir du stade HH10 chez le poulet. *Eif3a* et *Eif3m* sont largement exprimés dans les embryons à partir du stade HH10 mais leur expression est enrichie dans certains tissus à partir du stade HH22. L'expression de tous les candidats coïncide avec celle de *Pitx2c* dans la courbure du tube cardiaque. Seulement l'expression de *Srsf2* coïncide avec celle de *Pitx2c* dans le mésoderme de la plaque latérale gauche. Les fonctions des différents candidats suggèrent que ces partenaires potentiels d'interactions de la partie N-terminale de Pitx2c pourraient jouer un rôle important lors de la régulation de la transcription, la formation de l'ARN messager et la régulation de la traduction lors de la latéralité.

Acknowledgements

I am thankful to many people who have helped me throughout these two years with guidance, encouragement and assistance. First and foremost, I would like to express my gratitude to my supervisor, Dr. Aimee Ryan, for the opportunity to work in her lab and this project. Aimee, your support and confidence has made this journey possible and truly helped me grow into a better scientist and person. Thank you.

I also owe many thanks to the members of Dr. Ryan's lab, past and present. Thank you, Amanda Baumholtz, soon-to-be Dr. Michelle Collins, Halim Khairallah, Annie Simard, and Dora Siontas. All of you have contributed to my thesis in your own ways and made everyday in the lab a wonderful and unforgettable experience. I wish you all the best in your future endeavors.

I would also like to acknowledge Dr. Indra Gupta and Dr. Loydie Majewska and members of their lab for their feedback and discussion during our weekly meetings. Thanks also to my committee members, Dr. Daniel Bernard and Dr. Colin Crist for their suggestions, advice and guidance towards my project.

Last but not least, I am grateful to my parents and family for their love and understanding in both the good times and bad times and to my friends for their endless encouragement and emotional support.

List of Tables

List of Figures

List of Abbreviations

aa	Amino Acid
ActRIIA	Activin receptor IIa
Ade	Adenine
ADE2	Gene encoding phosphoribosylaminoimidazole carboxylase
AI506816	Expressed sequence AI506816, transcript variant 1, non-coding sequence
ARS1	Axenfeld-Rieger syndrome type 1
ASE	Left-side specific enhancer
Asf1b	Anti-silencing function 1, homolog B (S. Cerevisiae)
AUR1C	Gene encoding resistance to Aureobasidin A
Baz1b	Bromodomain adjacent to zinc finger domain, 1B
BCIP	5-bromo-4-chloro-3'-indolyphosphate
Bmp4	Bone morphogenetic protein 4
bp	Base pairs
cDNA	Complementary DNA
cfu	Colony forming units
CO-IP	Co-immunoprecipitation
Commd4	COMM domain containing 4
Daam2	Dishevelled associated activator of morphogenesis 2
DDO	Double drop-out medium without leucine and trptophan
DDO/X	Double drop-out medium with X-alpha-Galactose
DDO/X/A	Double drop-out medium with X-alpha-Galactose and Aureobasidin A
DEPC	Diethylpyrocarbonate
DTT	Dithiothreitol
E#	Embryonic day #
ECR	Evolutionarily conserved regions
EFEMP2	EGF-containing fibulin-like extracellular matrix protein 2
EGF-CFC	Epidermal growth factor-cripto/FRL-1/cryptic
Eif3	Eukaryotic translation initiation factor 3 complex
Eif3a	Eukaryotic translation initiation factor 3, subunit A
Eif3m	Eukaryotic translation initiation factor 3, subunit M
Fam96b	Family with sequence similarity 96, member B
Fgf8	Fibroblast growth factor 8
FoxC1	Forkhead box transcription factor C1
FoxH1	Forkhead box transcription factor H1
GAL4	Galectin 4
GDF1	Growth differentiation factor 1

GST	Glutathione S-transferase
H+-K+ ATPases	Hydrogen-potatssium ATPases
H+-V ATPases	Hydrogen-V type sodium ATPases
HEK293T	Human embryonic kidney 293T cells
HH	Hamburger and Hamilton
His	Histidine
HIS3	Gene encoding imidazoleglycerol-phosphate dehydratase
HMG17	Chromatin-associated high mobility group protein
hnRNP-U	Heterogeneous nuclear ribonucleoprotein U
hnRNP-K	Heterogeneous nuclear ribonucleoprotein K
Inv	Inversin
lacZ	Gene encoding β-galactosidase
LAMAT	Leucine-41, Methionine-43, Threonine-45 Pitx2cN Mutant
LB	Luria broth
Lefty1	Left-right determination factor 1
Lefty2	Left-right determination factor 2
Leu	Leucine
LPM	Lateral plate mesoderm
M	Methionine
MAO	Monoamine oxidase
Marcks	Myristoylated alanine rich protein kinase C substrate
Mef2A	Myocyte enhancing factor 2a
MEL	Gene encoding α-galactosidase
N4bl2l2	NEDD4 binding protein 2-like 2
NBT	Nitro-blue tetrazolium
Nkx2.5	NK2 homeobox 5
NLS	Nuclear localization signal
Npc2	Niemann-Pick C type 2
OAR	Otp and Aristaless domain
Pawr	Human PRKC apoptosis WT1 regulator
PBS	Phosphate buffered saline
PBT	Phosbase buffered saline with 10% tween
PCI	26S proteosome-COP9 signalosome-eukaryotic translation initiation factor 3
PFA	Paraformaldehyde
Pias1	Protein inhibitors of activated STAT proteins 1
Piasy	Protein inhibitors of activated STAT proteins gamma
Pit1	Pituitary-specific transcription factor 1
Pitx2c	Paired-like homeodomain transcription factor 2, isoform C
Pitx2cFL	Pitx2c full-length

Pitx2cN	Pitx2c N-terminus
Plod1	Procollagen-lysine, 2-oxoglutarate 5-dioxygenase 1
QDO	Quadruple drop-out medium without leu, trp, ade, his
QDO/A	Quadruple drop-out medium without leu, trp, ade, his with Aureobasidin A
QDO/X/A	Quadruple drop-out medium without leu, trp, ade, his with X-alpha-Galactose and Aureobasidin A
Rbpj	Recombining binding protein suppressor of hairless (Drosophila)
RS	Serine/arginine rich
SD	Synthetic defined yeast media
SDO	Single drop-out medium
SDS	Sodium dodecyl sulfate
Shh	Sonic hedgehog
Srsf1	Serine/arginine-rich splicing factor 1
Srsf15	Serine/arginine-rich splicing factor 15
Srsf2	Serine/arginine-rich splicing factor 2
Srsf3	Serine/arginine-rich splicing factor 3
SSC	Sodium saline citrate
T	Threonine
TGFβ	Transforming growth factor beta
Trp	Tryptophan
X-α-Gal	X-alpha-galactose
Y2H	Yeast two-hybrid
YB1	Y-box binding factor 1
YPD	Yeast extract peptone dextrose
YPDA	YPD supplemented with adenine hemisulfate
Zfp740	Zinc finger protein 740
Zfp845	Zinc finger protein 845

Chapter 1. Introduction

1.1. Overview of human laterality

Although the exterior of the human body appears symmetrical, the majority of the organs within the body cavity are positioned and formed asymmetrically along the left-right axis. This specific arrangement allows the organs to function and fit in the limited space of the body cavity. In fact, this asymmetry is evolutionarily conserved within all vertebrates.

Situs solitus refers to the normal asymmetric arrangement of the thoraco-abdominal organs (Aylsworth, 2001; Casey and Hackett, 2000; Kosaki and Casey, 1998). Generally in humans, the lungs form three lobes on the right side while forming only two lobes on the left side. The heart is compartmentalized in physiologically distinct left and right atriums and ventricles, a left-sided aorta and right-sided inferior vena cava. The liver is largely positioned on the right side along with the gallbladder, and the gastrointestinal tract loops toward the right, while the stomach and spleen are positioned on the left side.

Situs inversus is the mirror image reversal of the position of organs, such that what is normally on the right side is on the left side and vice versa. *Situs inversus* can occur completely (Fig. 1d), where all organs are reversed, or partially (Fig. 1c), where only some organs are reversed such as the thoracic organs only or the abdominal organs only. Usually, in complete *situs inversus*, also known as *situs inversus totalis*, all organs can function relatively normally, whereas partial

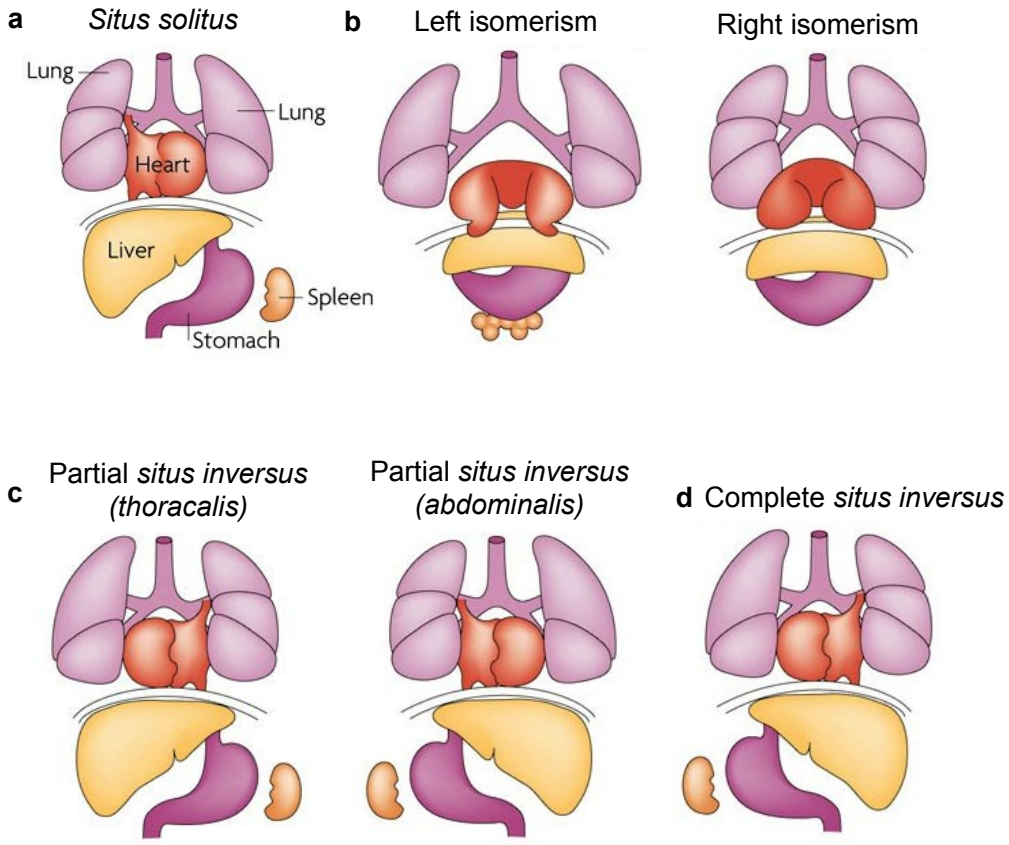

Figure 1. Categories of laterality defects in human. (a) Normal organ positioning is called *situs solitus.* In *situs solitus*, the right lung has three lobes while the left lung only has two lobes; the atrium and ventricles of the heart are positioned asymmetrically; the liver is positioned on the right while the stomach and spleen are positioned on the left. (b) Isomerisms present with bilateral symmetry of one side only: the left or the right. (c) Partial *situs inversus* is the reversal of some organ positions. Examples shown indicate *situs inversus thoracalis* where the only thoracic organs are reversed in position and *situs inversus abdominalis* where only the abdominal organs are reversed in position. (d) Complete *situs inversus* is the reversal of all organs. Reprinted with permission from Fliegauf et al. 2008.

situs inversus results in severe functional defects. Partial *situs inversus* is also referred to as *situs ambiguus* or heterotaxia. Right-sided isomerisms or asplenia describes the condition when both sides are right-sided (Fig. 1b). Conversely, left-sided isomerisms or polysplenia describes the condition where both sides are left-sided (Fig. 1b). No matter the side of isomerism, the malposition and malformation of the internal organs leads to life-threatening consequences (Aylsworth, 2001; Baum and Duncan, 2011; Kosaki and Casey, 1998).

In humans, laterality defects affect 1 in 10,000 individuals (Lin et al., 2000; Strife et al., 1998). Although the field has well-defined categories of laterality defects as described above, the severity and complexity of effects in each visceral organ ranges broadly between patients even within the same category (Applegate et al., 1999; Lee et al., 2006; Lin et al., 2000; Strife et al., 1998). To make matters more complicated, laterality defects can also be accompanied by defects in midline structures including musculoskeletal, urogenital, and craniofacial anomalies (Ticho et al., 2000). Most children affected by laterality defects come to clinical attention due to complex congenital heart defects, sepsis caused by immune deficiency due to the absence of the spleen, and bowel obstructions due to malrotation of the gastrointestinal tract (Applegate et al., 1999; Prendiville et al., 2010; Ruben et al., 1983; Waldman et al., 1977; Wu et al., 2002).

Complex congenital heart defects that commonly arise in patients with laterality defects are atrial septal defects, common atrioventricular canal, univentricular heart, transposition of the great arteries, and anomalous venous

connections including total anomalous pulmonary venous return (Applegate et al., 1999; Phoon and Neill, 1994). The incidence of having congenital heart defects in individuals with *situs solitus* is 0.6-0.8% (Strife et al., 1998). In comparison, the incidence rises to 3-5% in *situs inversus totalis* patients (Strife et al., 1998) and more dramatically to 50-100% in patients with heterotaxy (Applegate et al., 1999; Phoon and Neill, 1994). In addition to being more prevalent, prognosis of heterotaxy patients with complex congenital heart defects remain poor despite modern surgical techniques (Eronen et al., 2013; Serraf et al., 2010; Shiraishi and Ichikawa, 2012).

The spectrum of severity and number of organs affected in different individuals suggests there may be unique molecular determinants that are important in certain organs but not others. The variation in severity of defects between different organs suggests that some organs may be more sensitive to laterality cues than others. Nonetheless, the occurrence of multiple defective organs in heterotaxy patients is evidence that there is one common cascade that organizes laterality early on in development: the left-right patterning cascade.

1.2. Left-right axis formation

The laterality of the internal organs is established during embryogenesis downstream of left-right axis formation. The left-right axis is the last axis formed and forms perpendicular to the anterior-posterior and dorsal-ventral axes (Beddington and Robertson, 1999). The earliest morphological sign of left-right asymmetry is the rightward looping of the heart tube. This is observed at HH stage 11 in chick and at the end of embryonic day 8 (E8) in mouse (Abu-Issa and

Kirby, 2007; Lin et al., 2012). However, the molecular cues that drive left-right axis formation begin much earlier than any morphological sign of asymmetry. Many critical molecules have been implicated in the left-right patterning cascade.

The left-right patterning cascade can be divided into three stages (Komatsu and Mishina, 2013; Levin, 2005; Vandenberg and Levin, 2013). The first stage is the break of molecular symmetry at the node in mice, or Hensen's node in chick (Nakamura and Hamada, 2012; Vandenberg and Levin, 2013). The second stage is the propagation of left-right information from the node to, and through, the left lateral plate mesoderm via Nodal signaling (Collignon et al., 1996; Lowe et al., 1996; Nakamura et al., 2006). The third stage is the translation of left-right information in the left lateral plate mesoderm at the early stages of embryogenesis, to asymmetric organ morphogenesis during later stages by Pitx2c, a Bicoid-like homeodomain transcription factor (Ai et al., 2006; Campione et al., 1999; Kioussi et al., 2002; Kurpios et al., 2008; Logan et al., 1998; Ma et al., 2013; Piedra et al., 1998; Ryan et al., 1998; St. Amand et al., 1998; Welsh et al., 2013; Yoshioka et al., 1998; Zhou et al., 2007). While the evolutionary conservation of the initial break of molecular symmetry is not apparent, the left-right patterning cascade that results from this break is evolutionarily conserved in all vertebrates (Nakamura and Hamada, 2012; Vandenberg and Levin, 2013).

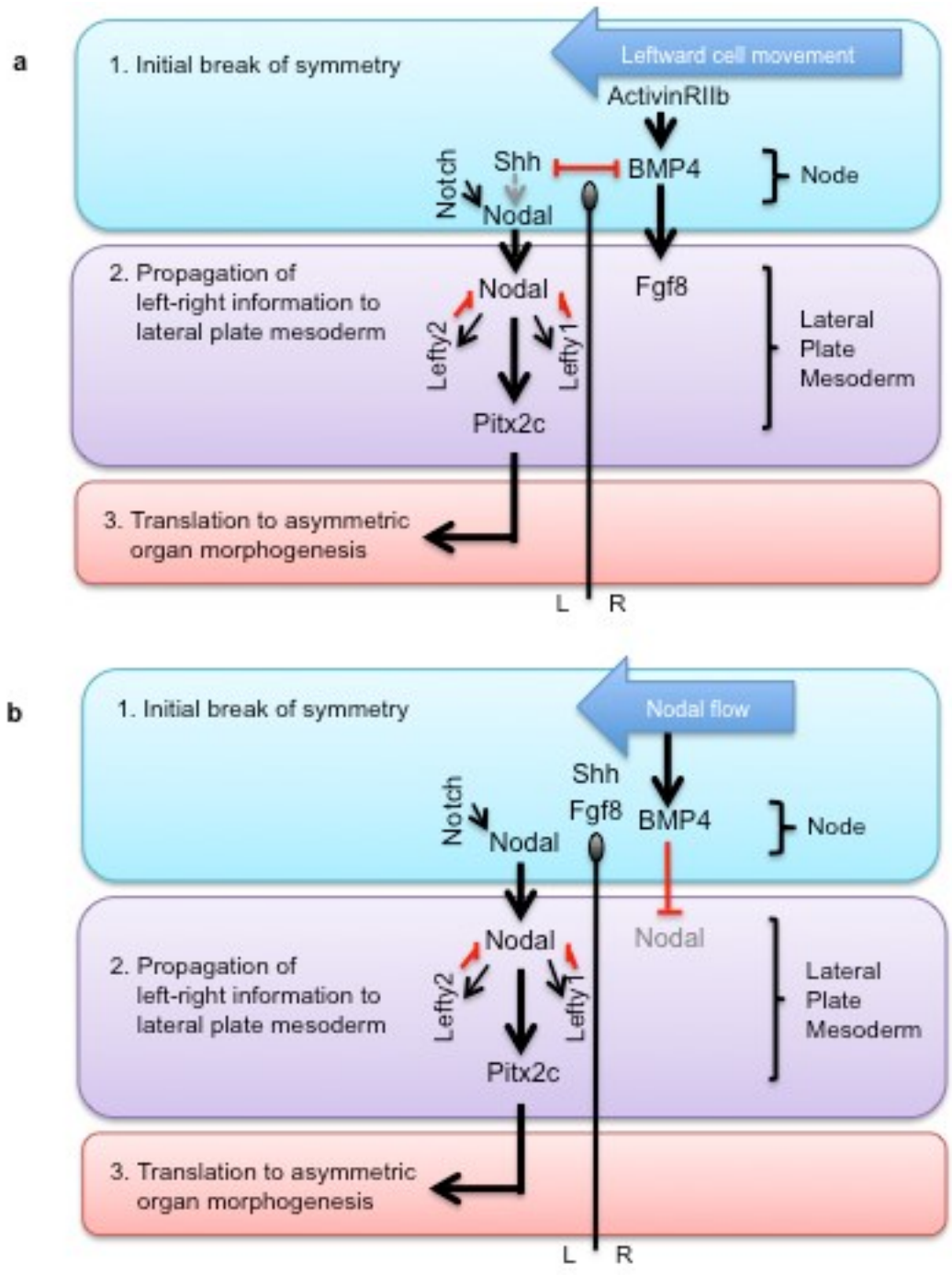

Figure 2. The three stages of left right patterning. (a) Left-right patterning in the chick and (b) in the mouse.

1.2.1. First stage – Part 1: Initial break of molecular symmetry

Between species, the initial break of molecular symmetry appears to be quite different (Levin, 2005; Levin and Palmer, 2007; Nakamura and Hamada, 2012; Vandenberg and Levin, 2013). In mice, the initial symmetry breaking event occurs at the node at E7.5 (Shiratori and Hamada, 2006). The rotational beating of inclined monocilium positioned posteriorly in the cells of the node causes a transient leftward nodal flow, which precedes and is required for the initiation of the left-right patterning cascade (Nonaka et al., 2002; Nonaka et al., 2005; Shinohara et al., 2012; Shiratori and Hamada, 2006; Tabin and Vogan, 2003). Mice with mutant ciliary genes have immotile cilia or no cilia, do not display nodal flow, and subsequently have laterality defects (Bangs et al., 2011; Ibañez-Tallon et al., 2002; Murcia et al., 2000; Nonaka et al., 1998; Okada et al., 1999; Takeda et al., 1999). When an artificial leftward fluid flow was applied to cilia mutated *inversus viscerum* (*iv*/*iv*) embryos, laterality was restored (Nonaka et al., 2002; Watanabe et al., 2003). Furthermore, when an artificial rightward fluid flow was applied to wild type embryos, embryos displayed *situs inversus* (Nonaka et al., 2002). Collectively, these data support the role of the cilia-driven leftward nodal flow at the node in directing left-right asymmetry in mice.

Although the chick equivalent of the node, Hensen's node also has cilia (Essner et al., 2002; Männer, 2001), the morphology of Hensen's node is not suitable for fluid flow establishment (Männer, 2001). Additionally, the *talpid*^{3} chick mutant, which lacks cilia, displays normal left-right patterning (Ede and Kelly, 1964). These data suggest another mechanism is responsible for the break

of symmetry in chick. It has been shown that ion transporters, H^+-K^+ and H^+-V ATPases, create an asymmetric membrane voltage potential across Hensen's node as early as Hamburger and Hamilton (HH) stage 3-4 and loss of either pump results in heterotaxia (Adams et al., 2006; Levin et al., 2002). Additionally, inhibition of Connexin 43 (a component of gap junctions) at Hensen's node during HH stage 5 also disrupts normal left-right patterning (Levin and Mercola, 1999). These data suggest a model whereby a unidirectional current of left-right determinant molecules distributed by ion transporters travels through gap junctions to one side of the embryo (Adams et al., 2006; Levin et al., 2002). When serotonin receptors and a serotonin regulator, monoamine oxidase (MAO), was blocked by pharmalogical means, laterality was randomized in chick embryos by HH stage 5 (Fukumoto et al., 2005). MAO was also shown to be asymmetrically expressed on the right side of the chick embryo (Fukumoto et al., 2005), suggesting that serotonin signaling is also important for left-right patterning. Downstream of asymmetric membrane voltage gradient and serotonin signaling, cell rearrangements occur, creating a leftward movement of cells in Hensen's node (Cui et al., 2009; Dathe et al., 2002; Gros et al., 2009). This leftward movement is required for activation of asymmetric gene expression at Hensen's node (Cui et al., 2009; Gros et al., 2009; Tsikolia et al., 2012).

In *Xenopus*, zebrafish and Medaka fish, motile cilia are observed in the gastrocoel roof plate of *Xenopus* and Kupffer's vesicle of both fish species—similar to what is observed in the mouse node—and cilia-dependent flow is also required to establish laterality (Nakamura and Hamada, 2012). However, *Xenopus*

laterality is also dependent on the asymmetric expression of H^+-K^+ ATPases and accumulation of serotonin prior to cilia formation (Aw et al., 2008; Beyer et al., 2012; Fukumoto et al., 2005; Walentek et al., 2012). In *Xenopus*, it has been shown that the role of serotonin, gap junctions and ion transporters precedes and determines cilia flow (Beyer et al., 2012; Walentek et al., 2012), suggesting that perhaps there could be evolutionarily conserved symmetry breaking events which require further investigation. Nonetheless, the initial break of symmetry event appears variable and complex between vertebrates (Levin, 2005; Levin and Palmer, 2007; Vandenberg and Levin, 2013).

1.2.2. First stage – Part 2: Asymmetric gene expression at the node

Once symmetry is broken, genes are expressed asymmetrically at the node. Like the initial event of symmetry breaking, downstream gene expression also occurs variably between vertebrates. In the chick, activin receptor IIa (ActRIIA) and its substrate, activin βB, are the first proteins known to be asymmetrically expressed on the right side of Hensen's node after the initial break of symmetry (Levin et al., 1995; Levin et al., 1997). These two molecules then activate the expression of bone morphogenetic protein 4, *Bmp4* (Monsoro-Burq and Le Douarin, 2001). Initially sonic hedgehog (*Shh*) is bilaterally expressed at Hensen's node (Levin et al., 1995). However, Bmp4 and Shh then begin to reciprocally antagonize the expression of each other such that *Bmp4* is maintained on the right side and *Shh* on the left side (Monsoro-Burq and Le Douarin, 2001). Bmp4 induces fibroblast growth factor 8 (*Fgf8*) on the right side of the Hensen's node to repress the expression of *Bmp4* antagonists (Boettger et al., 1999; Esteban

et al., 1999) while Shh induces the expression of inhibitors of *Bmp4* on the left side (Esteban et al., 1999; Katsu et al., 2012; Yokouchi et al., 1999; Zhu et al., 1999). Shh also induces the expression of *Nodal* on the left side of Hensen's node (Levin et al., 1995). Notch signaling is also important for the expression of *Nodal* at Hensen's node (Raya et al., 2004).

In the mouse, *Shh* and *Fgf8* appear to play opposite roles compared to the chick. *Fgf8* appears to be a left determinant in mouse: *Fgf8* hypomorph mutants display right isomerisms and Fgf8 induces the expression of *Nodal* on the left side of the node (Meyers and Martin, 1999). Conversely, *Shh* appears to be a right determinant: *Shh*-/- mice display left isomerisms (Hildreth et al., 2009; Tsukui et al., 1999) and *Nodal* is expressed in the absence of *Shh* (Meyers and Martin, 1999). As in chick, *Bmp4* remains expressed at higher levels on the right side of the node where it inhibits *Nodal* expression, while Bmp4 inhibitors on the left side continue to promote *Nodal* expression (Mine et al., 2008). *Nodal* expression is also activated by Notch signaling in the mouse via the functional interaction between Rbpj, a transcriptional mediator of Notch signaling, and the node enhancer element in the *Nodal* promoter (Adachi et al., 1999; Krebs et al., 2003; Norris and Robertson, 1999; Raya et al., 2003). Notch signaling also appears to regulate canonical Wnt signaling through *Wnt3* to repress the expression of *Nodal* inhibitor, *Cerberus-like 2*, thereby enhancing the expression of *Nodal* on the left side of the node (Kitajima et al., 2013).

In rabbits, Fgf8 was also found to be a right determinant similar to what is seen in chick, however *Shh* is bilaterally expressed much like what is seen in the

mouse (Fischer et al., 2002). Contrary to both chick and mouse, Bmp4 appears to induce *Nodal* expression in rabbits (Fischer et al., 2002). Like mouse, Bmp signaling is also important for right sidedness in *Xenopus* (Hyatt and Yost, 1998; Ramsdell and Yost, 1999). In zebrafish, it is apparent that Fgf signaling is important in left-right patterning as *Fgf8* null embryos exhibit randomized laterality (Albertson and Yelick, 2005; Hong and Dawid, 2009).

Thus, it appears that while the same molecular determinants are involved in the initial asymmetric gene expression stage of left-right patterning, the role of each molecule is not evolutionarily conserved. Nevertheless, what is evolutionarily conserved is the most important outcome following the initial break of symmetry and initial asymmetric gene expression: the asymmetric expression of *Nodal* at the left side of the node. This event is a prerequisite for the asymmetric expression of *Nodal* in the left lateral plate mesoderm and the initiation of the Nodal signaling cascade (Brennan et al., 2002; Saijoh et al., 2003).

1.2.3. Second stage: Stabilizing left identity in the lateral plate mesoderm

The molecular events that occur at the second stage are highly conserved in all vertebrates including mouse, chick, *Xenopus*, zebrafish, quail and rabbit (Levin, 2005; Raya and Belmonte, 2006). On the right side of the embryo, asymmetrically expressed Fgf8 induces the expression of *Snail* in the right lateral plate mesoderm (LPM) by inhibiting the expression of a *Snail* repressor, *Nodal* (Boettger et al., 1999). Snail further maintains right identity by repressing expression of *Pitx2*, a left determinant, in the right LPM (Isaac et al., 1997; Murray and Gridley, 2006; Patel et al., 1999).

On the left side of the embryo, *Nodal* is asymmetrically expressed in the left LPM and is strictly restricted to this region. *Nodal* expression in the LPM is positively regulated by GDF1 (Peterson et al., 2013; Ramsdell and Yost, 1999; Tanaka et al., 2007), a member of the TGFβ family, as well as members of the Nodal co-receptor family, epidermal growth factor-cripto/FRL-1/cryptic (EGF-CFC) (Gaio et al., 1999; Gritsman et al., 1999; Yan et al., 1999) and Nodal itself (Saijoh et al., 2000). While Nodal expression is induced by these molecules in the LPM, left-right determination factor 1 (Lefty1) at the midline restricts *Nodal* expression to the left side of the embryo (Bisgrove et al., 1999; Lenhart et al., 2011; Meno et al., 1998; Sakuma et al., 2002) and left-right determination factor 2 (Lefty2) in the left LPM refines the expression of *Nodal* by repressing the lateral expansion of *Nodal* expression (Meno et al., 1999; Meno et al., 2001; Sakuma et al., 2002). Both *Lefty1* and *Lefty2* expression are positively regulated by Nodal signaling creating a negative feedback loop controlling *Nodal* expression (Saijoh et al., 2000; Yamamoto et al., 2003). Bicoid-like homeodomain transcription factor 2 (*Pitx2*), a direct target of Nodal signaling, stabilizes the left identity of the embryo once it is induced by Nodal (Shiratori et al., 2001). *Pitx2* expression persists longer than *Nodal* expression and is maintained by autoregulation (Schweickert et al., 2000) and Nkx2.5 (Shiratori et al., 2001). It is also expressed on the left side of asymmetrically formed organ primordia (Logan et al., 1998; Ryan et al., 1998; Semina et al., 1996; St. Amand et al., 1998; Yoshioka et al., 1998). Although the role of Pitx2 as the most downstream effector of this cascade is well characterized and evolutionary conserved, much of how it directs asymmetric organ morphogenesis is not understood.

1.2.4. Third stage: Asymmetric organ morphogenesis

Organs that undergo asymmetric morphogenesis often do this via differential cell behaviours including proliferation, migration and adhesion (Levin, 2005). In the heart, the cardiac outflow tract divides and positions the two great arteries of the right and left ventricle, the ascending aorta and pulmonary trunk (Miquerol and Kelly, 2013). Proper formation of the outflow tract requires continued proliferation and delayed differentiation of the secondary heart field and migration of cells from the secondary heart field to the developing heart tube (Bajolle et al., 2006; Miquerol and Kelly, 2013). Pitx2 is necessary for both of these processes in the heart by regulating the expression of growth controlling genes (Ai et al., 2006; Kioussi et al., 2002; Ma et al., 2013; Zhou et al., 2007). It was shown in C2C12 murine myoblast cells and αT_3-1 pituitary cells that Pitx2 induces gene activation of Cyclin D2, a growth control gene of the G_1 phase, to promote proliferation (Kioussi et al., 2002).

In the gut, looping is initiated by a leftward tilt in the dorsal mesentery, a structure that holds the gut to the dorsal body wall (Klezovitch and Vasioukhin, 2013; Kurpios et al., 2008). The morphology of the dorsal mesentery begins as symmetrical sparse mesenchyme and cuboidal epithelium but begins to differ when the left-sided mesenchyme condenses and the left-sided epithelium becomes columnar while the right side remains the same (Klezovitch and Vasioukhin, 2013; Kurpios et al., 2008). As the mesenchyme condenses on the left side, it induces a leftward tilt to the gut tube. Recently, it was shown that Pitx2 activates N-cadherin mediated intracellular adhesion complexes in the actin cytoskeleton

via a Wnt signaling target, *Daam2*, to facilitate polarized condensation of left dorsal mesentery (Kurpios et al., 2008; Plageman Jr et al., 2011; Welsh et al., 2013). Thus, it appears that the role of Pitx2 as a transcription factor is important in regulating transcription of genes required for different cell behaviours on the left and right sides of developing organs.

1.3. Bicoid-like homeodomain transcription factor Pitx2

1.3.1. Pitx2 gene structure and isoforms

Pitx2 is one of three members of the RIEG/Pitx homeobox family. The *Pitx2* locus contains 6 exons and encodes 3 major isoforms, Pitx2a, Pitx2b and Pitx2c (Gage and Camper, 1997; Kitamura et al., 1999; Kitamura et al., 1997; Smidt et al., 2000). These isoforms are derived from alternative transcription start sites at either exon 1 or exon 4 and from alternative splicing via the inclusion or exclusion of exon 3 for isoforms that use the transcription start site at exon 1.

Recently, additional isoforms of Pitx2 have been discovered. Lamba and colleagues (2008) identified and characterized two novel isoforms: Pitx2cβ, derived from an alternative translation start site within exon 4 of the *Pitx2c* mRNA, and *Pitx2b2*, derived from an alternative 3' splice acceptor site in exon 3. In humans, *PITX2D* was cloned from a human craniofacial cDNA library (Cox et al., 2002). *PITX2D* is generated from the same promoter as *PITX2C*, but contains

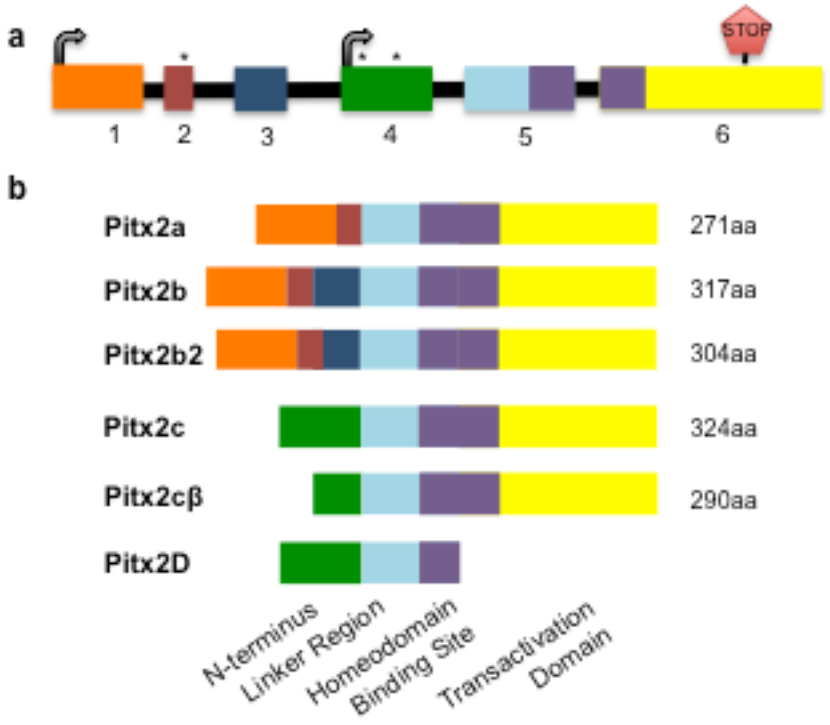

Figure 3. *Pitx2* locus and its protein isoforms. Gradient arrows indicate transcription start sites. Asterisks indicate translation start sites. Stop sign indicates translation stop sites. (b) Three protein isoforms are expressed in all vertebrates, Pitx2a, Pitx2b and Pitx2c. Pitx2b2 is generated by an alternative splicing of exon 3. Pitx2cβ is generated by an alternative translation start site in exon 4. Pitx2D is generated by alternative splicing of exon 6 and is only expressed in human. Amino acid (aa) lengths refer to murine isoforms.

a truncated homeodomain due to a 3' splice acceptor site within exon 5 (Cox et al., 2002). As a result, PITX2D does not bind to DNA and functions to inhibit the transcriptional activity of other PITX2 isoforms (Cox et al., 2002). *Pitx2d* has not yet been described in other species.

Pitx2 isoforms demonstrate differential transcriptional activity on different promoters, including distaless-homeobox 2 *(Dlx2)*, procollagen-lysine, 2-oxoglutarate 5-dioxygenase 1 *(Plod1)*, and *Prolactin*, and different isoforms can hetero- and homodimerize to induce synergistic transactivation at these promoters (Cox et al., 2002). Specifically Pitx2b acts together with both Pitx2a and Pitx2c at all promoters, while Pitx2a and Pitx2c only appear to synergize at certain promoters (Cox et al., 2002). It has been suggested that Pitx2a and Pitx2b can induce the expression of *Pitx2c*, in addition to activating their own expression (Schweickert et al., 2000).

1.3.2. Pitx2 protein domains

All three major Pitx2 isoforms share identical linker regions, homeodomains, and C-terminal domains and differ only at their N-termini. All homeobox transcription factors have a characteristic 60 amino acid homeodomain that determines DNA binding specificity. Like Bicoid, Pitx2 is characterized by a lysine at residue 50 within the homeodomain (Hanes and Brent, 1989). This lysine residue causes Pitx2 to selectively recognize and bind 5'-TAATCC-3' (Amendt et al., 1998; Wilson et al., 1996). Additionally, it also acts as an interaction domain with other proteins, including transcription factors and chromatin binding proteins (Fig. 4).

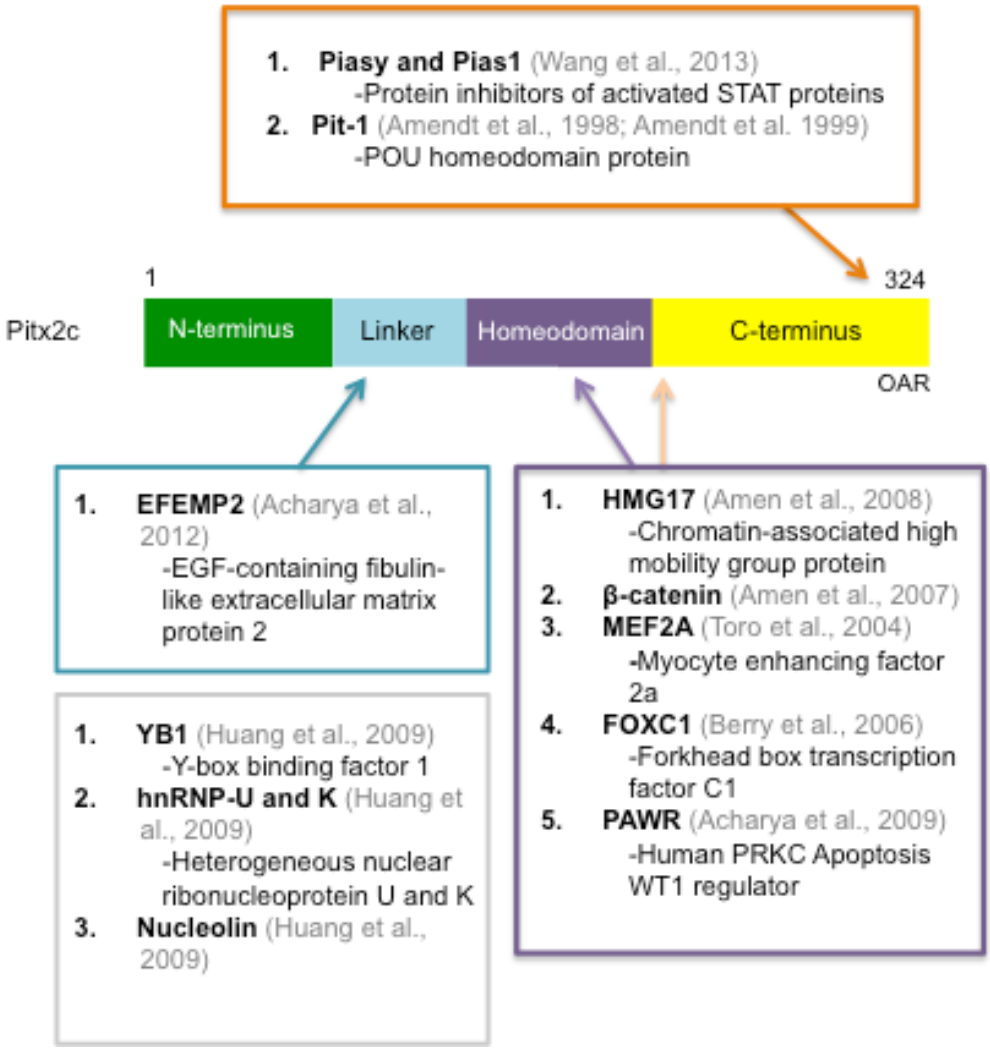

Figure 4. Known interaction partners of Pitx2c. Proteins in the blue box are known to interact with the linker region. Proteins in the purple box are known to interact with the homeodomain and the C-terminus. Proteins in the orange box are known to interact with the C-terminus. Proteins in the grey box are known to interact with Pitx2c, however the interaction region has not been mapped.

The C-terminal region of Pitx2 contains a 14 amino acid region, the OAR (Otp and Aristaless) domain, which is highly conserved amongst other homeodomain proteins, including Otp and Aristaless from which the region derives its name (Gage and Camper, 1997; Semina et al., 1996). The OAR in the C-terminus serves as an interaction domain with other transcription factors to allow synergistic activation of target genes (Amendt et al., 1999; Saadi et al., 2006; Smidt et al., 2000) and also intrinsically inhibits the DNA binding capacity of the homeodomain in Pitx2a by interacting with a region in the N-terminus (Amendt et al., 1999; Saadi et al., 2006). It was also shown that phosphorylation by Protein Kinase C in the C-terminus is important to facilitate Pitx2 interactions with other proteins and successive changes in transactivation activity (Espinoza et al., 2005).

The function of the unique N-terminal domains between isoforms is not clear. However, a role for the N-terminus of the Pitx2c isoform was recently identified in our lab (Simard et al., 2009) and will be discussed in detail at the end of this chapter.

1.3.3. Pitx2 expression pattern during embryogenesis

The expression of *Pitx2* during embryogenesis is highly conserved amongst species (Campione et al., 1999; Kitamura et al., 1999; Logan et al., 1998; Ryan et al., 1998; Schweickert et al., 2000; Semina et al., 1996; St. Amand et al., 1998; Yoshioka et al., 1998). However, only *Pitx2a* and *Pitx2c* are expressed during embryogenesis in chick (Yu et al., 2001). Additionally, *Pitx2a* does not

exist in *Xenopus* (Schweickert et al., 2000), while *Pitx2b* is undetectable in zebrafish (Essner et al., 2000).

Pitx2 is symmetrically expressed in the head mesenchyme during early gastrulation stages and continues to be symmetrically expressed in the face mesenchyme, pharyngeal arches and clefts, pituitary gland, eyes, somites, muscle progenitors of the limbs, kidneys, umbilicus, and tooth primordia as organogenesis progresses (Arakawa et al., 1998; Gage and Camper, 1997; Hjalt et al., 2000; Kitamura et al., 1997; Logan et al., 1998; Mucchielli et al., 1997; Piedra et al., 1998; Ryan et al., 1998; Semina et al., 1996; St. Amand et al., 1998; Yoshioka et al., 1998).

Additionally, *Pitx2* also exhibits asymmetric expression. Of the 3 isoforms, *Pitx2c* is the only isoform expressed asymmetrically in chick, mouse, and *Xenopus* (Kitamura et al., 1999; Liu et al., 2001; Schweickert et al., 2000; Yu et al., 2001). *Pitx2c* is asymmetrically expressed in the left lateral plate mesoderm. This asymmetric expression continues in the left side of organs that are positioned and formed asymmetrically including the heart, gut, and lungs (Arakawa et al., 1998; Gage and Camper, 1997; Hjalt et al., 2000; Kitamura et al., 1997; Logan et al., 1998; Mucchielli et al., 1997; Piedra et al., 1998; Ryan et al., 1998; Semina et al., 1996; St. Amand et al., 1998; Yoshioka et al., 1998).

Since Nodal-induced expression of *Pitx2* in the left lateral plate mesoderm is a hallmark of the left signaling cascade, the inducibility of *Pitx2* isoforms by Nodal was assessed and the results showed that only *Pitx2c* expression is

inducible by Nodal (Schweickert et al., 2000). The asymmetric expression of *Pitx2c* is mediated by FoxH1, a transcription factor, via an intronic left side-specific enhancer (ASE) (Shiratori et al., 2001).

1.3.4. Pitx2 mutations in humans

PITX2 was first discovered as the RIEG gene responsible for Axenfeld-Rieger syndrome type 1 (ARS1, MIM 180500), an autosomal-dominant, haploinsufficient disorder found in humans (Semina et al., 1996). ARS1 patients present with ocular, craniofacial, dental and umbilical anomalies and occasionally abnormalities in cardiac, limb and pituitary development, but no laterality defects such as lung or gut malformations have been reported (Chang et al., 2012; Hjalt and Semina, 2005; Jorgenson et al., 1978; Semina et al., 1996). Cardiac anomalies, including abnormality of the cardiovascular outflow tract and atrial septal defects, are observed in ARS1 patients (Bekir and Güngör, 2000; Chang et al., 2012; Cunningham et al., 1998). These cardiac defects are identical to those observed in heterotaxy patients, suggesting that problems establishing laterality completely still remain in a small proportion of ARS1 patients.

Most of the *PITX2* mutations responsible for ARS1 are point mutations in the coding region and generally affect the homeodomain and C-terminal domain, although some mutations have also been found in regulatory elements of *PITX2* (D'haene et al., 2011; Maciolek et al., 2006; Reis et al., 2012; Trembath et al., 2004; Tumer and Bach-Holm, 2009; Volkmann et al., 2011). Mutations in the N-terminal domain of *PITX2* have yet to be discovered. Chromosomal aberrations at the *PITX2* locus such as rearrangements, deletions and duplications affecting copy

number have also been described (D'haene et al., 2011; Flomen et al., 1997; Makita et al., 1995; Tumer and Bach-Holm, 2009). Both gain- and loss-of-function mutations in *PITX2* result in ARS1 (Amendt et al., 2000; Holmberg et al., 2004; Lines et al., 2002; Saadi et al., 2006), suggesting that the appropriate level of PITX2 expression is also important.

1.3.5. Pitx2 mutations in mice

Consistent with human ARS1 patients, heterozygous null *Pitx2* mice display defects in ocular and dental formation (Gage et al., 1999). In contrast, homozygous deletion of *Pitx2* also display rare ARS1 defects, including pituitary malformations, omphalocele and cardiac laterality defects such as abnormalities of the cardiac outflow tract and atrioventricular septal defects (Gage et al., 1999; Kitamura et al., 1999; Lin et al., 1999; Lu et al., 1999). Additionally, homozygous null *Pitx2* mice display defects not observed in ARS1 patients; unique laterality defects include abnormal body rotation, absence of gut looping, right pulmonary isomerism, and transposition of the great arteries (Gage et al., 1999; Kitamura et al., 1999; Lin et al., 1999; Lu et al., 1999). Unlike heterozygous null mutations, homozygous deletion of *Pitx2* in mice is embryonic lethal, providing possible explanation as to why there are no human ARS1 patients characterized with laterality defects.

In *Pitx2ab*$^{-/-}$ mice where only the *Pitx2c* isoform is expressed, laterality defects are rescued (Liu et al., 2001). By using different alleles of *Pitx2c* expressing different levels of *Pitx2c*, it appears that each asymmetrically formed organ requires different thresholds of *Pitx2c* expression (Liu et al., 2001). Low

levels of *Pitx2c* in *Pitx2c* hypomorph mice were able to rescue the cardiac defects observed in *Pitx2* null mice suggesting normal heart development requires low levels of *Pitx2c* expression. This may explain why cardiac defects are rarely observed in ARS1 patients. Only high levels of *Pitx2c* expression in *Pitx2ab*$^{-/-}$ mutants were able to rescue right pulmonary isomerism (Liu et al., 2001). Although rotation of the gut tube was restored with low levels of *Pitx2c*, direction was randomized. At intermediate levels of *Pitx2c* expression, direction was completely reversed. At high levels of *Pitx2c* expression, rotation and direction of gut looping was rescued. This suggests that normal gut development requires a specific threshold of Pitx2c expression to maintain proper laterality (Liu et al., 2001).

1.3.6. Pitx2 gain-of-function and loss-of-function in chick, Xenopus, and zebrafish

All *Pitx2* isoforms have been reported to affect organ *situs* when misexpressed on the right side of embryos (Essner et al., 2000; Logan et al., 1998; Schweickert et al., 2000; Yu et al., 2001), but this is most likely due to the induction of *Pitx2c* expression by other isoforms (Schweickert et al., 2000). Conversely, only the loss of *Pitx2c* expression on the left side of embryos affects organ *situs* (Yu et al., 2001). Similarly when a dominant-negative form of *Pitx2c* was expressed on the left side of embryos, organ *situs* was affected, while a dominant-negative form of Pitx2a showed no effect (Yu et al., 2001).

1.3.7. Pitx2c N-terminus in left-right patterning

Since Pitx2c differs from Pitx2a and Pitx2b only at the N-terminus, the unique role of Pitx2c in left-right patterning may be associated with its unique N-terminus. Recently in our lab, the function of the *Pitx2c* N-terminus in left-right patterning was investigated (Simard et al., 2009). Misexpression of *Pitx2c's* N-terminal domain (*Pitx2cN*) on the left side of the embryo (where *Pitx2c* is endogenously expressed) randomized the direction of heart looping. Site-directed mutagenesis identified leucine-41 and to a lesser extent threonine-45 as being critical for the ability of the Pitx2cN to interfere with rightward looping of the heart tube.

The mutations within the N-terminus do not affect full-length *Pitx2c's* (*Pitx2cFL*) transactivation function. However, cotransfection of a vector expressing *Pitx2cN* did interfere with the synergistic activation of the *Plod-1* promoter by Pitx2cFL and Nkx2.5. Importantly, the cotransfection of LAMAT *Pitx2c* N-terminus mutants carrying site mutations at L41, M43, and T45 did not affect the ability of Pitx2cFL and Nkx2.5 to synergistically activate the *Plod-1* promoter. Additionally, Pitx2c and Nkx2.5 require another protein intermediate in order to act on the *Plod1*-promoter since they do not directly interact with each other, but are required to be in close proximity to synergistically activate the *Plod1*-promoter (Ganga et al., 2003). Together, these results suggest that there is a critical interaction domain in the Pitx2c N-terminus, involving leucine-41, by which Pitx2c interacts with other proteins to form transcription factor complexes that synergistically activate genes. Protein interactions with this domain may also

be important for Pitx2c's role in left-right patterning. Although there are known proteins that interact at the homeodomain and C-terminus of Pitx2, including transcription factors and other types of proteins, no interactors of the Pitx2c N-terminus have been identified (Fig. 4).

1.4. Hypothesis and objectives

The essential role of Pitx2c in left-right patterning is evident; however how Pitx2c orchestrates asymmetric organogenesis throughout development is not well understood. Recently in our lab, we identified a critical interaction domain in the unique N-terminus of Pitx2c that is required for its function in left-right patterning. We hypothesize that there are protein interaction partners of the Pitx2c N-terminus that are required for Pitx2c's function in patterning left-right asymmetry during embryogenesis.

To test this hypothesis, I sought to identify protein interaction partners of the Pitx2c N-terminus using a yeast two-hybrid screen with the mouse Pitx2c N-terminus as bait and the mouse E11 two-hybrid cDNA library as prey. This approach was chosen for it's unbiased nature and advantage over classic biochemical or genetic approaches in that it is performed in an *in vivo* system. Only candidates isolated at least twice from the screen were prioritized for further analysis. Prioritized candidates were verified to be coding sequences and screened for false positive interactions. Putative interaction regions with Pitx2cN were confirmed in yeast via yeast co-transformations. The expression patterns of candidate protein interaction partners of the Pitx2c N-terminus were characterized during embryogenesis using whole mount *in situ* hybridization in chick embryos. As candidate expression patterns should overlap with that of *Pitx2c* for interactions to be important *in vivo,* candidate expression patterns were compared with the known expression pattern of *Pitx2c* to further prioritize candidates. Lastly, I reviewed the known functions of candidate interaction partners and

discussed the feasibility and function of potential Pitx2c-candidate interactions in left-right patterning.

2. Materials and Methods

2.1. Yeast strains

Saccaromyces cerevisiae strain, Y2HGold (*MATa, trp1-901, leu2-3, 112, ura3-52, his3-200, gal4Δ, gal80Δ, LYS2::GAL1$_{UAS}$–Gal1$_{TATA}$–HIS3, GAL2$_{UAS}$–Gal2$_{TATA}$–ADE2, URA3::MEL1$_{UAS}$–Mel1$_{TATA}$-AUR1-C, MEL1*) from Clontech (Palto Alto, CA) was used to transform bait fusion plasmids for the yeast-two hybrid screen. The mouse E11 cDNA library was generated in *Saccaromyces cerevisiae* strain, Y187 (*MAT* α, *ura3-52*, *his3–200*, *ade2–101*, *trp1–901*, *leu2–3*, *112*, *gal4*Δ, *gal80*Δ, *met-, URA3::GAL1$_{UAS}$-GAL1$_{TATA}$-lacZ, MEL1)* by Clontech. A working population of *S. cerevisiae* Y2Hgold were grown at 30°C on yeast YPD supplemented with adenine hemisulfate (YPDA) agar plates for 3-5 days and stored at 4°C for up to 1 month.

2.2. Generation of the bait construct and prey library

A cDNA encoding the N-terminal domain of mouse Pitx2c (*Pitx2cN*; aa 1-68) was cloned previously in the lab into the pGBKT7 vector (Clontech, Palo Alto, CA) to generate the bait, *Pitx2cN*, and *GAL4*-DNA binding domain fusion plasmid (Fig. 5). The yeast two-hybrid embryonic day 11 mouse Mate and Plate cDNA library was purchased from Clontech. Clontech generated the library by cloning cDNAs derived from whole embryos into the pGADT7 prey vector and transforming the library into the Y187 yeast strain. The candidate-pGADT7 vector expresses proteins fused to the GAL4 activation domain (Fig. 5).

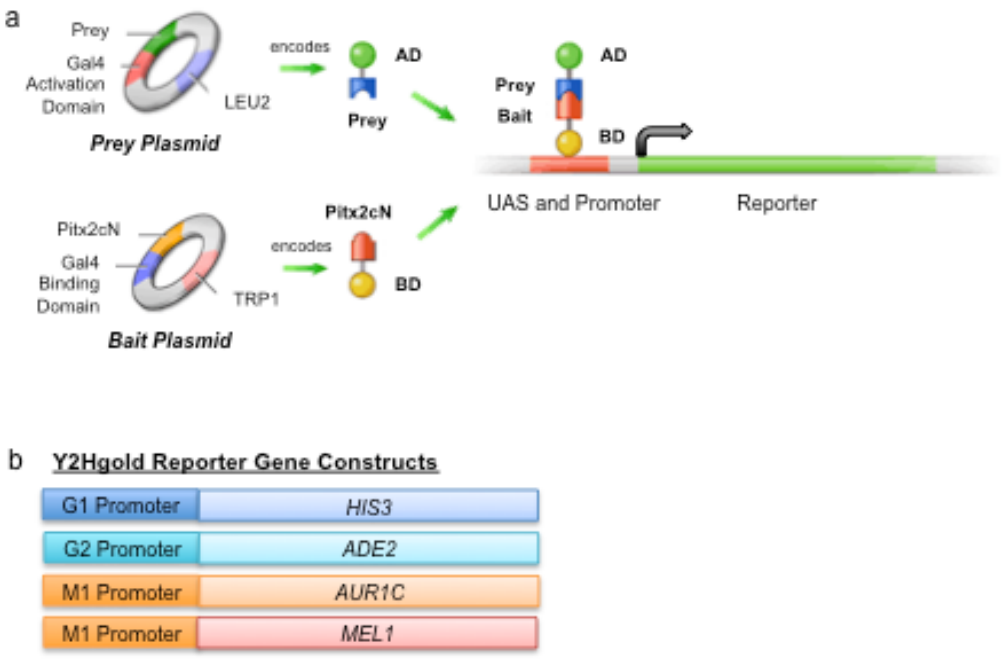

Figure 5. Principle of the two-hybrid screen. (a) The Clontech Yeast Two Hybrid System kit divides yeast Gal4 transcription factor into two domains: activation domain and DNA binding domain. The two domains are then fused to two separate proteins, bait and prey. If there are protein interactions between the bait and prey protein, the activation domain and DNA binding domain will be brought together to complete the GAL4 transcription factor. Image adapted from The Science Creative Quarterly, http://sqc.ubc.ca, yeasttwohybrid by Jiang Long. (b) Four reporter genes are present in the Y2HGold yeast strain: HIS3, a imidazoleglycerol-phosphate dehydratase encoding gene, ADE2, an phosphoribosylaminoimidazole carboxylase encoding gene, AUR1-C, an Aureobasidin A resistance gene, and MEL1, an alpha-galactosidase encoding gene. Image adapted from Clontech.

2.3. Yeast selection criteria and reporters used

To select for yeast colonies containing the pGBKT7 and/or the pGADT7 vectors as well as for positive interacting colonies, nutritional selection, chromogenic selection and anti-fungal resistance were used. The pGADT7 vector contains a gene encoding β-isopropylmalate dehydrogenase (*LEU2*), an essential component of leucine synthesis, and the pGBKT7 vector has a gene encoding phosphoribosylanthranilate isomerase (*TRP1*), an essential component of tryptophan synthesis (Fig. 5). Medium absent of leucine (Leu; SDO-Leu) and/or tryptophan (Trp; SDO-Trp) was used to select for the presence of one or both plasmids. Medium deficient of one amino acid was termed single drop-out (SDO) while medium deficient of both amino acids was termed double drop-out (DDO).

To detect positive protein interactions, growth medium was manipulated to take advantage of four reporter genes present in the Y2Hgold yeast strain: a gene encoding imidazoleglycerol-phosphate dehydratase (*HIS3*), an essential component of histidine synthesis; a gene encoding phosphoribosylaminoimidazole carboxylase (*ADE2*), a component essential for adenine synthesis; *AUR1-C*, a gene encoding Aureobasidin A (A) resistance; and *MEL-1*, a gene encoding α-galactosidase which hydrolyzes colourless X-α-galactose (X) into a blue substrate (Fig. 5). Medium absent of all four amino acids, leucine, tryptophan, histidine (His) and adenine (Ade) was termed quadruple drop-out (QDO). For ease of picking positive interacting colonies by eye, X-α-galactose, a chromogenic substrate, was used. For increased stringency to select for positive interacting colonies, Aureobasidin A, an antifungal reagent was used.

2.4. Yeast transformation to test autoactivity and toxicity of bait vector

To test for autoactivation of reporter genes and toxicity to cells, *Pitx2cN*-pGBKT7 or *p53*-pGBKT7 (Clontech) was transformed into Y2Hgold cells using the Yeastmaker^{TM} Yeast Tranformation System 2 (Clontech), as per manufacturer's instruction. Yeast transformations were spread onto SDO-Trp and SDO-Trp/X/A plates at a 1/10 dilution or undiluted. Growth and colour were assessed after 4 days of incubation at 30°C.

2.5. Yeast two-hybrid screen

A yeast two-hybrid screen was performed using the Matchmaker Gold Yeast Two-Hybrid System (Clontech). To begin the yeast two-hybrid screen, a liquid culture of *Pitx2cN*-pGBKT7 transformed in Y2Hgold cells (bait strain) was cultured at 30°C until OD_{600} reached 0.800. The library strain (Clontech) was combined with 4mL of this bait strain and incubated at 30°C with slow shaking to allow the two strains to mate. The success of mating, determined by the presence of zygotes, was checked at 20, 24 and 27 hours by examining a small sample of mated culture on a slide under the Axiophot upright microscope (Zeiss). Once zygotes were observed, 100µl of 1/10, 1/100, 1/1,000, and 1/10,000 dilutions of the mated culture were spread on SDO-Trp, SDO-Leu and DDO plates. The remainder of the mated culture was spread on DDO/X/A plates. Each plate was spread with 200µl of mated culture. All plates were incubated at 30°C for 4 days. Colony growth and colour were assessed to determine positive interacting colonies. The number of screened clones was determined by the number of colonies formed on DDO plates. The mating efficiency was determined by the

percentage of diploids. This was calculated by the number of colonies on DDO divided by the lower number of colonies either on the SDO-Trp or SDO-Leu plates. Blue colonies on DDO/X/A plates were patched out onto QDO/X/A plates and incubated at 30°C for 4 days. Growth and colour were assessed. Blue colonies were restreaked again according to colour intensity onto a second round of QDO/X/A plates and incubated at 30°C for 4 days. Growth and colour were assessed.

2.6. Plasmid isolation from yeast

Plasmids of positive interacting colonies were isolated using the Easy Yeast Plasmid Isolation Kit (Clontech) as per manufacturer's instructions. Inserts were PCR amplified using vector-specific primers, Matchmaker AD LD-Insert Screening Amplimers (Clontech) and sequenced at the McGill University and Genome Quebec Innovation Center using a T7 primer. Sequences of clones obtained were searched in NCBI BLAST and UCSC BLAT to determine identity. PCR products of candidate interaction partners were also digested using DpnII (New England Biolabs) and separated on a 1% agarose gel to identify duplicate clones.

2.7. Separating prey plasmids in yeast colonies

Some colonies contained multiple plasmids. The colonies with multiple plasmids were streaked repeatedly on DDO/X medium to separate the prey plasmid responsible for the Pitx2cN protein-protein interaction (Fig. 6). Once restreaked, the blue and white colonies both appeared indicating separation of,

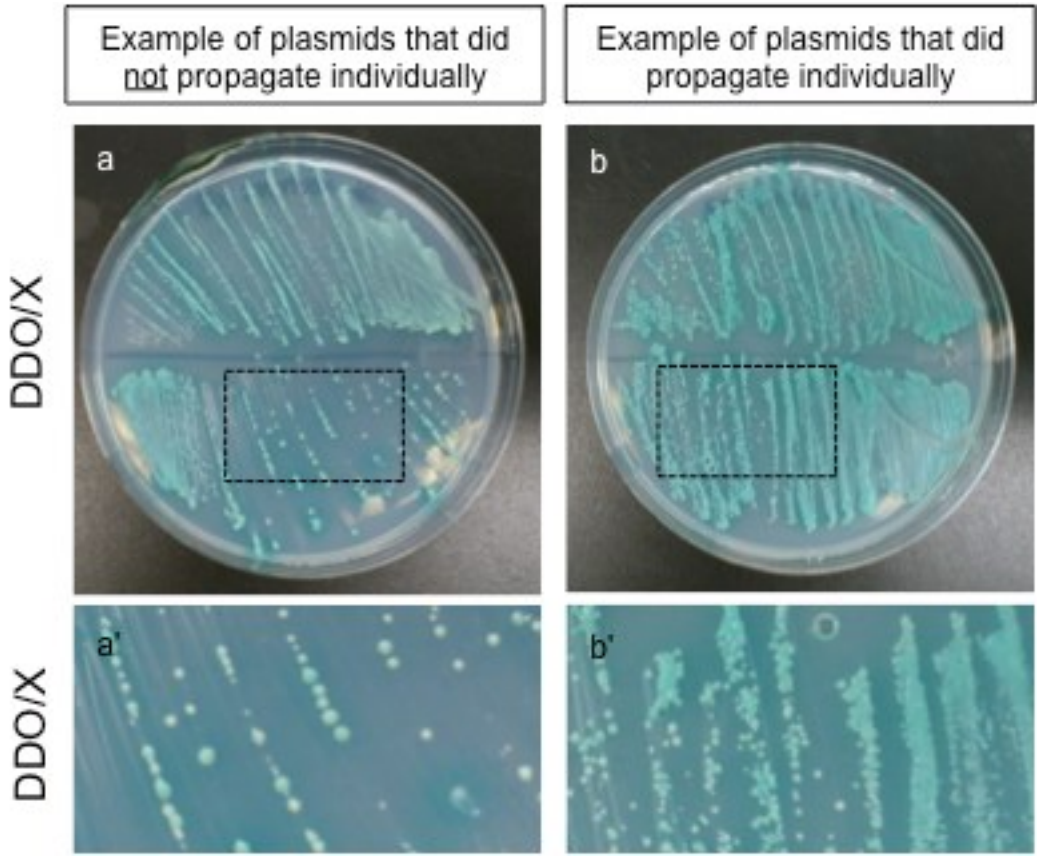

Figure 6. Sample plates showing restreaking process to separate colonies with multiple plasmids: (a) Shown is a plate at initial stages of restreaking. Note the variation of colony colour from white to different intensities of blue. (a') is a magnified view as indicated by the dotted box in (a). (b) Shown is a plate at final stages of restreaking. Note the uniformity of blue colour in all colonies. (b') is a magnified view as indicated by the dotted box in (b).

interacting versus non-interacting prey plasmids, respectively (Fig 6a-a'). Blue colonies were selected and re-streaked. When only blue colonies were observed plasmids from these colonies were isolated and sequenced as described previously (Fig 6b-b').

2.8. Re-cloning yeast plasmids

Isolated plasmids were PCR amplified using the Matchmaker AD LD-Insert Screening Amplimers (Clontech) vector-specific primers. PCR products were then digested with NdeI (New England Biolabs) and BamHI (New England Biolabs) for 1 hour at 37°C and ligated with linearized pGADT7 and pGBKT7. Ligations were transformed into competent DH5α *E. coli* cells, plated on LB agar plates containing 100µg/ml ampicillin (Fisher) for pGADT7 or 50µg/ml kanamycin (Fisher) for pGBKT7, and incubated at 37°C. Colonies were picked and cultured overnight in liquid LB with 100µg/ml of ampicillin (Fisher) or 50µg/ml kanamycin (Fisher). The STET (8% sucrose, 50 mM Tris-HCl pH 8, 0.5% Triton X-100, 50 mM EDTA)/boiling miniprep method was performed to isolate plasmid DNA from bacterial cultures as described in Siontas, 2011. Isolated plasmids were digested with NdeI (New England Biolabs) and BamHI (New England Biolabs) for 1 hour at 37°C and separated on 1% agarose gels to visualize the insert and plasmid to identify plasmids with inserts. Plasmids with inserts were then sequenced using T7 primers at the McGill University and Genome Quebec Innovation Centre. *In silico* analysis of sequences was performed to determine their identity. Plasmid DNA were isolated using the Plasmid Midi

Kit (Qiagen) as per manufacturer's instructions. Plasmids were resuspended in double distilled water and stored at -20°C until use.

2.9. Yeast transformations to test autoactivity of candidates and to confirm and validate candidate-Pitx2cN interactions

To assess interactions, vectors were transformed using the small-scale version of Yeastmaker^{TM} Yeast Tranformation System 2 (Clontech) as per manufacturer's instructions. Equal amounts of each vector were transformed for a total of 100ng in each transformation and plated on DDO/X medium. Plates were incubated at 30°C. Colony growth and colour were assessed 4 days after plating. Blue colonies were streaked onto QDO/A or QDO/X/A agar plates and incubated at 30°C for 4 days. Growth and colour were assessed.

To eliminate false positives, Y2Hgold yeast cells were transformed with candidate-pGADT7 and empty-pGBKT7 vectors. To confirm the interaction of putative candidate interaction regions with Pitx2cN, Y2H gold yeast cells were transformed with candidate-pGADT7 and *Pitx2cN*-pGBKT7 vectors. To validate protein expressions, Y2H gold yeast cells were transformed with candidate-pGBKT7 and *Pitx2cN*-pGADT7 vectors.

2.10. Sequence alignment of interaction regions of confirmed potential candidates with full length candidate proteins

Insert sequences were translated using ExPASy (Swiss Institute of Bioinformatics) and aligned to full length proteins obtained from the NCBI

database using ClustalW2 (EMBL-EBI). Literature review was performed to determine the functional domains residing in each interaction region.

2.11. Handling and dissection of chick embryos

Fertilized eggs were obtained from Couvoir Simentin (St-Canut, QC). Eggs were incubated at 38.5°C for various hours depending on age of chick embryo desired. Chick embryos were dissected from eggs and placed in 1X DEPC PBS on ice. For RNA isolation, chick embryos were immediately flash-frozen in liquid nitrogen. For whole-mount *in situ* hybridization, chick embryos were fixed in 4% paraformaldehyde (PFA) overnight, dehydrated and stored in 100% methanol at -20°C.

2.12. cDNA cloning of chick candidate protein interaction partners

Total RNA was isolated using the Absolutely RNA Miniprep Kit (Stratagene) from HH stage 12 chick embryos as per manufacturer's instructions. Isolated RNA was stored at -20°C until use. mRNA for *Npc2, Srsf15, Eif3a* and *Eif3m*, were reverse transcribed and PCR amplified using the Superscript® One-Step RT-PCR System with Platinum® *Taq* DNA Polymerase (Invitrogen) from total RNA collected as described above using primers that were designed to amplify the entire coding region. Primer sequences used and PCR product sizes can be found in Table 1. Synthesized cDNA was stored at -20°C until use.

cDNA products and pBluescriptKS II+ vectors (Stratagene) were digested using EcoRI (New England Biolabs) for 1 hour at 37°C and ligated at room temperature overnight using T4 DNA ligase (Invitrogen) as per manufacturer's

Table 1. Primers used for cDNA cloning of chick candidates

Candidate	Primer Sequences (5'→3')	PCR Product Size (bp)
Npc2	Forward: CCAAAGACGGAAGCATTCAAGAGG Reverse: GCAGCTCCAAGTTAGTTGATAGTGC	450
Srsf15	Forward: GCACCCAAGGAGTCGCAC Reverse: CCTCAAAACAATAGGGATGTG	842
Eif3a	Forward: GCGAATATGAAAACAGTTTAACC Reverse: CCAGATAGTTAATTGTAATTCTGC	448
Eif3m	Forward: CGTTCATCGACATCACGG Reverse: GAATGCATGTCTTCTTTAAACC	1125

instructions. Ligated plasmids were transformed into competent DH5α *E. coli* cells and incubated on LB agar with 100μg/ml ampicillin. Colonies were picked and cultured overnight in liquid LB with 100μg/ml of ampicillin. The STET/boiling miniprep method was performed to isolate plasmids from bacterial cultures as described in Siontas, 2011. Isolated plasmids were digested with EcoRI (New England Biolabs) for 1 hour at 37°C to identify plasmids with inserts. Digestions were separated on 1% agarose gels to visualize the insert and plasmid. Plasmids with inserts were then sent for sequencing. *In silico* analysis of sequences was performed to confirm identity and orientation of insert. Plasmid DNA were isolated using the Plasmid Midi Kit (Qiagen) as described above and plasmids were resuspended in double distilled water and stored at -20°C until use.

2.13. RNA probe preparation

Npc2-, *Srsf15*-, *Eif3m*-, and *Eif3a*-pBluescript KS II+ were linearized with BamHI, ClaI or SmaI (New England Biolabs) for 2 hours at 25°C and 37°C, respectively. Antisense RNA was generated using 5X transcription buffer (Invitrogen), 100mM DTT (Invitrogen), digoxygenin labeled UTP (Roche) and T3 or T7 RNA polymerases (Invitrogen) depending on the orientation of the inserts (Table 2). After 2 hours of incubation at 37°C, RNA probes were precipitated and resuspended in 100mM DTT. A small sample was separated on 1% agarose gels to determine the amount of RNA transcribed. RNA probes were diluted in hybridization solution (50% formamide, 5X sodium saline citrate (SSC) pH 5.0, 50μg/mL yeast tRNA, 1% SDS, and 50μg/mL heparin) to a final concentration of 1μg/mL and stored at -20°C until use.

Table 2. Polymerase and enzymes used for RNA probe preparation

Candidate	RNA Polymerase Used	Restriction Enzyme Used to Linearize Plasmid
Npc2	T3	Sma1
Srsf15	T3	BamH1
Eif3a	T3	Sma1
Eif3m	T7	Cla1

2.14. Whole mount *in situ* hybridization

Whole-mount *in situ* hybridization of chick embryos was performed at: HH stage 10, when the linear heart tube is formed; HH stage 12, when the heart tube has looped to the right; HH stage 18, when the Rathke's pouch is formed; and HH stages 24 and 26, when the limb buds are developing. Fixed embryos were dehydrated sequentially with 25% methanol in PBS with 10% tween (PBT), 50% methanol in PBT, 75% methanol in PBT, and 100% methanol prior to rehydration into PBT. After being bleached with 6% hydrogen peroxide, embryos were treated with 10µg/mL proteinase K in PBT at room temperature. Incubation time was dependent on the age of the embryo and stopped with 0.2% glycine. Embryos were fixed again using a solution of 4% PFA and 0.2% gluteraldehyde in PBT for 20 minutes on ice. Embryos were then incubated with pre-hybridization solution at 65°C for 2 hours. Pre-hybridization solution was replaced with antisense RNA probes in hybridization solution and embryos werer incubated overnight at 65°C. Following this incubation, embryos were washed with prewarmed solution 1 (50% formamide, 5X SSC pH4.5 and 1% SDS) for 4x20 minutes at 65°C and then washed with prewarmed solution 3 (50% formamide, 2X SSC pH 4.5) for 4x20 minutes at 65°C. Embryos were then washed with 2mM levamisole in 1X TBST (25mM Tris-HCl pH 7.5, 137 mM NaCL, 2.7 mM KCl) for 3x10 minutes. After these washes, embryos were blocked in 10% sheep serum in 1X TBST for 1.5 hours at room temperature. Embryos were then incubated overnight at 4°C in antibody mix containing 10%

sheep serum, and 0.05% of anti-digoxygenin conjugated with alkaline phosphatase (Roche) in TBST. After incubation, embryos were washed with 2mM levamisole in 1X TBST for 3x5 minutes and then washed 5x1 hour at room temperature. Subsequently, embryos were washed with NTMT solution (100mM NaCL, 100mM Tris-HCl pH 9.5, 40mM MgCl2, and 0.1% Tween) for 3x10 minutes and transferred to new NTMT solution containing 0.25% BCIP (Roche) and 0.25% NBT (Roche). Embryos were incubated at room temperature until desired colour development was achieved.

2.15. Tissue sectioning

Whole mount *in situ* embryos were dehydrated gradually in 30% ethanol, 50% ethanol, 70% ethanol, 100% ethanol, and finally xylene for 30 minutes each at room temperature. Dehydrated embryos were placed in melted paraffin and incubated in a vacuum oven at 60°C for 2 hours. Embryos were then placed in fresh liquid paraffin and positioned as desired for sectioning. Embryos were sectioned at 10µm using the Leica RM2155 microtome and sections were mounted onto Superfrost Plus slides (Fisher). Paraffin was removed from sections in two 3 minute xylene washes and slides were coverslipped with Permount mounting medium (Fisher). Sectioned whole mount *in situ* embryos were imaged with a Zeiss AxioCam MRm or MRc attached to an Axiophot upright microscope (Zeiss) via a Leica Adaptor.

Chapter 3. Results

3.1. Identification of potential protein interaction partners of the Pitx2c N-terminus

3.1.1. Autoactivity and cytotoxicity of Pitx2cN-pGBKT7

Before beginning the screen with the *Pitx2c* N-terminus, it was necessary to ensure that the *Pitx2c* N-terminus in the bait vector (*Pitx2cN*-pGBKT7) would not autoactivate reporter genes in the yeast strain used or cause cytotoxicity to the yeast cells. An initial small-scale transformation of *Pitx2cN*-pGBKT7 in Y2Hgold yeast cells resulted in similar numbers and sizes of yeast formed on SDO/-Trp plates (Fig. 7b) as compared to a yeast colonies transformed with the control plasmid, *p53*-pGBKT7 (Fig. 7a). These data indicate that *Pitx2cN*-pGBKT7 does not cause cytotoxicity to the Y2Hgold yeast strain. Colonies transformed with the *Pitx2c* N-terminus vector did not grow on SDO/-Trp/X/A plates (Fig. 7d), indicating that *Pitx2cN*-pGBKT7 does not autoactivate reporter genes in the Y2Hgold yeast strain. Therefore, *Pitx2cN*-pGBKT7 was suitable for use as bait in the yeast two-hybrid screen.

3.1.2. Identifying potential protein interaction partners using a yeast two-hybrid screen

Pitx2cN-pGBKT7-transformed Y2Hgold yeasts mated with the mouse E11 cDNA library-transformed Y187 yeasts yielded zygotes 27 hours after mating (Fig. 8). The transformation efficiency of *Pitx2cN*-pGBKT7 was 7.55×10^5 cfu/μg (Table 3). The number of clones present in the cDNA library was 1.70×10^9

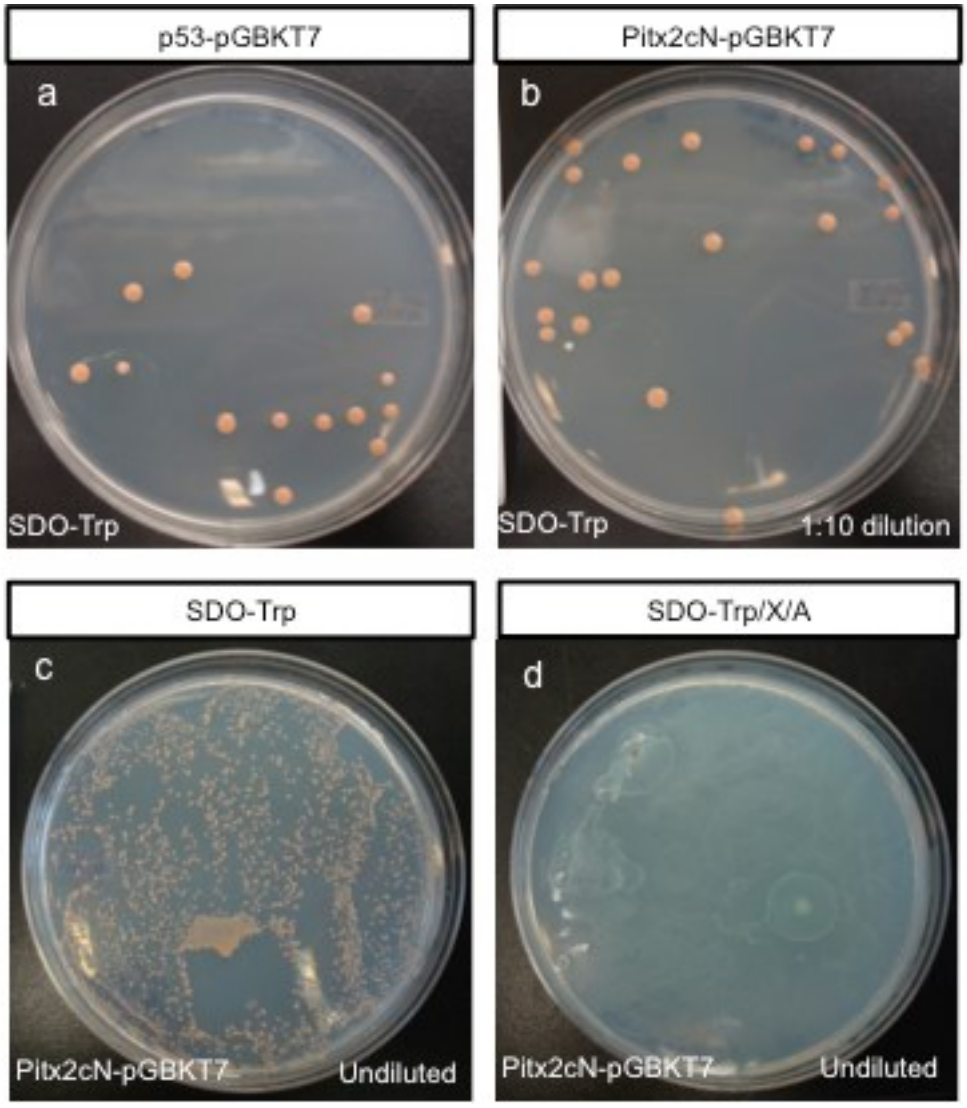

Figure 7. Pitx2cN-pGBKT7 does not autoactivate reporter genes or cause toxicity in yeast cells: (a) Y2Hgold yeast colonies transformed with a control plasmid, p53-pGBKT7, grown on SDO-Trp medium and plated at a 1:10 dilution. Y2Hgold yeast colonies transformed with Pitx2cN-pGBKT7 grown on SDO-Trp medium and plated at a 1:10 dilution (b) and undiluted (c). (d) Y2Hgold yeast colonies transformed with Pitx2cN-pGBKT7 grown on SDO-Trp/X/A and plated undiluted.

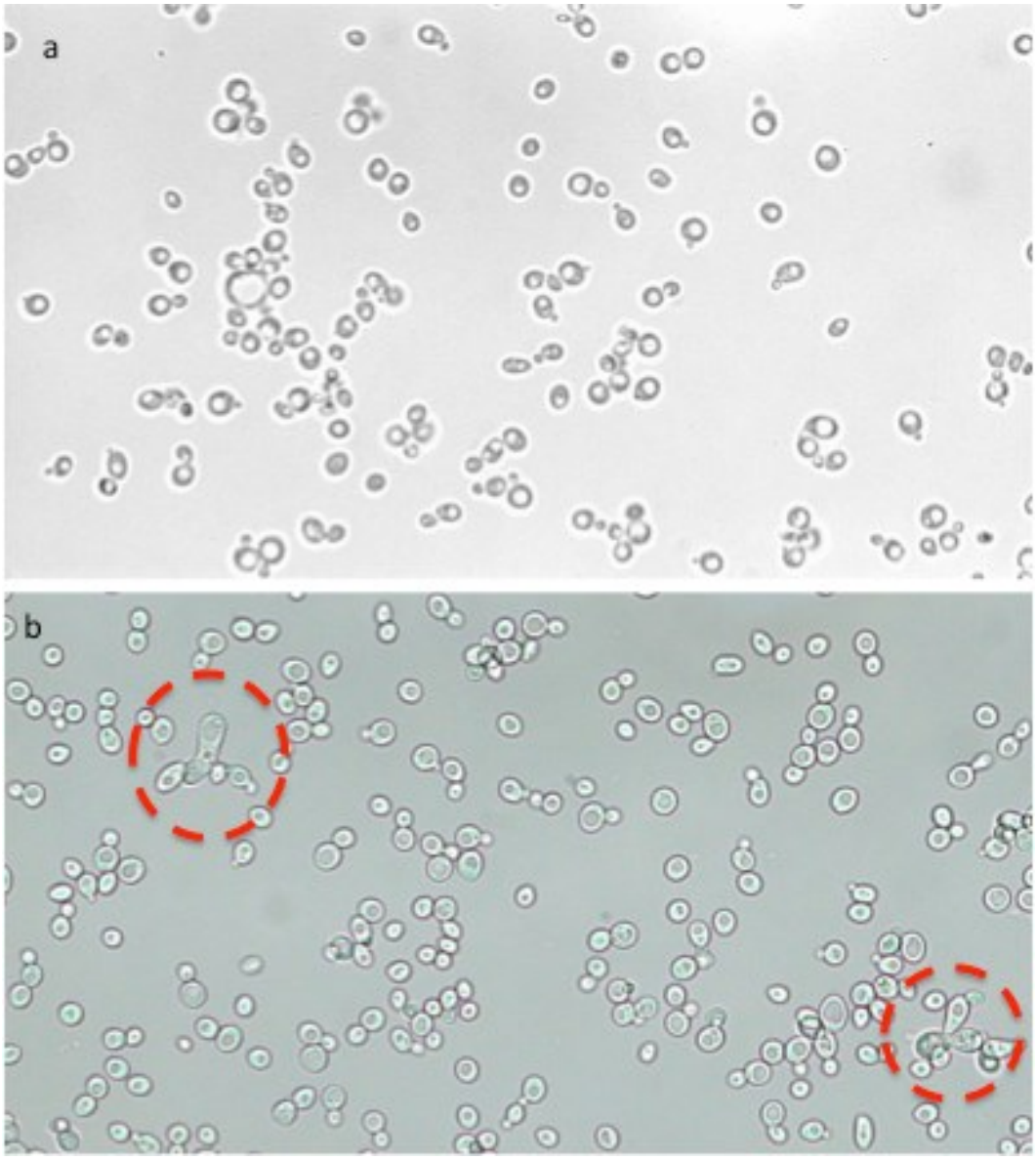

Figure 8. Formation of zygotes after yeast mating: (a) A sample of yeast culture after 24 hours of mating. (b) A sample of yeast culture after 27 hours of mating. Note the presence of zygotes circled in red.

Table 3. Efficiency of the yeast two-hybrid screen

Mouse Pitx2c N-terminus & Mouse E11 cDNA library	
Transformation efficiency of Pitx2c N-terminus	7.55×10^5 cfu/µg
Number of clones in cDNA library	1.70×10^9 cfu/µg
Mating efficiency	22.4%
Number of clones screened	4.05×10^7
Number of clones streaked (low stringency – DDO/X/A)	318
Number of blue colonies (high stringency – QDO/X/A)	128

cfu/μg (Table 3). The mating efficiency was determined to be 22.4% and a total of 4.05 x10^7 clones were screened (Table 3).

A total of 318 clones were selected on low stringency DDO/X/A plates (Fig. 9a). When these colonies were patched onto high stringency QDO/X/A plates, 128 colonies continued to grow (Fig. 9b). 58 of these were dark blue colonies, indicating stronger protein interactions, while 70 grew as light blue colonies, indicating weaker protein interactions. Since it is possible that stronger interacting colonies could support the growth of weaker interacting colonies nearby by breaking down the antifungal reagent, colonies were streaked onto high stringency plates a second time (Fig. 9c). All 58 dark blue colonies continued to grow, while only 11 of the 70 light blue colonies were able to grow (Fig. 9c), giving a combined total of 69 colonies.

3.1.3. Prioritization of candidate interaction partners

Sequence analysis identified 32 unique genes among the 69 prey clones (Table 4). Fourteen candidates that were isolated two or more times were prioritized as potential protein interaction partners for further analysis (shown in bold in Table 4). In order from the most frequently isolated to the least frequently isolated, these candidates were Niemann-Pick C type 2 (*Npc2*), Eukaryotic translation initiation factor 3, subunit A (*Eif3a*), Krab-box Zinc Finger Protein (*Zfp845*), Serine/arginine-rich splicing factor 2 (*Srsf2*), Eukaryotic translation initiation factor 3, subunit M (*Eif3m*), NEDD4 binding protein 2-like 2 (*N4bp2l2*), Anti-silencing function 1 homolog B (*S. cerevisiae*) (*Asf1b*), Bromodomain adjacent to zinc finger domain, 1B (*Baz1b*), COMM domain

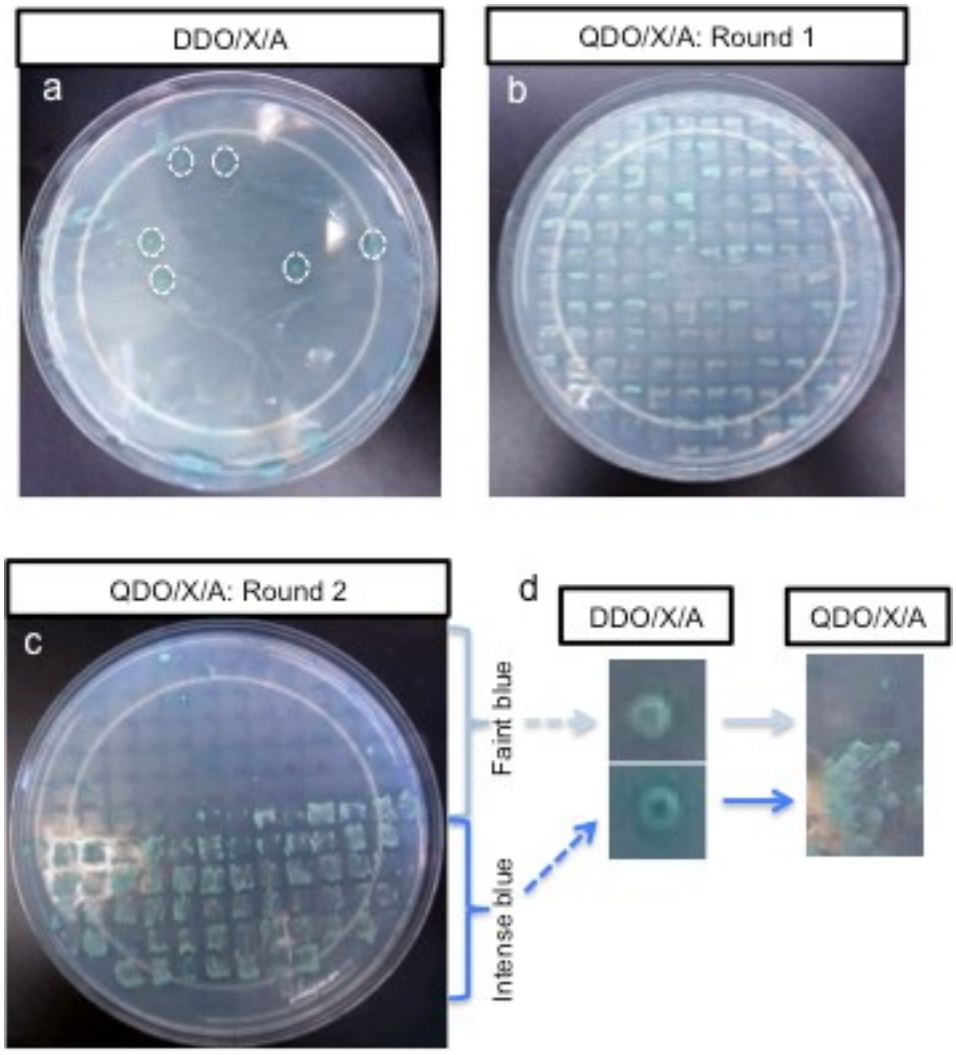

Figure 9. Analysis of colony formation on different stringency plates: Shown are a low stringency DDO/X/A plate (a) and a high stringency QDO/X/A plate (b) from the yeast two hybrid screen. Blue colonies indicated by white circles on DDO/X/A plates were picked and patched onto 1 cm by 1 cm squares on QDO/X/A plates. Colonies that grew in the first round of high stringency QDO/X/A plates (b) were streaked onto a second round of high stringency QDO/X/A plates (c) based on the intensity of colour in (b). (d) Shown are magnified views of colonies of different intensities on DDO/X/A plates and the resultant patches of these colonies on QDO/X/A plates.

Table 4. Interacting prey candidates isolated in the screen.

Frequency	Prey Insert
7	**Niemann-Pick type C2 (Npc2)**
4	**Eukaryotic translation initiation factor 3, subunit A (Eif3a)**
4	**Krab-box Zinc Finger Protein (Zfp845)**
4	**Serine/arginine-rich splicing factor 2 (Srsf2)**
3	**Eukaryotic translation initiation factor 3, subunit M (Eif3m)**
3	**NEDD4 binding protein 2-like 2 (N4bp2l2)**
2	**ASF1 anti-silencing function 1 homolog B (*S. cerevisiae*)**
2	**Bromodomain adjacent to zinc finger domain, 1B (Baz1b)**
2	**COMM domain containing 4 (Commd4)**
2	**Expressed sequence AI506816 (AI506816), transcript variant**
2	**Family with sequence similarity 96, member B (Fam96b)**
2	**Myristoylated alanine rich protein kinase C substrate**
2	**Serine/arginine-rich splicing factor 15 (Srsf15)**
2	**Zinc finger protein 740 (Zfp740)**
1	5' UTR of Sec24 related gene family, member B (*S. cerevisiae*)
1	Collagen, type III, alpha 1 (Col3a1)
1	DIS3 mitotic control homolog (S. cerevisiae)-like (Dis3l), transcript
1	DnaJ (Hsp40) homolog, subfamily B, member 6 (Dnajb6),
1	Insulin-like growth factor 2 mRNA binding protein 2 (Igf2bp2)
1	Phospholipase C, gamma 1 (Plcg1)
1	Polymerase (RNA) II (DNA directed) polypeptide B (Polr2b)
1	Protein tyrosine phosphatase, non-receptor type 2 (Ptpn2),
1	RIKEN cDNA 1110034A24 gene (1110034A24Rik)
1	RIKEN cDNA 9130401M01 gene (9130401M01Rik)
1	Ring finger protein 2 (Rnf2)
1	Syntaxin 5A (Stx5a), transcript variant 2
1	Ubiquitin C (Ubc)
1	Rho family GTPase 2 (Rnd2)
1	Glyceraldehyde-3-phosphate dehydrogenase (GAPDH)

*Candidates in bold were isolated at least twice in the screen and prioritized for further analysis

containing 4 (*Commd4*), Expressed sequence AI506816, transcript variant 1, non-coding sequence (*AI506816*), Family with sequence similarity 96, member B (*Fam96b*), Myristoylated alanine rich protein kinase C substrate (*Marcks*), Serine/arginine-rich splicing factor 15 (*Srsf15*), and Zinc finger protein 740 (*Zfp740*). Of these 14 candidates, *Baz1b*, *Marcks*, *Zfp740*, and *AI506816* clones contained 3' UTR non-coding sequences and were not analyzed further.

The remaining ten candidates were next tested in a series of yeast co-transformations to eliminate false-positive candidates, confirm protein interactions, and validate the initial yeast two-hybrid screen. Candidates were first tested to ensure that the candidate protein could not independently activate (autoactivate) the reporter genes. Colonies transformed with *Zfp845*, *Fam96b*, *N4bl2l2* or *Commd4*-pGADT7 and empty-pGBKT7 appeared blue and grew well on QDO/X/A plates, while colonies transformed with *Npc2*, *Eif3a*, *Srsf2*, *Eif3m*, *Asf1b* or *Srsf15*-pGADT7 and empty-pGBKT7 did not grow as well and were white on QDO/X/A plates (Fig. 10a). Therefore, I concluded that clones encoding *Zfp845*, *Fam96b*, *N4bp2l2* and *Commd4* could independently autoactivate reporter genes and were therefore considered to be false-positive interactions and were removed from further analysis.

The remaining six candidates were next tested to confirm their positive interactions with the Pitx2c N-terminus using yeast cotransformations and selection plates as described previously. Colonies transformed with *Npc2*, *Srsf2*, *Srsf15*, *Eif3a*, *Eif3m*, or *Asf1b*-pGADT7 and *Pitx2cN*-pGBKT7 met all selection criteria supporting that they were dependent on the presence of the Pitx2c N-terminus to activate reporter gene expression (Fig. 10b).

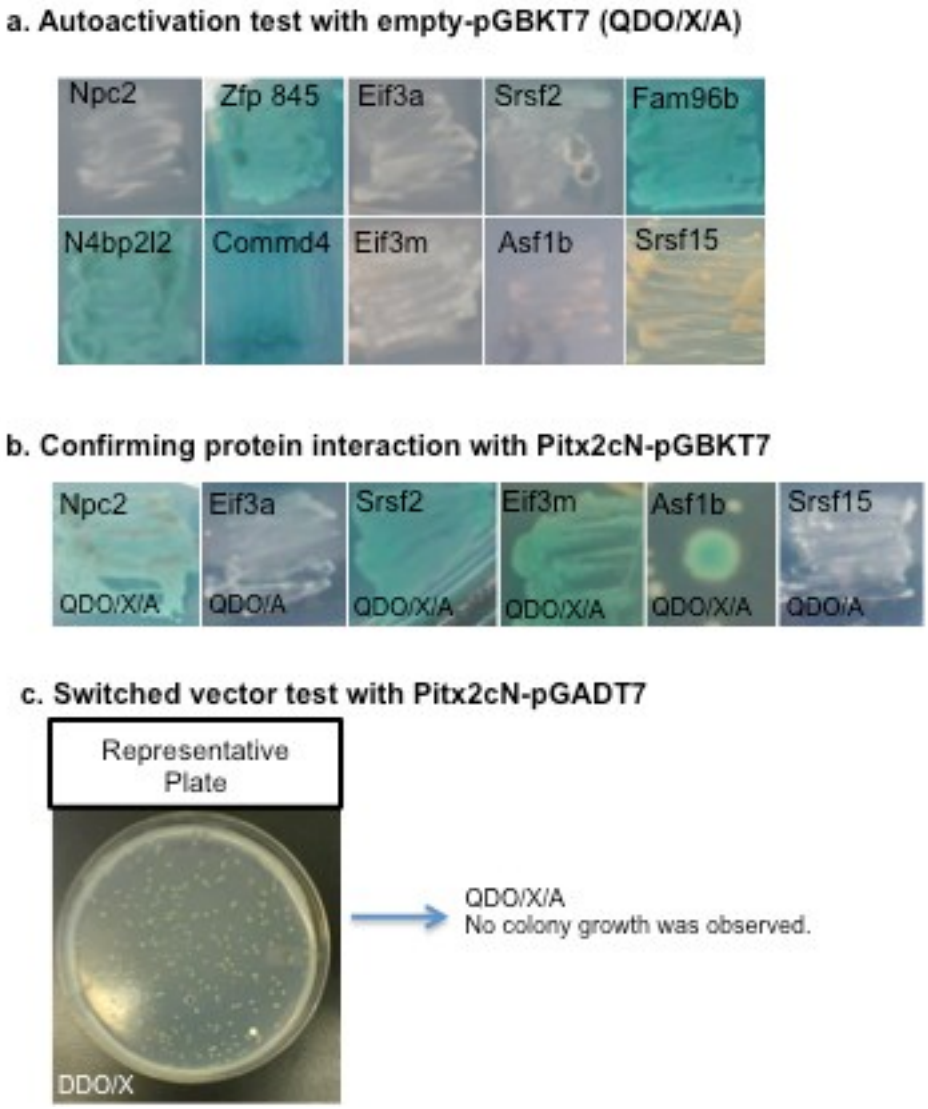

Figure 10. Prioritizing candidate protein interaction partners: (a) Y2Hgold cells were transformed with candidates in pGADT7 and empty-pGBKT7, plated on DDO/X medium and blue colonies were subsequently streaked onto QDO/X/A medium. Blue growth on QDO/X/A indicates autoactivity. (b) Y2Hgold cells were transformed with candidates in pGADT7 and Pitx2cN-pGBKT7 and plated on DDO/X medium. Blue colonies on DDO/X medium were streaked onto QDO/X/A or QDO/A medium. As1b colony growth was directly assessed on QDO/X/A. Colony growth confirms interaction of candidates with Pitx2cN. (c) Y2Hgold cells were transformed with candidates in pGBKT7 and Pitx2cN-pGADT7. Shown is a representative DDO/X plate showing white colonies only and no growth on QDO/X/A plates.

To validate positive protein interactions identified from the screen, candidates and the *Pitx2c* N-terminus were swapped from their original vectors and cloned into the opposing vector. All interactions tested showed white colonies on DDO/X plates and no colony growth on QDO/X/A plates (Fig. 10c), suggesting that the proteins do not interact with Pitx2cN. Inserts were sequenced to confirm that no mutations had been acquired during subcloning. It is unlikely that none of these candidates would interact with the Pitx2c N-terminus in the swap-vector approach. One potential explanation is that the Pitx2cN-fusion is not functional in this context. These results will be discussed in Chapter 4. Initial attempts at other approaches, including co-immunoprecipitation of tagged proteins in transfected cells, were inconclusive. Additional methods to map these interactions are discussed in Chapter 6.

3.1.4. Analyzing Pitx2cN interacting domains in candidate interaction partners

3.1.4.1. Clone alignment of anti-silencing function 1 homolog B (S. cerevisiae) (Asf1b)

Two identical clones of *Asf1b* were identified in the screen. However, depending on the reading frame (shift of two nucleotides), the protein sequence aligned to either the N-terminal region from amino acid 1 to 36 or the C-terminal region from amino acid 76 to 202 (Fig. 11b). This was due to the fact that the clones from the library were missing exon 2 and one nucleotide from the full length *Asf1b* mRNA sequence. This anomaly may have been a result of the yeast two-hybrid cDNA library creation process. Since the yeast cells used tolerate

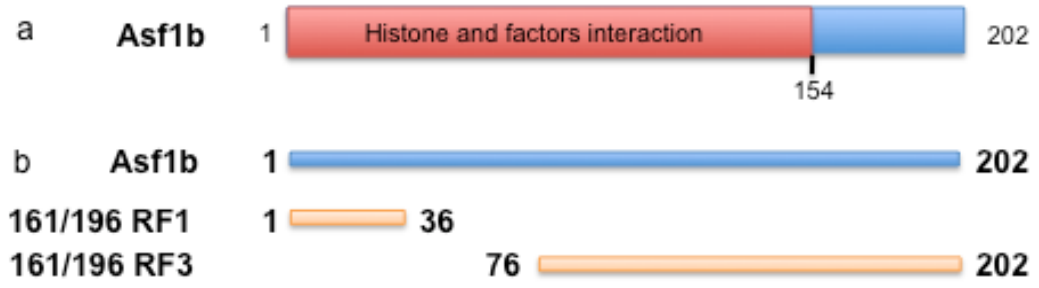

Figure 11. Alignment of Asf1b clones: (a) Schematic of domains of mouse Asf1b adapted from coordinates retrieved from Entrez Conserved Domains Database (Marchler-Bauer et al., 2003). The red region represents the domain that interacts with histones and other nucleosome assembly factors. Numbers indicate amino acid positions. (b) Protein sequence alignment of Asf1b clones with full length Asf1b (blue bar) using ClustalW2 Multiple Sequence Alignment. Schematic of sizes of Asf1b clones (orange) in two different reading frames in comparison to full length Asf1b (blue). RF indicates reading frame.

translational frameshifts, either frame or region could contain the candidate interaction domain. Colonies with both clones grew well but varied in intensity of blue colour on the high stringency selection plate, which could be due to the reading frame used by the yeast.

3.1.4.2. Clone alignment of eukaryotic translation initiation factor 3, subunits A and M (Eif3a and Eif3m)

The four clones of *Eif3a* identified by the screen aligned to the C-terminal end of Eif3a, with the shortest clone aligning to amino acid 1257 to 1344 and the longest clone aligning to 1200 to 1344 (Fig. 12b). This interaction region contains a bipartite nuclear localization signal (Saletta et al., 2010). All four clones resulted in well-grown, intense blue colonies on the high stringency selection plate. The three identical clones of *Eif3m* align to the C-terminal end of Eif3m from amino acid 15 to 374 (Fig. 13b). This interaction region contains a putative proteasome, COP9, initiation factor 3 (PCI) domain (Marchler-Bauer et al., 2003). All three clones resulted in well-grown, blue colonies with one growing better but with less blue colour on the high stringency selection plates.

3.1.4.3. Clone alignment of Niemann-Pick C type 2 (Npc2)

Seven clones encoding *Npc2* were isolated from the yeast two-hybrid screen, three of which were identical. All clones aligned to the majority of Npc2, excluding the N-terminus (Fig. 14b). The shortest of the clones aligned to amino acids 83 to 149 while the longest of the clones aligned to amino acids 26 to 149 (Fig. 14a). This candidate interaction region contains two evolutionarily conserved regions, one of unknown function and another required for cholesterol

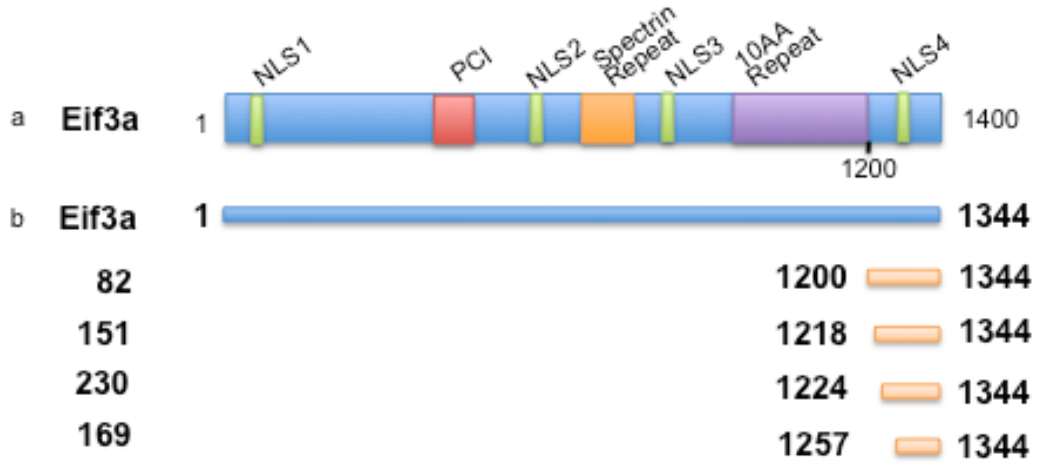

Figure 12. Alignment of Eif3a clones: (a) Schematic of domains of human Eif3a adapted from Saletta et al., 2010. The green regions represents potential bipartite nuclear localization signals (NLS). The red region represents the Proteosome, COP9, Initiation Factor 3 (PCI) domain. The orange region from represents the spectrin domain. The purple region represents a region of 10 amino acid repeats. Numbers indicate amino acid positions. (b) Protein sequence alignment of Eif3a clones with full length mouse Eif3a using Clustal W2 Multiple Sequence Alignment. Schematic of sizes of Eif3a clones (orange) in comparison to full length Eif3a (blue).

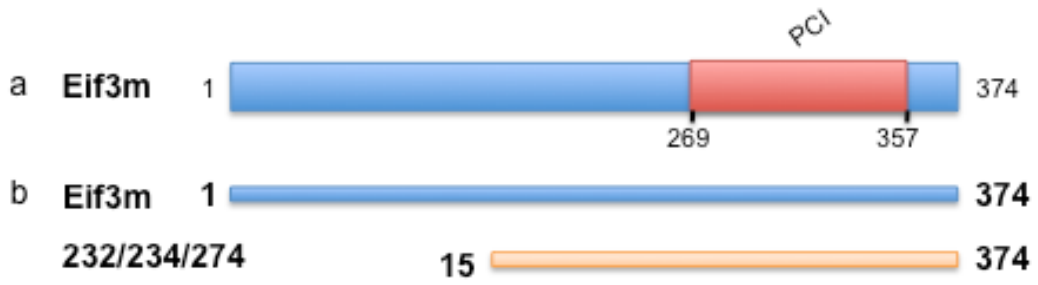

Figure 13. Alignment of Eif3m clones: (a) Schematic of domains of mouse Eif3m adapted from coordinates retrieved from Entrez Conserved Domains Database (Marchler-Bauer et al., 2003). The red region represents the Proteosome, COP9, Initiation Factor 3 (PCI) domain. Numbers indicate amino acid positions. (b) Protein sequence alignment of Eif3m clones with full length Eif3m using Clustal W2 Multiple Sequence Alignment. Schematic of sizes of Eif3m clones (orange) in comparison to full length Eif3m (blue).

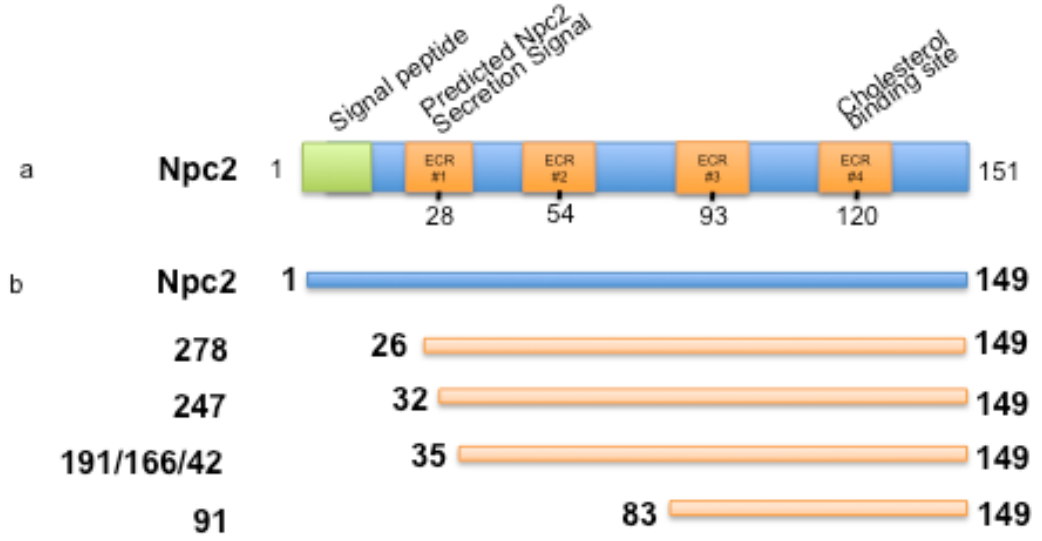

Figure 14. Alignment of Npc2 clones: (a) Schematic of domains of human Npc2 adapted from Vanier et al., 2004. The green region represents the signaling peptide portion. The orange regions represent the evolutionary conserved regions of Npc2. The first region is predicted to be a secretion signal and the last region a cholesterol binding sites. The function of the second and third region still remains to be understood. Numbers indicate amino acid positions. (b) Protein sequence alignment of Npc2 clones with full length mouse Npc2 using Clustal W2 Multiple Sequence Alignment. Schematic of sizes of Npc2 clones (orange) in comparison to full length Npc2 (blue).

binding (Vanier et al., 2004). All clones with the exception of the longest clone resulted in well-grown, intense blue colonies on the high stringency selection plate. Colonies with the longest clone were slower growing and had a fainter blue colour.

3.1.4.4. Clone alignment of serine/arginine-rich splicing factor 2 and 15 (Srsf2 and Srsf15)

Four clones encoding Srsf2 were isolated from the screen, however there were only 2 unique clones. The longest clones aligned to amino acid 133 to 221, while the shortest clones aligned to amino acid 168 to 221 at the C-terminus of Srsf2 (Fig. 15b). This candidate interaction region contains the serine-arginine rich (RS) domain (Fig. 15a) (Fu et al., 1992). Colonies of all clones varied in growth rate but were all intensely blue on the high stringency selection plate.

Two identical clones of *Srsf15* were isolated, which align to amino acids 989 to 1209 at the C-terminal end of Srsf15 (Fig. 16b). Both clones resulted in colonies that grew well and were intense blue in colour on the high stringency selection plate.

3.2. Potential protein interaction partners and Pitx2c co-expression in the chick embryo from HH stage 10 to 26

The yeast two-hybrid screen isolated Pitx2 interaction partners in the context of yeast cells, an environment very different from the embryo. For these interactions to be relevant to *Pitx2c* function *in vivo*, the candidates must be expressed in the same tissues as *Pitx2c* in the embryo. A review of the literature

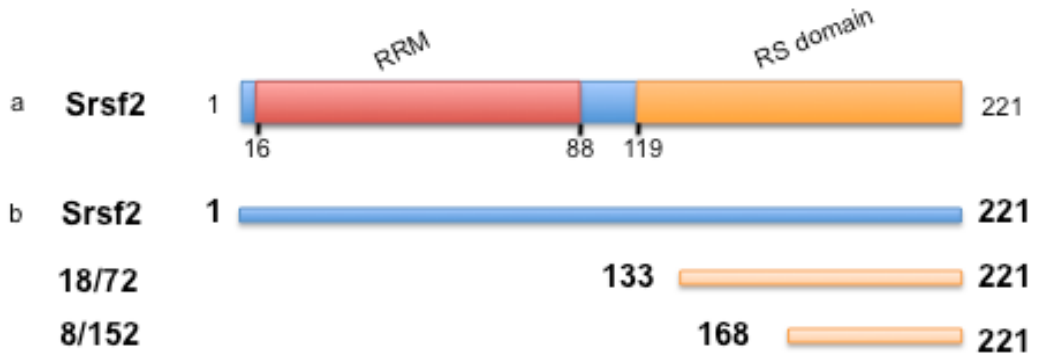

Figure 15. Alignment of Srsf2 clones: (a) Schematic of domains of Srsf2 adapted from (Meggendorfer et al., 2012). The red region represents RNA recognition motif. The orange regions represents the serine-arginine rich (RS) domain. Numbers indicate amino acid positions. (b) Protein sequences alignment of Srsf2 clones with full length Srsf2 using Clustal W2 Multiple Sequence Alignment. Schematic of sizes of Srsf2 clones (orange) in comparison to full length Srsf2 (blue).

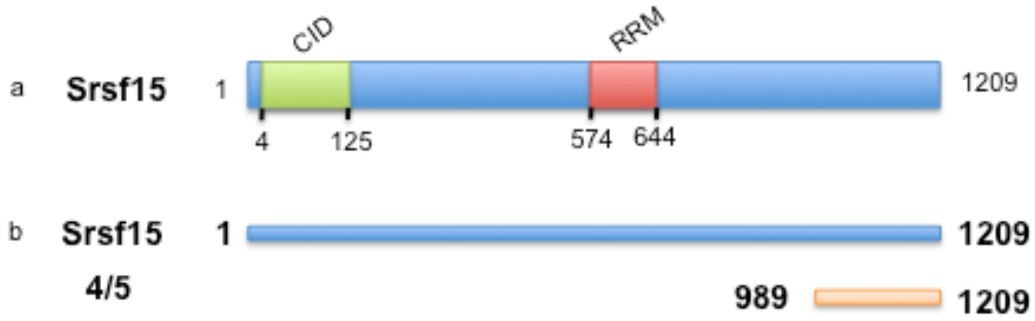

Figure 16. Alignment of Srsf15 clones: (a) Schematic of domains of mouse Srsf15 adapted from coordinates retrieved from Entrez Conserved Domains Database (Marchler-Bauer et al., 2003). The green region represents the C-terminal-domain-of-RNA-polymerase-II-interacting domain (CID). The red region represents the RNA recognizing motif (RRM). Numbers indicate amino acid positions. (b) Protein sequence alignment of Srsf15 clones with full length Srsf15 using Clustal W2 Multiple Sequence Alignment. Schematic of sizes of Srsf15 clones (orange) in comparison to full length Srsf15 (blue).

showed that only the expression of *Srsf2* had been examined in chick embryos although limited expression pattern information exists for other candidates in the mouse. As such, mRNA expression of these candidates was characterized and compared with *Pitx2c* expression in chick embryos. Briefly, *Pitx2c* is expressed symmetrically in the head mesenchyme and asymmetrically in the left lateral plate mesoderm starting at HH stage 8 until HH 10 (Ryan et al., 1998; GEISHA Database, ID O21; Fig. 17a). *Pitx2c* is symmetrically expressed in the head mesenchyme and asymmetrically expressed in the heart tube at HH stage 12 (Ryan et al., 1998; GEISHA Database, ID O21; Fig. 17b). At HH stage 14, *Pitx2c* is expressed bilaterally in the first pharyngeal arch and asymmetrically in the heart (Ryan et al., 1998; GEISHA Database, ID O21; Fig. 17c). At later stages of organogenesis (HH stage 19-25), *Pitx2c* is also expressed symmetrically in the pituitary gland, periocular mesenchyme in the eyes, somites, and mesenchyme in the limbs, and asymmetrically in the mesentery of the gut tube and the endocardium and myocardium in the heart (Furtado et al., 2011; Logan et al., 1998; Ryan et al.,1998; Fig. 17d, e).

3.2.1. mRNA expression analyses of candidate interaction partners

Using the NCBI database, chick homologs of the mouse candidate protein interaction partners were identified for *Eif3a, Eif3m, Npc2, Srsf2, Srsf15* and *Asf1a* in the chick genome. However, the *Asf1b* chick homolog was not identified in the chick genome. Therefore, *Asf1b* mRNA expression was not analyzed in the chick embryo. Chick homologs were cloned and synthesized into antisense riboprobes to analyze expression by whole mount *in situ* hybridization.

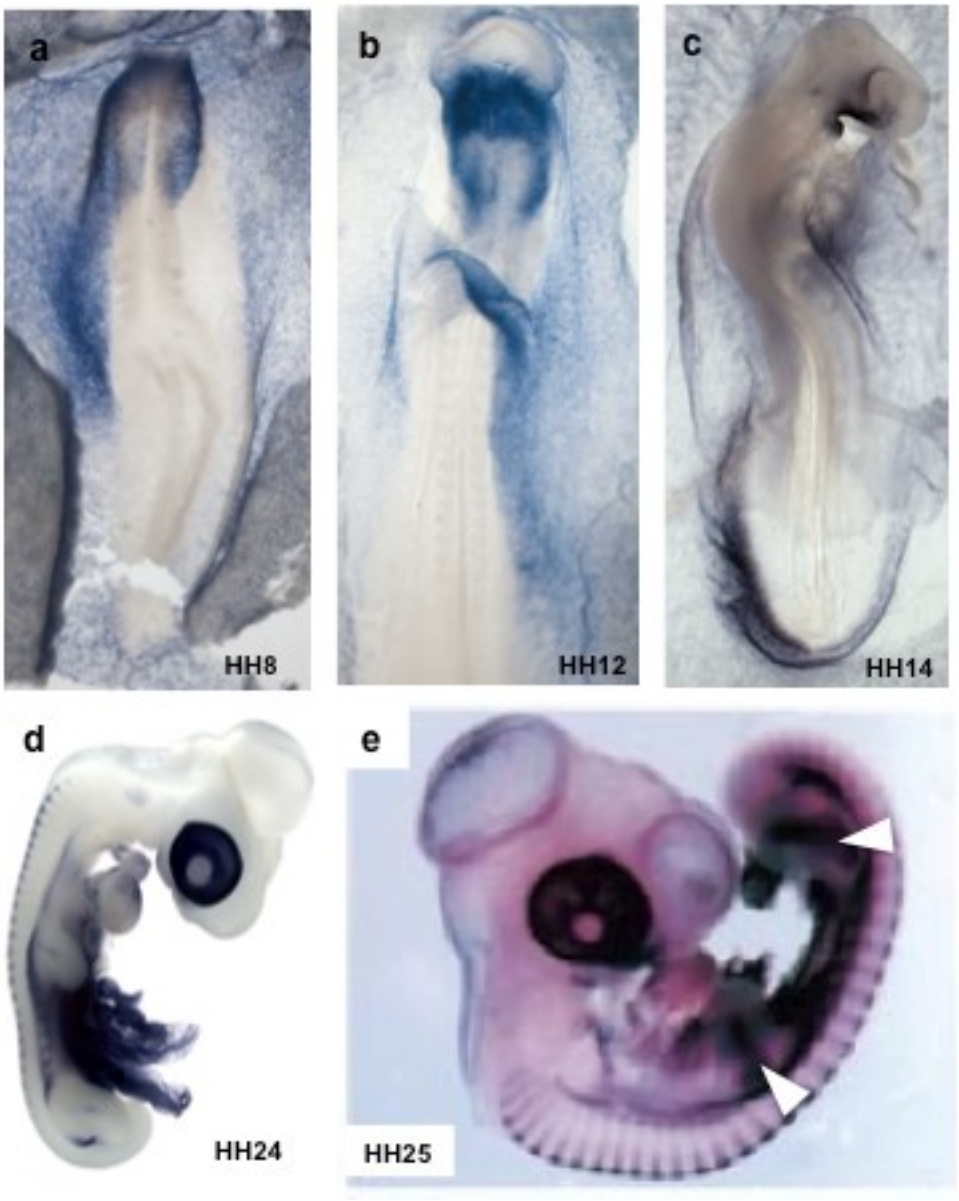

Figure 17. *Pitx2* expression from HH stage 8 to 25. (a) Dorsal view of a HH stage 8 embryo showing *Pitx2* expression symmetrically in the head mesenchyme and asymmetrically in the left lateral plate mesoderm. (b) Ventral view of the HH stage 12 embryo showing symmetric *Pitx2* expression in the head mesenchyme and asymmetric *Pitx2* expression in the looping heart tube. (c) Dorsal view of an embryo at HH stage 14 indicating expression in the face mesenchyme, heart. Dorsal views of embryos showing *Pitx2* expression at HH stage 24 (d) and HH stage 25 (e). White arrowheads in e indicate expression of *Pitx2* in the hind limb buds. Images taken from Ryan et al., 1998 (e) and GEISHA Database, University of Arizona ,Tucson, ID: O21 (a-d).

3.2.2.1. Expression of eukaryotic translation initiation factor 3, subunit A (Eif3a)

At HH stage 10 and 12 in the chick, *Eif3a* was expressed almost ubiquitously in the embryo including in the endocardium of the heart tube or looping heart tube as shown by sections (Fig. 18a, b, c). However, *Eif3a* is not expressed in the lateral plate mesoderm (Fig. 18a, b). By HH stage 18, *Eif3a* was ubiquitously expressed throughout the whole embryo (Fig. 18d, e), including the optic cup and lens of the eyes (Fig. 18e). In the heart, *Eif3a* expression is enriched in the endocardium (Fig. 18e'). At HH stage 26, expression of *Eif3a* remained ubiquitously expressed at low levels in the whole embryo (Fig. 18f, g) including the heart and limb buds (Fig. 18g, h) and became enriched in the periocular mesenchyme of the eyes (Fig. 18g').

3.2.2.2. Expression of eukaryotic translation initiation factor 3, subunit M (Eif3m)

Like *Eif3a*, *Eif3m* expression was absent in the lateral plate mesoderm but was otherwise expressed almost ubiquitously at HH stage 10 and 12 in the chick (Fig. 19a, b). Sections at these stages confirm *Eif3m* expression in the head mesenchyme and the endocardium of the looping heart tube (Fig. 19c). By HH stage 16, *Eif3m* was ubiquitously expressed (Fig. 19d, e). Sections through the heart show *Eif3m* expression in the endocardium (Fig. 19e'). At HH stage 22 and 26, *Eif3m* was ubiquitously expressed at low levels (Fig. 19f, g, i), including in periocular mesenchyme in the eyes (Fig. 19g), in the endocardium of the heart (Fig. 19g') and the mesenchyme and ectoderm of the limb buds (Fig. 19h).

3.2.2.3. Expression of Niemann-Pick C type 2 (Npc2)

In the chick embryo, *Npc2* was expressed in the area opaca of the extraembryonic tissue during early stages of embryogenesis (HH stage 10 and 12; Fig. 20a, b). The onset of symmetrical *Npc2* expression in the looping heart tube is observed between HH stage 10 and 12 (Fig. 20a', b'). Expression of *Npc2* was enriched in the heart tube at stage 16 (Fig. 20c, d) and was also present in the aortic arches, the carotid arteries, and the dorsal aorta (Fig. 20c). *Npc2* expression in these blood vessels continued into HH stage 26. Expression of *Npc2* is also observed in the blood vessels of the extraembryonic tissue (Indicated by black arrows in Fig. 20d). Sections of HH stage 18 embryos showed enriched *Npc2* expression in the head mesenchyme (Fig. 20f) and the endocardium of the heart (Fig. 20g). At stage 24-26, *Npc2* was also broadly expressed throughout the whole embryo (Fig. 20h, j). Sections through these embryos show *Npc2* expression in the head mesenchyme, the endocardium of the heart, the trabeculae of the heart (Fig. 20i), and the mesenchyme of the limbs buds. At HH stage 24, *Npc2* is expressed in the mesenchyme of the hindlimb bud (Fig. 20h, h'), and becomes more restricted to the condensing mesenchyme of the digits and long bones at HH stage 26 (Fig. 20j, j').

3.2.2.4. Expression of serine/arginine-rich splicing factor 2 (Srsf2)

Srsf2 is the only candidate interaction partner that has been previously characterized in the chick embryo. *Srsf2* is expressed symmetrically in the surface ectoderm, lateral plate mesoderm, and intermediate mesoderm at HH stage 9 (GEISHA Database, ID: G53) (Fig. 21a and 21a'). At HH stage 16, *Srsf2*

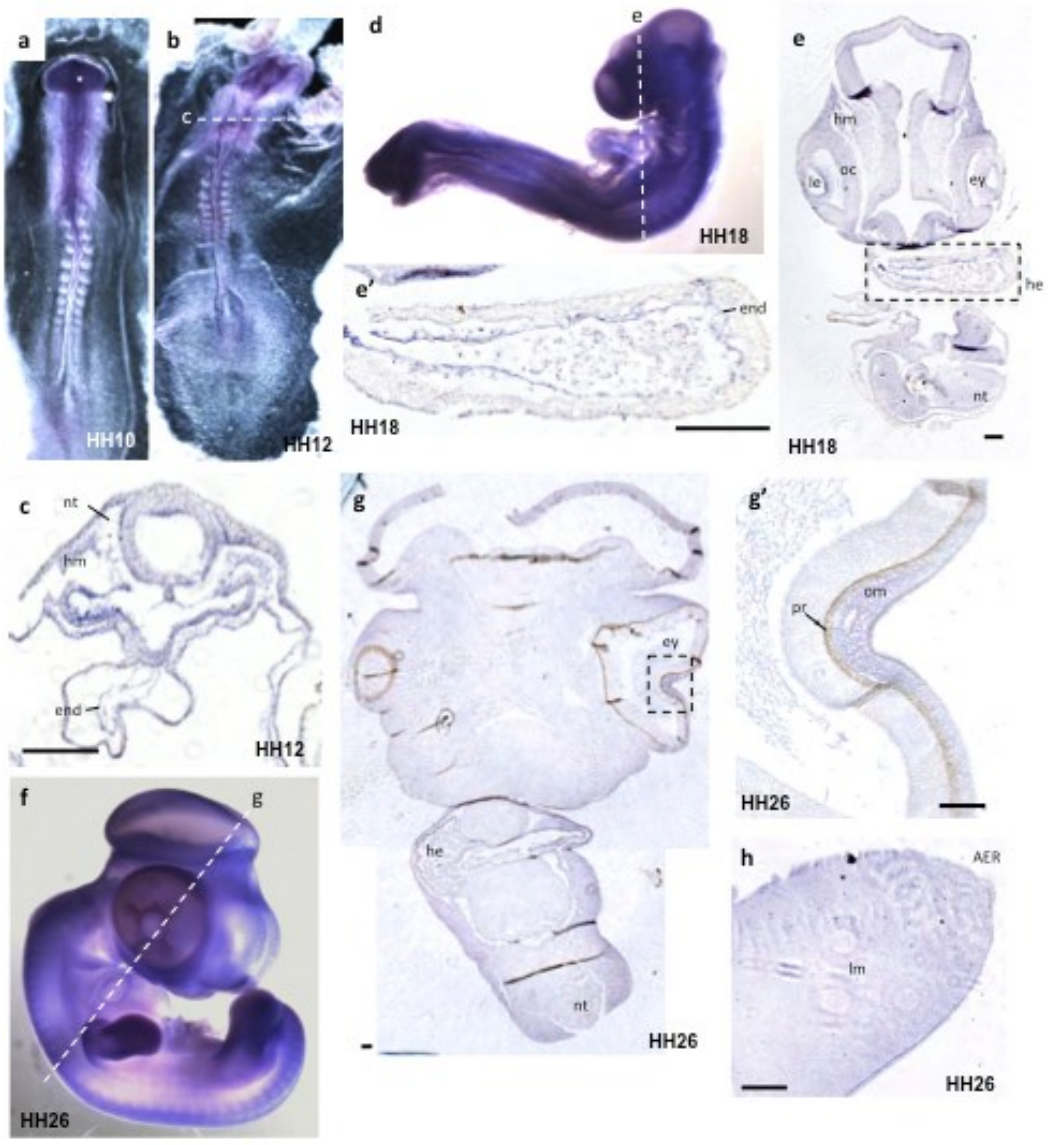
a
HH10
b
c
HH12
d
e
HH18
e'
end
HH18
e
hm
oc
ey
le
he
nt
HH18
c
nt
hm
end
HH12
g
ey
he
nt
HH26
g'
om
pr
HH26
f
g
HH26
h
AER
lm
HH26

Figure 18. **Expression of *Eif3a* from HH stage 10 to 26.** Ventral view of HH stage 10 (a) and dorsal view of HH stage 12 (b) embryos showing expression of *Eif3a*. (c) Transverse section at the level of the dashed line in b showing expression in the head mesenchyme and endocardium of the heart. (d) Lateral view of HH stage 18 embryos. (e) Transverse section of HH stage 18 embryo as indicated by the dashed line in d. (e') Magnified view of the heart is shown at HH stage 18 as indicated by the dashed box in e showing expression of *Eif3a* in the endocardium of the heart. (f) Lateral view of HH stage 26 embryo. (g) Transverse section of HH stage 26 embryo as indicated by the dashed lines in f. Magnified views of the eye (g'), as indicated by the dashed box in g, and the limb bud (h) at HH stage 26. Asterisks indicate trapped antisense riboprobe. All scale bars represent 0.1mm. Abbreviations: AER, apical ectodermal ridge; end, endocardium; ey, eyes; he, heart; hm, head mesenchyme; le, lens; lm, limb mesenchyme; ne, neural ectoderm; nt, neural tube; oc, optic cup; om, periocular mesenchyme; pr, pigmented layer of the retina.

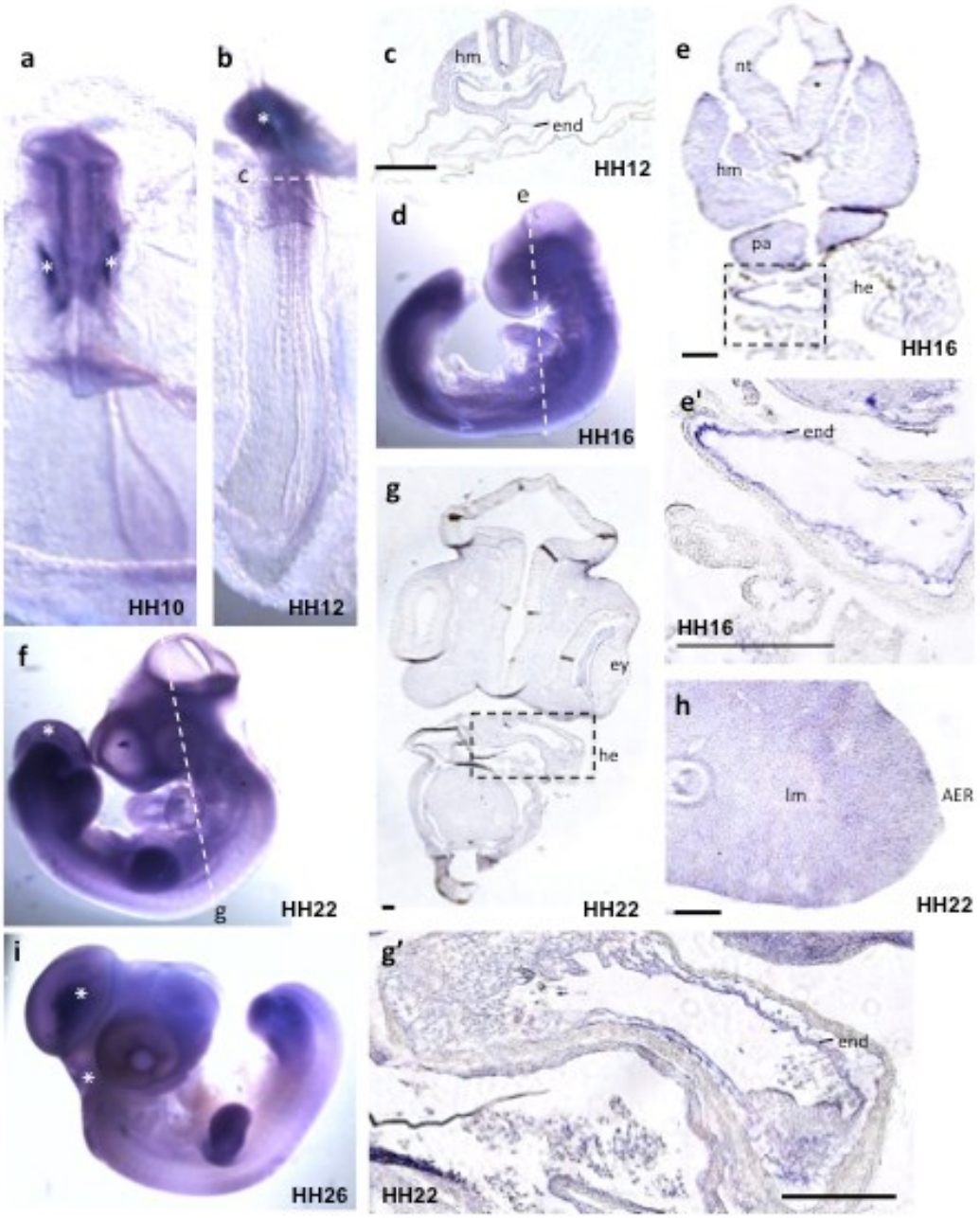
a
HH10
b
c
HH12
c
hm
end
HH12
d
e
HH16
e
nt
hm
pa
he
HH16
e'
end
HH16
f
g
HH22
g
ey
he
HH22
h
lm
AER
HH22
i
HH26
g'
end
HH22

Figure 19. **Expression of *Eif3m* from HH stage 10 to 26.** Ventral views of HH stage 10 (a) and HH stage 12 (b) embryos showing expression of *Eif3m*. (c) Transverse section at the level of the dashed line in b showing expression at the head mesenchyme and endocardium of the heart. (d) Lateral view of HH stage 16 embryo showing expression of *Eif3m*. (e) Transverse section of HH stage 16 embryo as indicated by the dashed lines in d. (e') Magnified view of the heart is shown at HH stage 16 indicating expression in the endocardium. (f) Lateral view of HH stage 22 embryo showing expression of *Eif3m*. (g) Transverse section of an HH stage 22 embryo as indicated by the dashed lines in f. Magnified views of the heart (g') and limb bud (h) at HH stage 22. (i) Lateral view of a HH stage 26 embryo. White asterisks indicate trapped antisense riboprobe. All scales represent 0.1mm. Abbreviations: AER, apical ectodermal ridge; end, endocardium; ey, eyes; he, heart; hm, head mesenchyme; lm, limb mesenchyme; nt, neural tube; pa, pharyngeal arch.

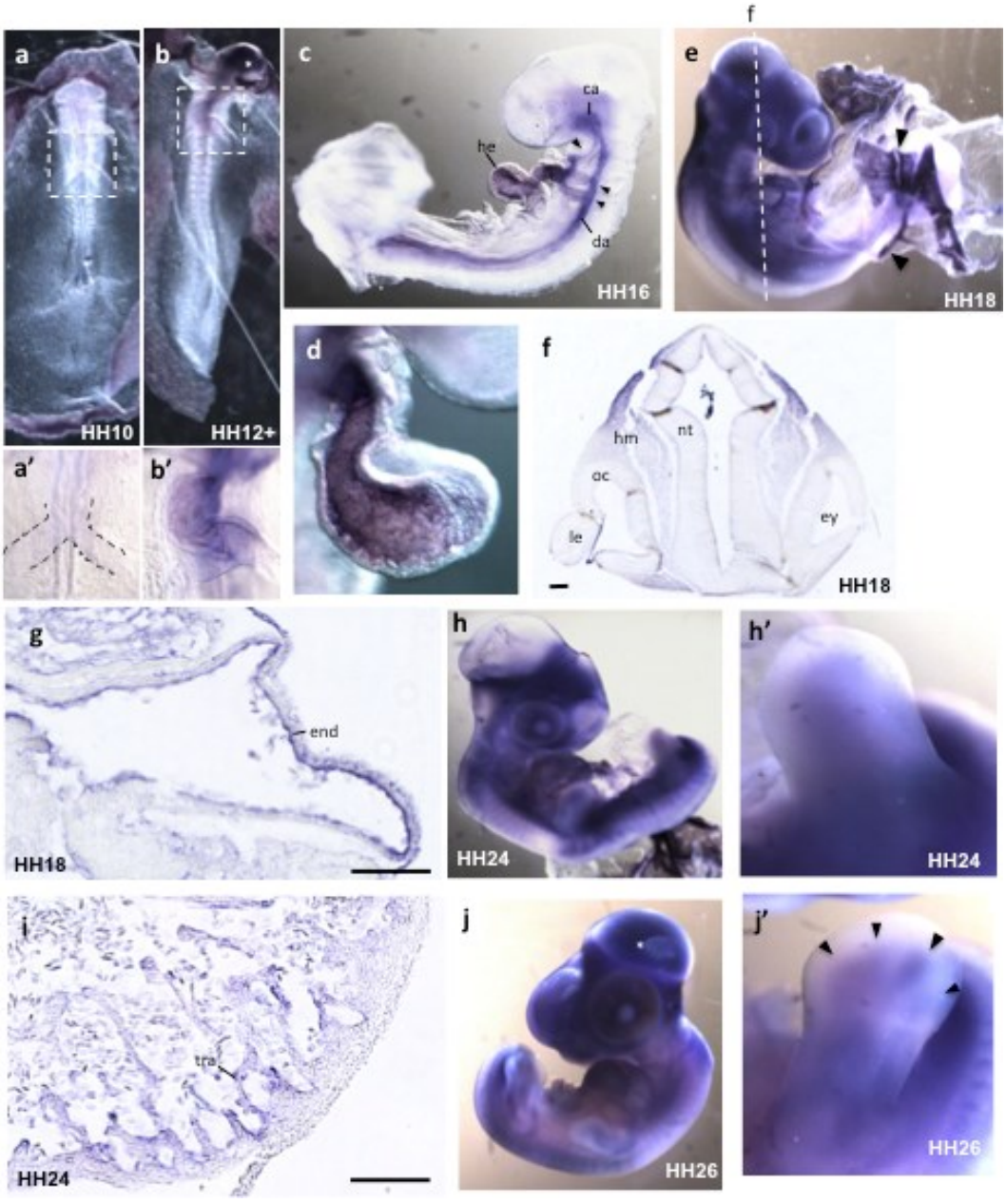
a
HH10
b
HH12+
a'
b'
c
ca
he
da
HH16
d
f
e
HH18
f
hm
nt
oc
ey
le
HH18
g
end
HH18
h
HH24
h'
HH24
i
tra
HH24
j
HH26
j'
HH26

Figure 20. Expression of *Npc2* from HH stage 10 to 26. Ventral views of HH stage 10 (a) and HH stage 12 (b) embryos showing expression of *Npc2.* Lateral views showing expression of *Npc2* at HH stage 16 (c) and HH stage 18 (e). Arrows in c indicate the aortic arches. Arrows in d indicate extraembryonic vessels and tissue. Magnified view of the heart at HH stage 10 (a'), HH stage 12 (b'), and HH stage 16 (d). Dotted lines in a' outline the heart tube. (f) Transverse section of HH stage 18 embryo as indicated by the dashed lines in e. (g) Magnified view of the and heart at HH stage 18 shows expression in the endocardium. (h) Lateral view of HH stage 24 embryo showing *Npc2* expression. (h') Magnified view of a whole mount hindlimb. (i) Transverse section of the heart at HH stage 24 as showing expression in the trabeculae. (j) Magnified view of a transverse section through the eyes. (k) Lateral view of HH stage 26 embryo showing *Npc2* expression. (j') Magnified view of the whole mount hindlimb at HH stage 26. Arrows in j' indicate expression of *Npc2* in the condensing mesenchyme of the digit and long bones. Asterisks indicate trapped antisense riboprobe. All scales represent 0.1mm. Abbreviations: AER, ectodermal ridge; ca, carotid artery; da, dorsal aorta; end, endocardium; ey, eyes; he, heart; hm, head mesenchyme; le, lens; nt, neural tube; oc, optic cup; tra, trabeculae

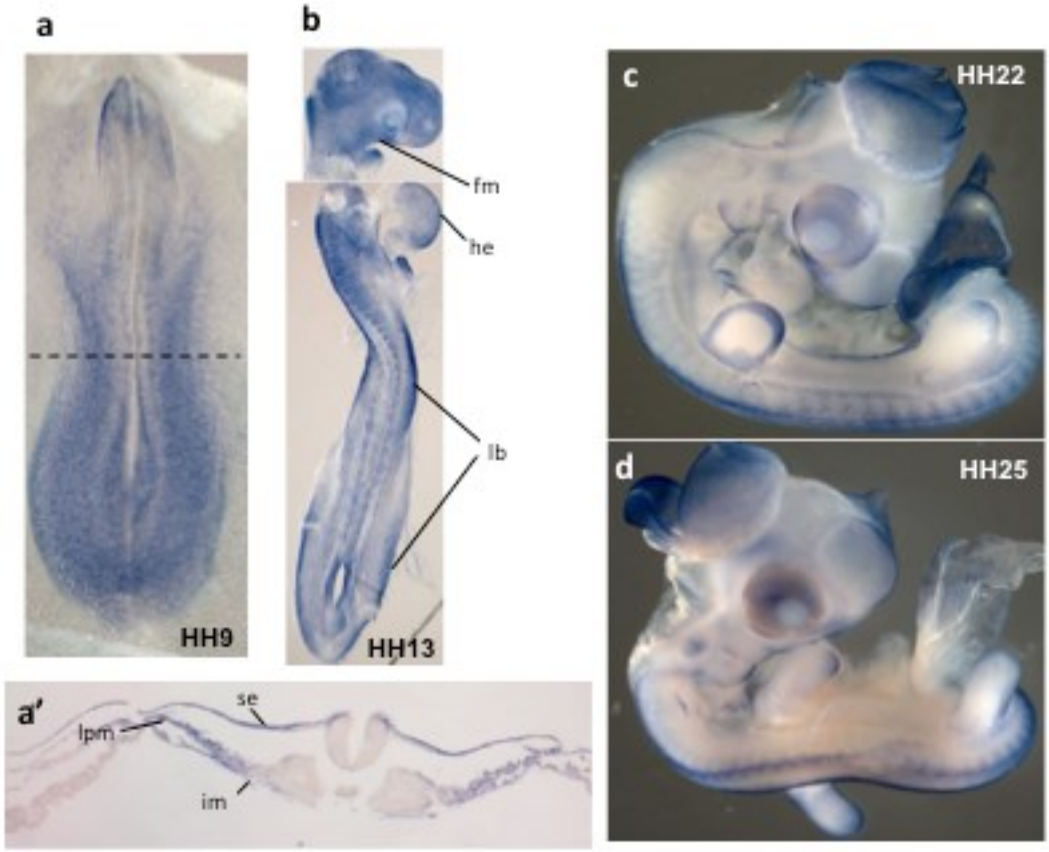

Figure 21. **Expression of *Srsf2* from HH stage 9 to 25.** (a) Ventral view of a HH stage 9 embryo. Transverse section (a') taken from the position indicated at the level of the dashed line shows expression in the surface ectoderm, lateral plate mesoderm and intermediate mesoderm. (b) Dorsal view of a HH stage 13 embryo showing expression in the face mesenchyme, heart, eyes, somites, and limb buds. Lateral views of HH stage 22 (c) and HH stage 25 (d) embryos showing *Srsf2* expression in the eyes, pharyngeal arch and clefts, heart, somites and limb. Abbreviations: fm, face mesenchyme; he, heart; im; intermediate mesoderm; lb, limb bud; lpm, lateral plate mesoderm; se, surface ectoderm. Images taken from GEISHA ISH Analysis, ID: G53.

expression is observed in the face mesenchyme, somites, limb buds, and heart (GEISHA Database, ID: G53; Fig. 21b). At HH stage 22-24, shows continued *Srsf2* is expressed in the eyes, limb buds, pharyngeal arches and somites (GEISHA Database, ID: G53) (Fig. 21c, d). Based on the whole mount embryo view, it appears that *Srsf2* is expressed in the ectoderm of the limb buds.

3.2.2.5. Expression of serine/arginine-rich splicing factor 15 (Srsf15)

Unlike *Srsf2*, *Srsf15* expression was not observed at early stages of embryogenesis (HH stage 12; Fig. 22a). At HH stage 16, *Srsf15* appeared to be weakly expressed throughout the embryo (Fig. 22b). At HH stage 18, *Srsf15* was expressed ubiquitously (Fig. 22c), including in the optic cup and lens in the eyes (Fig. 22d), in the head mesenchyme (Fig. 22d), and the endocardium of the heart (Fig. 22d'). At HH stage 24-26, *Srsf15* expression became increasingly restricted (Fig. 22e, h). In the limbs, *Srsf15* expression was enriched in the mesenchyme (Fig. 22g). In the heart, *Srsf15* continued to be expressed in the endocardium (Fig. 22f). While hindlimb expression of Srsf15 appeared to be ubiquitous in the mesenchyme at HH stage 24 (Fig. 22g), at HH stage 26 hindlimb expression of *Srsf15* was restricted to the condensing mesenchyme of the digits and long bones (Fig. 22h').

3.2.2.6. Summary of overlapping expression between candidates and Pitx2c

A comparison between the expression patterns of the candidate interaction partners and *Pitx2* showed that only *Srsf2* and *Pitx2c* overlapped in the lateral

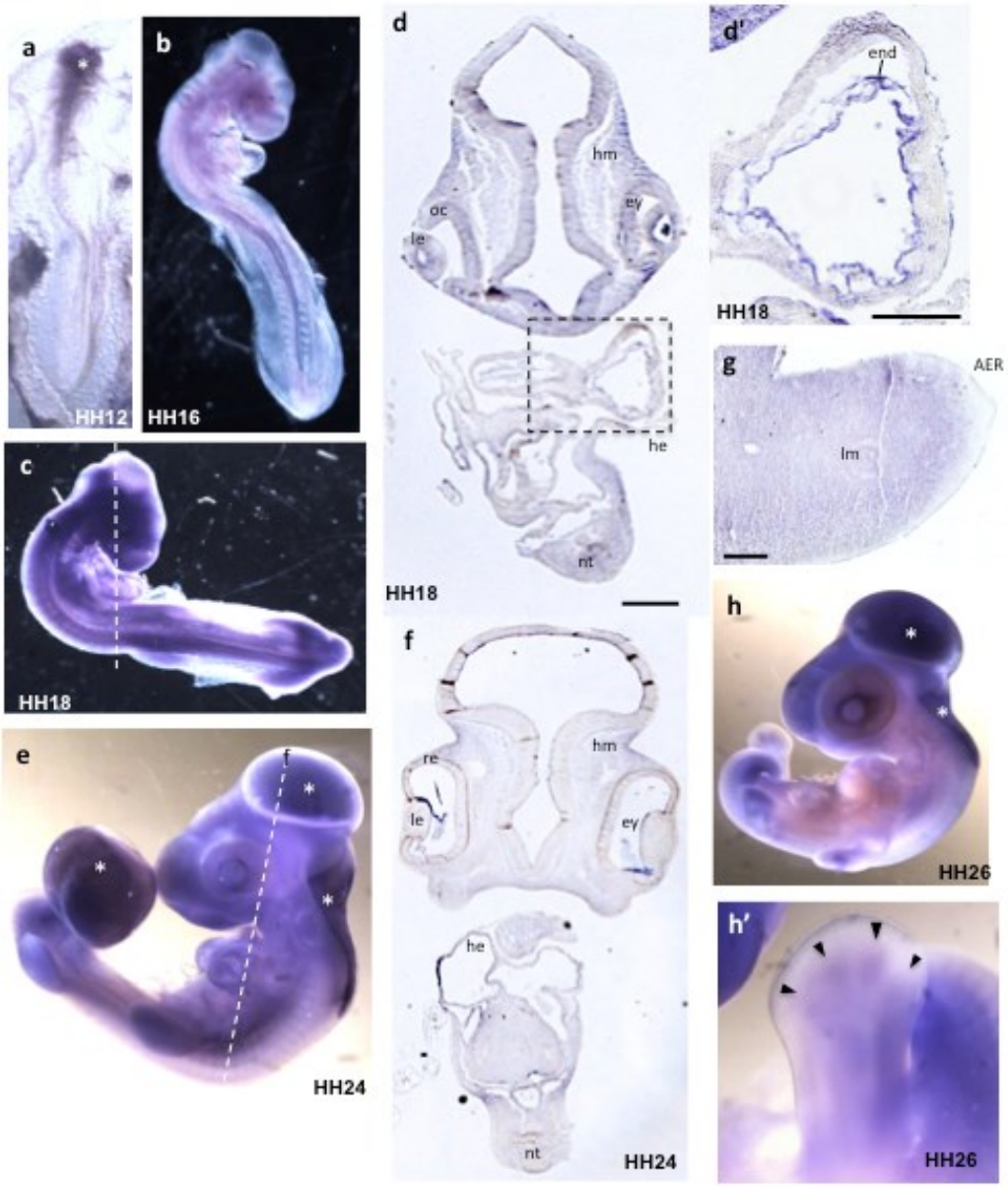
a
HH12
b
HH16
c
HH18
d
hm
ey
oc
le
he
nt
HH18
d'
end
HH18
g
AER
lm
h
HH26
h'
HH26
e
f
HH24
f
hm
re
le
ey
he
nt
HH24

Figure 22. **Expression of *Srsf15* from HH stage 12 to 26.** (a) Ventral view of a HH stage 12 embryo showing *Srsf15* expression. (b) Dorsal view of a HH stage 16 embryo showing *Srsf15* expression. (c) Lateral view of a HH stage 18 embryo. (d) Transverse section of HH stage 18 embryo as indicated by the dashed line in c. (d') Magnified view of the heart as indicated by the dashed box in d showing expression of *Srsf15* in the endocardium. (e) Lateral view of a HH stage 24 embryo. (f) Transverse section of HH stage 24 embryo as indicated by the dashed lines in e. (g) Magnified view of the sectioned limb at HH stage 24 showing expression in the mesenchyme. (h) Lateral view of a HH stage 26 embryo. (h') Magnified view of the hind limb at HH stage 26 with arrows indicating *Srsf15* expression in the condensing mesenchyme of digits and long bones. Asterisks indicate trapped antisense riboprobe. All scales represent 0.1mm. Abbreviations: AER, apical ectodermal ridge; end, endocardium; ey, eyes; he, heart; hm, head mesenchyme; le, lens; lm, limb mesenchyme; nt, neural tube; oc, optic cup; re, retina.

plate mesoderm as early as HH stage 9. Only *Npc2*, *Eif3a* and *Eif3m* were expressed with *Pitx2c* in the looping heart tube at HH stage 12 although they were expressed symmetrically, in contrast to *Pitx2c*, which is expressed asymmetrically. As the heart develops further after HH stage 16, all candidates overlapped with *Pitx2c's* expression in the endocardium of the heart. At later stages of organ morphogenesis (after HH stage 16), only *Eif3a* and *Eif3m* overlapped with *Pitx2c* in expression in the periocular mesenchyme of the eyes, and all candidates except *Srsf2* overlapped with *Pitx2c* expression in the mesenchyme of the limb buds. A summary of expression pattern comparison between candidate interaction partners and *Pitx2c* is provided in Table 5.

Table 5. Summary of mRNA expression patterns of Pitx2 and candidate protein interaction partners

	HH10		HH12	After HH16		
	Lateral plate mesoderm	Heart tube	Looping heart tube	Heart	Eyes	Limb mesenchyme
Pitx2	+	+	+	+	+	+
Npc2	-	-	+	+	-	+
Eif3a	-	-	+	+	+	+
Eif3m	-	-	+	+	+	+
Srsf2	(+)	U	U	(+)	(-)	(-)
Srsf15	-	-	-	+	-	+

* - indicates absent expression, + indicates positive expression, ( ) indicates expression based on previously described data, U indicates unknown

Chapter 4. Discussion

Asymmetric organogenesis is a complex event that requires a combination of cell behaviours including proliferation, differentiation and migration, which are differentially regulated on the left and right side. The asymmetric expression of *Pitx2c* on the left side of organ primordia is essential for asymmetric formation of these organs, including the heart and gut (Campione et al., 1999; Logan et al., 1998; Piedra et al., 1998; Ryan et al., 1998; St. Amand et al., 1998; Yoshioka et al., 1998). It has been shown that Pitx2c orchestrates differential cell behaviours on the left and right side of the heart and gut (Ai et al., 2006; Kioussi et al., 2002; Kurpios et al., 2008; Ma et al., 2013; Welsh et al., 2013; Zhou et al., 2007). Although a better understanding of how Pitx2c regulates gut looping has been published very recently (Welsh et al., 2013), the molecular mechanisms of how Pitx2c orchestrates asymmetric organ morphogenesis in other organs still requires much research. Additionally, an interaction at the N-terminus of Pitx2c is important for its function in left-right patterning (Simard et al., 2009). My thesis research identified proteins that may interact with the Pitx2c N-terminus, potentially regulating processes such as cholesterol transport, translational regulation, mRNA processing in addition to transcriptional regulation.

4.1. Identification of six potential protein interaction partners of the Pitx2c N-terminus

I first identified 69 clones which represent 32 unique potential protein interaction partners of the Pitx2c N-terminus using a yeast two-hybrid screen with the mouse Pitx2c N-terminus as bait and mouse E11 cDNA two-hybrid library as

prey. Fourteen candidates were isolated at least twice from the screen and these were selected for further analysis. After eliminating non-coding sequences and false positive interactions and confirming protein interactions, six potential protein interactors of the Pitx2c N-terminus remained: Anti-silencing factor 1b (*S. Cerevisiae*) (Asf1b), Eukaryotic translation initiation factor 3 subunit a (Eif3a), Eukaryotic translation initiation factor 3 subunit m (Eif3m), Niemann Pick C type 2 (Npc2), Serine-arginine rich splicing factor 2 (Srsf2), and Serine-arginine rich splicing factor 15 (Srsf15).

4.2. Validating the screen: Switch vector issue

To validate protein interactions, I applied the switch vector approach. Candidates were swapped into the bait vector while Pitx2c was swapped into the library vector. Unfortunately, none of the candidate interactions were validated. Since this result was unexpected, I examined possible problems with the switch vector approach. Sequence analysis demonstrated that all inserts were in-frame with the fusion protein and no mutations were introduced during cloning. This leaves the possibility that there is an incompatibility of fusion proteins. The switched candidate bait vectors encode a candidate-gal4 DNA binding domain fusion protein and the switched Pitx2cN prey vector encodes a fusion Pitx2cN-gal4 activation domain protein. It is possible that the new arrangement and change in proximity between the candidate or Pitx2cN with the relative GAL4 transcription factor domains interfered with the function of the GAL4 transcription factor and thus inhibited the activation of reporter genes. The prey protein may have prevented DNA binding or Pitx2cN may have prevented

activation of reporter genes. Since no interactions were detected, I predict that the problem is most likely due to the Pitx2cN-activation domain fusion protein. Other methods that can be performed to validate the interactions isolated from the screen are described in Chapter 6.

4.3. Limitations of the yeast two-hybrid screen to identify proteins relevant to left-right patterning

A key feature of the yeast two-hybrid screen is that it is unbiased and, since a whole embryo cDNA library was used, it was also a broad search approach. Since Pitx2c is also involved in symmetric organ development, this screening approach does not differentiate between candidates that are required for symmetric or asymmetric organ development. Therefore, it is possible that these candidates may be important for organogenesis but dispensable in asymmetric organ morphogenesis.

Since the youngest library that was available was mouse E11, some earlier events of asymmetric organogenesis may not have been represented including the initial looping of the heart. However other events of asymmetric organogenesis including gut looping occur during this stage (Burn and Hill, 2009). The limited availability of commercial yeast two-hybrid cDNA libraries makes it difficult to overcome this limitation. One solution would be to make a custom library at an earlier stage such as E9 when the heart is looping (Abu-Issa and Kirby, 2007) or E8 when Pitx2c is expressed asymmetrically in the LPM (Campione et al., 1999). Candidates could also be compared between libraries of different species to determine if there are candidates that are evolutionarily conserved.

Another limitation of the yeast two-hybrid screen is the possibility of false negative candidates. These candidates could interact *in vivo*, however, in the context of a yeast cell, they may not be revealed. A solution to this would be to use a different method of screening for protein interactions. Some other methods that could be used include GST-pull down or tandem affinity purification with embryo extracts to isolate protein interaction partners, followed by mass spectrometry to identify proteins.

4.4. Comparison of Pitx2c and candidate expression to potential function of interaction

Expression patterns of the candidate interaction partners were analyzed to determine if they overlap in expression with *Pitx2c* during embryogenesis. Overlapping in expression between *Pitx2c* and candidates is essential to support a biologically relevant role *in vivo*. *Srsf2* and *Pitx2c* are coexpressed in the left LPM and after HH stage 14. Additionally, I have shown that *Npc2*, *Srsf15*, *Eif3a*, and *Eif3m* are coexpressed with *Pitx2c* after HH stage 12 in the chick embryo using whole mount *in situ* hybridization. These results support a potential functional role during embryogenesis for the protein-protein interactions identified by the yeast two-hybrid screen. The mRNA expression patterns that I characterized for *Npc2*, *Srsf15*, *Eif3a* and *Eif3m* between HH 10 and 26 in the chick have not been previously described. Below I discuss which of these potential interactions are most likely to be relevant to *Pitx2c's* role in left-right patterning.

4.4.1. Anti-silencing function 1, homolog B (Asf1b)

Asf1b is a histone H3-H4 chaperone required for nucleosome assembly and disassembly (Henikoff, 2008; Munakata et al., 2000). The N-terminal region of Asf1b is known to bind to histones and other nucleosome assembly factors (Loyola and Almouzni, 2004) while the function of the C-terminus is unknown (Fig. 11a). Based on the identification of a full length *Asf1b* clone from the screen and functions of Asf1b domains, the Pitx2c N-terminus could bind to the N- or C-terminal domain of Asf1b.

The *Asf1b* homolog was not identified in the chick genome. Therefore, I was unable to characterize its expression in the chick embryo. In the mouse, *Asf1b* is expressed in the maxillary process, first and second pharyngeal arches and limb buds at E10.5 (EMAGE ISH analysis; ID 2219). This expression becomes more enriched and also appears in the thymus and liver at E11 (EMAGE ISH analysis; ID 2218). *Pitx2c* is also expressed in these regions, with the exception of the thymus. Although Asf1b overlaps in expression with Pitx2c, it is not expressed in asymmetrically formed organs; therefore, it is unlikely to have a role in left-right asymmetry. Asf1b knockout models do not exist, thus its role in development is unclear.

Asf1-mediated nucleosome disassembly and -interaction with transcription initiation machinery is required for the transcriptional activation of genes (Adkins et al., 2004; Umehara and Horikoshi, 2003). Given that Pitx2c is a transcription factor, we could postulate that the potential interaction between Pitx2c and Asf1b

may be a necessary step in transcriptional activation of Pitx2c target genes in tissues where they are co-expressed.

4.4.2. Eukaryotic initiation factor 3, subunit A and M (Eif3a and Eif3m)

Eif3a and Eif3m are components of the eukaryotic translation initiation factor 3 complex (Damoc et al., 2007). The shortest isolated clone of *Eif3a* contains a bipartite nuclear localization signal (NLS) (Saletta et al., 2010). Given that Pitx2c is mainly a nuclear protein, this NLS may be related to the function of the potential Pitx2c-Eif3a interaction. The putative interacting region in Eif3m contains a predicted 26S proteasome-COP9 signalosome-eukaryotic translation initiation factor 3 (PCI) domain from amino acid 269 to 357 domain. PCI domains allow protein–protein interactions between subunits of multi-protein complexes (Pick et al., 2009). Given that Pitx2c does not contain a PCI domain, there is most likely another domain in this region facilitating the potential Pitx2c-Eif3m interaction.

While Eif3a is a core component in the Eif3 complex, Eif3m can be replaced by other Eif3 subunits (Zhou et al., 2005). Since the expression of *Eif3m* is the same as *Eif3a*, Eif3m is most likely the accessory subunit to the core Eif3 complex during these stages of development in the chick. This is further supported by evidence in the mouse demonstrating that Eif3m is required in the Eif3 complex during embryogenesis (Zeng et al., 2013). *Eif3a* and *Eif3m* mRNA expression was ubiquitous in the chick embryo and was only enriched in certain tissues at later stages of organogenesis. In the mouse, western blot analysis showed that Eif3a was expressed in multiple asymmetrically formed organs and

expression was higher in embryonic tissues compared to adult tissues for almost all organs (Liu et al., 2007; Pincheira et al., 2001). *In vitro*, decreased Eif3a expression led to increased differentiation of intestinal cells (Liu et al., 2007). Examination of *Eif3a* mutant mice to identify specific effects of Eif3a on laterality and organ development is yet to be reported. The *Eif3m* mutant mice were recently characterized. *Eif3m* null and hypomorph mice die by E9.5 and exhibit severe growth retardation (Zeng et al., 2013). *Eif3m* heterozygous mice were viable and fertile, however there was a proliferation defect resulting in significantly reduced organ sizes (Zeng et al., 2013). These data provide evidence suggesting a pivotal role for the Eif3 complex and translational regulation during organogenesis.

Eif3a is known to interact with crucial components of translation including other eukaryotic translation initiation factors, ribosomal subunits, other receptors, and cytoskeletal components, while no evidence has been reported of interactions with any transcription factors (Kouba et al., 2012; Lin et al., 2001; MacDonald et al., 1999). Eif3a is primarily found in the cytoplasm, however limited proteolysis allows Eif3a to enter the nucleus (Dong and Zhang, 2006; Saletta et al., 2010; Severin et al., 1997). Although Eif3a and Eif3m would have conventionally been thought to function in the cytoplasm, the functions of eukaryotic translation initiation factors in the nucleus are slowly coming to light (Strudwick and Borden, 2002). Both Eif3a and Eif3m interact with nuclear proteins *in vitro* (Proshkin et al., 2011). Another translation initiation factor, Eif4E functions in the nucleus to modulate the ability of nuclear factors to retain transcripts in the nucleus and facilitate the transport of transcripts to the cytoplasm (Lai and Borden, 2000;

Rousseau et al., 1996). Perhaps Pitx2c's potential interaction with the Eif3 complex is required for regulating gene expression pre-translation at the mRNA level in the nucleus. Further analysis of the nuclear localization of Eif3 components would be required.

Alternatively Pitx2c may have a role in regulating cytoplasmic translation of its target genes. To initiate translation, Eif4e binds to the 5' cap of the mRNA and recruits the Eif3 complex, which brings the ribosome to the transcript. Bicoid, another homeodomain transcription factor, has been shown to bind to the 3'UTR of its target transcripts (Chan and Struhl, 1997; Dubnau and Struhl, 1996; Rivera-Pomar et al., 1996). In addition to Bicoid's ability to bind RNA, it recruits Eif4E homologous proteins (4EHP) to the 5' cap of the target transcript and blocks Eif4e from binding and initiating translation (Cho et al., 2005; Macdonald, 2005). Given that Pitx2c is a Bicoid-like transcription factor, it may also provide transcript specificity and regulate translation initiation via interaction with the Eif3 complex.

Although *Eif3a* and *Eif3m* do not clearly link to left-right patterning given the studies thus far, they affect cellular behaviours that are required for organogenesis including differentiation and proliferation. Additionally, Eif3a and Eif3m could have functions in the nucleus by interacting with Pitx2c, despite their conventional role in cytoplasmic translation. Conversely, Pitx2c may have a novel role in regulating cytoplasmic translation.

4.4.3. Niemann-Pick Type 2 (Npc2)

Npc2 encodes for a small, soluble, sterol-binding glycoprotein that regulates lysosomal transport of cholesterol (Sleat et al., 2004; Storch and Xu,

2009). The putative Pitx2c interaction region contains an evolutionarily conserved region of unknown function and another containing a cholesterol binding site (Verot et al., 2007). Since the structure of Pitx2c is unlike cholesterol, the putative Pitx2c interaction region would occur in a region outside of the cholesterol-binding site.

In humans, *NPC2* mutations result in 5% of all cases of Niemann-Pick Type C (NPC) disease, which is characterized by neurodegeneration due to intracellular cholesterol accumulation. *Npc2* hypomorphic mice with mutations in the carboxyl terminal domain also mimic this milder form of NPC in humans. These mice are viable and have no abnormalities until 55 days of age (Sleat et al., 2004). No laterality defects due to *Npc2* mutations in humans or mice have been reported, suggesting that *Npc2* does not have a role in asymmetric organ morphogenesis. Alternatively, the low levels of Npc2 remaining may be sufficient for left-right patterning.

As described above, *Npc2* and *Pitx2c* mRNA are both expressed in the heart. However, *Npc2* does not appear to be expressed until after the heart has looped. Additionally, Npc2 is localized in the cytoplasm and Pitx2c is mostly localized in the nucleus. Altogether, the interaction between Npc2 and Pitx2c *in vivo* seems unlikely.

4.4.4 Serine/arginine-rich splicing factor 2 and 15 (Srsf2 and Srsf15)

Srsf2 and *Srsf15* are members of the serine/arginine-rich family of splicing factors. Although Srsf2 is a well-studied member, little is known about

Srsf15. It is inferred from sequence orthology that Srsf15 contains similar elements to that of its family members (Marchler-Bauer et al., 2003). Even though the RS domain is not one of the elements mapped by orthology, these domains are generally found at the C-terminus of all serine/arginine-rich splicing factors (Cazalla et al., 2002). Based on clone alignment to the C-terminus of both Srsf2 and Srsf15, Pitx2c potentially interacts with the RS domain in both these splicing factors (Fig. 15a and 16a). Consistent with its potential as a site of Pitx2c interaction, the RS domain has multiple functions including nuclear localization and protein–protein interactions (Amrein et al., 1994; Cáceres et al., 1997).

In the chick, *Srsf2* is expressed symmetrically in the lateral plate mesoderm, overlapping *Pitx2c* expression in the left LPM and in the heart until HH stage 22. *Srsf2* is also expressed in other maturing tissues in which *Pitx2c* is expressed. These expression data suggest that *Srsf2* may have a role in left-right patterning early on but is most likely not involved at HH stage 22 or later.

Unlike *Srsf2*, *Srsf15* is only expressed in later stages during chick embryogenesis starting at HH stage 15 where is it weakly expressed ubiquitously. *Srsf15* expression does become restricted and enriched in specific tissues including the heart where it overlaps with *Pitx2c* expression up to HH stage 24. These expression data suggest that *Srsf15* may have a role in heart development from HH stage 15 to 24.

Consistent with its housekeeping role in constitutive and alternative splicing in cells, no human diseases have been directly linked to *SRSF* mutations (Xiao et al., 2007). Germline deletion of *Srsf2* in mice causes embryonic lethality at E7.5 suggesting that *Srsf2* is required for early embryonic development,

however a complete analysis of this phenotype has not been described (Ding et al., 2004; Wang et al., 2001). Since the loss of *Srsf2* precludes analysis of its function later in organogenesis, tissue-specific ablation of *Srsf2* has been used to define its function in various organs.

Mice with a conditional deletion of *Srsf2* in differentiated cardiomyocytes in the heart survived into adulthood but developed dilated cardiomyopathy (Ding et al., 2004). It would be interesting to examine a conditional *Srsf2* knockout in the secondary heart field where *Pitx2c* is expressed and where proliferation and migration is essential for proper formation and positioning of the two great arteries of the left and right ventricle (Ai et al., 2006; Kioussi et al., 2002; Ma et al., 2013; Zhou et al., 2007). A conditional deletion of *Srsf2* in the pituitary gland showed severe anterior pituitary agenesis (Xiao et al., 2007). This was caused by a reduction in cell proliferation (Xiao et al., 2007) similar to what is observed in *Pitx2* null mice (Gage et al., 1999; Kitamura et al., 1999; Lin et al., 1999; Lu et al., 1999). Although the role of *Srsf2* in asymmetric organ morphogenesis is not clear, it is required for cell behaviours that are important in organogenesis including cell proliferation during pituitary development. More importantly, *Srsf2* expression and function overlap with *Pitx2c* in pituitary development suggesting that the potential protein–protein interaction identified from the screen may be required for essential biological processes *in vivo*.

No functional studies have been performed for *Srsf15*. However, *Srsf* generally appears to have an essential role in cell or embryo survival. In addition to *Srsf2* (Ding et al., 2004; Wang et al., 2001), *Srsf1* is required for cell viability in a chicken B-cell line, DT40, (Wang et al., 1996) and *Srsf3* germline deletion

causes death by E3.5 (Jumaa et al., 1999). Since *Srsf15* is expressed during embryogenesis, it would be interesting to investigate the effects of *Srsf15* on organ formation using a germline deletion or conditional mutation of *Srsf15* in mice or gain- and/or loss-of-function in chick.

It is evident from the embryonic lethality caused by *Srsf* knockouts in mice that splicing is important for embryogenesis. Pitx2c's involvement in regulating splicing has yet to be demonstrated. As mentioned previously, Pitx2c may also have the ability to bind RNA since it contains a Bicoid-type homeodomain. Therefore, Pitx2c may confer transcript specificity and recruit Srsf by protein–protein interactions to cause differential splicing of transcripts on the left and right side of the embryo. Further investigation would be required to determine Pitx2c's role in regulating differential splicing as well as the potential role of Srsf in asymmetrical and symmetrical organ morphogenesis.

4.5. Summary of functions for Pitx2c-candidate interactions in left-right patterning

Through analysis of each candidate, some themes of how Pitx2c may orchestrate organogenesis are apparent. It is suggested that these potential interactions with Pitx2c may be involved in cell proliferation and for some, cell differentiation in multiple organs. These could be mediated by transcriptional regulation in the case of Asf1b, mRNA processing via Srsf2 and Srsf15, or by translational regulation by interactions with Eif3a and Eif3m. Given that no known role of mRNA processing and translation regulation by Pitx2c has been reported, it would be an interesting focus for further research.

Due to the minimal localization of Pitx2c in the cytoplasm, the site of protein–partner interaction most likely occurs in the nucleus. With the exception of Npc2, all candidates appear to be able to localize in the nucleus. By examining the overlap in expression of Pitx2c and candidates in the chick embryo, I was able to narrow down sites of biological relevance for each potential protein-protein interaction. Although Asf1b is not expressed in asymmetrically formed organs, its expression still overlapped with Pitx2c in other symmetrically formed organs. In terms of left-right patterning, Pitx2c-Srsf2 interaction may be important in the lateral plate mesoderm during early gastrulation stages while Pitx2c interactions with Srsf15, Eif3a and Eif3m may be important for the laterality of the heart after the initial looping of the heart tube. Further analysis would be required to confirm that Pitx2c-candidate interactions are required at these sites to orchestrate left-right patterning.

Chapter 5. Conclusions

Pitx2c has long been known to be important for left-right patterning (Gage et al., 1999; Kitamura et al., 1999; Lin et al., 1999; Lu et al., 1999); however how Pitx2c orchestrates asymmetric organogenesis still remains largely unclear. In this study, I identified six potential protein interaction partners of the Pitx2c N-terminus out of 32 unique genes isolated from a yeast two-hybrid screen using mouse Pitx2cN as bait and mouse E11 yeast two-hybrid cDNA library as prey. With these six candidates, I showed that these clones encoded proteins, their interactions with Pitx2cN were not false positives, and confirmed the putative interaction region of the candidates with Pitx2cN individually in yeast. These six candidates were Anti-silencing function 1 homolog B (*S. cerevisiae*) (*Asf1b*), Eukaryotic translation initiation factor 3, subunit A (*Eif3a*), Eukaryotic translation initiation factor 3, subunit M (*Eif3m*), Niemann-Pick C type 2 (*Npc2*), Serine/arginine-rich splicing factor 2 (*Srsf2*), and Serine/arginine-rich splicing factor 15 (*Srsf15*).

I have demonstrated that these candidates overlap in expression with *Pitx2c* during embryogenesis suggesting biological relevance *in vivo*. Additionally, I have also shown novel expression pattern data for *Npc2, Eif3a, Eif3m* and *Srsf15* during chick embryogenesis. While *Npc2* and *Srsf15* have more tissue-specific expression patterns in the chick, *Eif3a* and *Eif3m* are more broadly expressed throughout the embryo and only become enriched in particular tissues at later stages of development. Based on literature review, the interactions of these candidates with Pitx2c are likely to regulate transcription via Asf1b, mRNA

processing via Srsf2 and Srsf15 and translation via Eif3a and Eif3m. Considering expression data and known functions of Srsf2, it is the most interesting candidate with respect to the left-right patterning functions of Pitx2c in the lateral plate mesoderm.

This project has been able to identify potential new molecules that could be involved in symmetrical and/or asymmetrical organogenesis. Ultimately, this project provides insight into possible molecular mechanisms by which *Pitx2c* orchestrates left-right patterning and is a foundation for identifying novel molecules involved in asymmetric organ morphogenesis that could be responsible for some variants of laterality defects in humans.

Chapter 6. Future directions

Since candidates were prioritized for further analysis based on the number of times they were isolated, this may have excluded potential protein interaction partners of Pitx2c. Further analysis of the rest of the list could be performed to determine if candidates that were isolated once could be of interest. As indicated by analysis of each candidate and known literature, the yeast two-hybrid screen did identify some promising candidate interaction partners that may be required for Pitx2c's function in left-right patterning. Further research is necessary to validate and determine the mechanisms of these interactions and the downstream effects on left-right patterning.

The potential interactions identified by the yeast two-hybrid screen need to be validated using an alternative method in a vertebrate system and with full-length candidates. To validate these interactions, co-immunoprecipitation (CO-IP) should be performed. This can be performed using embryonic lysates if there are antibodies available or in a transfected mammalian cell line including HEK293T where proteins can be tagged and expressed. Interactions should be tested between the putative interaction regions of the candidates and the Pitx2c N-terminus as well as with full-length candidates and full length Pitx2c. It is important to test the full-length proteins since they may contain localization signals not present in the interaction region that may promote or hinder the interaction. Although a domain may be fully accessible when a portion of the protein is expressed, the tertiary structure of a full-length candidate protein may mask this domain and block interactions. If these results also show interaction

between candidates and Pitx2c, these data will validate the interaction obtained from the screen as well as ensure that interactions are maintained in full-length proteins and thus biologically relevant.

Cellular localization of full-length candidate proteins should also be determined and compared with Pitx2c. Immunofluorescence could be performed in embryos if good antibodies are available or in transfected mammalian cells including HEK293T where candidates could be tagged and detected with an anti-tag antibody. Full-length Pitx2c can be detected by a custom antibody made by our laboratory or a commercially available Pitx2 antibody. This would allow us to determine if these proteins colocalize with Pitx2c in the same cellular compartments.

Potential protein interaction partners should also be tested for interaction with the LAMAT Pitx2c N-terminus mutant, as we have previously shown that these are the residues required for Pitx2c's function in left-right patterning. This could be done in a yeast two-hybrid assay as performed in this project or by coimmunoprecipitation as described above. These data would help prioritize candidates that may be important for Pitx2c's function in left-right patterning for further functional analysis.

Next, functional studies could be performed in chick—a more amenable model than the mouse embryo—to determine if each candidate has an effect on laterality *in vivo*. For *Srsf2*, laterality can be assessed by the direction of heart looping since it is expressed during early stages of gastrulation. Due to the

expression of *Npc2*, *Srsf15, Eif3a* and *Eif3m* only after the heart tube has looped, laterality should be assessed by looking at asymmetric features of the developed heart including sizes of the left and right atriums and ventricles, septation, and position of the great arteries. Loss of function analysis can be performed by depleting expression of the candidate via morpholino or antisense oligos on both sides of the embryo. Conversely, overexpression of putative candidate interaction domains only can be performed using retroviral particles in the same stages as above; as was done previously in our lab to determine the importance of the Pitx2c N-terminus. Injection of retroviral particles and electroporation of morpholino or antisense oligos would be performed on both sides of the lateral plate mesoderm just prior to HH stage 9 for *Srsf2*, on both sides the looping heart tube just prior to HH stage 12 for *Npc2*, *Eif3a,* and *Eif3m* and just prior to HH stage 16 for *Srsf15*. If candidates have a role in left-right patterning, manipulated embryos would be expected to exhibit laterality defects. Once candidates prove to be important for laterality in chick, transgenic knockdown or knockout mice can be created for candidates with no known transgenic model and thoroughly examined to determine if the effects of candidates on laterality and organ morphogenesis are evolutionarily conserved.

Another area of investigation would be the mechanism by which each candidate interacts with Pitx2c. Fragments of putative interaction region of each candidate can be tested to determine where the exact location of interaction with Pitx2c N-terminus lies. This can be performed by a yeast two-hybrid assay or by coimmunoprecipitation.

Since Pitx2c is a transcription factor, it would be of interest to determine if interactions with candidates have an effect on Pitx2c's transcription factor function. Candidates can be transfected with full-length *Pitx2c* and a *bicoid*-luciferase reporter construct. Luciferase activity can be measured by a luminometer to determine if Pitx2c's transactivation function has been affected. Similarly, the effect of candidates on Pitx2c's function to synergistically activate genes with other transcription factors can be analyzed. Candidates can be transfected with full-length *Pitx2c, Nkx2.5* and *Plod1*-lucerifase reporter construct as previously performed in our lab and analyzed as described above.

Additional candidate specific experiments can also be performed based on the possible molecular pathways Pitx2c-candidate interactions could regulate. The downstream gene targets of transcriptional regulation by Pitx2c and Asf1b can be determined by transcriptome analysis using chromatin-immunoprecipitation and high throughput sequencing. Srsf2 and Srsf15 splicing targets can be determined by coding transcriptome analysis using mRNA sequencing or splicing microarrays and compared to known Pitx2c targets or by determining if Srsf splicing targets contain bicoid-type homeodomain binding sites, also known as bicoid response elements. Proteome analysis using mass spectrometry can be performed to identify differentially expressed proteins as a result of translational regulation by Pitx2c and the Eif3 complex. These data would provide evidence of what Pitx2c-candidate interactions regulate during transcription, splicing or translation and further advocate the biological relevance of Pitx2c-candidate interactions.

Overall, it would be important to validate the interactions identified by the screen, determine if the interactions are feasible in the context of the cells of the embryo and determine if the candidates have a role in organizing left right patterning. Additionally, it would be interesting to further examine how these candidates affect Pitx2c's function and how their interaction affects laterality of developing organs in the embryo.

References

Abu-Issa, R., Kirby, M.L., 2007. Heart Field: From Mesoderm to Heart Tube. Annual Review of Cell and Developmental Biology 23, 45-68.

Adachi, H., Saijoh, Y., Mochida, K., Ohishi, S., Hashiguchi, H., Hirao, A., Hamada, H., 1999. Determination of left/right asymmetric expression of nodal by a left side-specific enhancer with sequence similarity to a lefty-2 enhancer. Genes & Development 13, 1589-1600.

Adams, D.S., Robinson, K.R., Fukumoto, T., Yuan, S., Albertson, R.C., Yelick, P., Kuo, L., McSweeney, M., Levin, M., 2006. Early, H+-V-ATPase-dependent proton flux is necessary for consistent left-right patterning of non-mammalian vertebrates. Development 133, 1657-1671.

Adkins, M.W., Howar, S.R., Tyler, J.K., 2004. Chromatin Disassembly Mediated by the Histone Chaperone Asf1 Is Essential for Transcriptional Activation of the Yeast PHO5 and PHO8 Genes. Molecular Cell 14, 657-666.

Ai, D., Liu, W., Ma, L., Dong, F., Lu, M.-F., Wang, D., Verzi, M.P., Cai, C., Gage, P.J., Evans, S., Black, B.L., Brown, N.A., Martin, J.F., 2006. Pitx2 regulates cardiac left-right asymmetry by patterning second cardiac lineage-derived myocardium. Developmental Biology 296, 437-449.

Albertson, R.C., Yelick, P.C., 2005. Roles for fgf8 signaling in left-right patterning of the visceral organs and craniofacial skeleton. Developmental Biology 283, 310-321.

Amendt, B.A., Semina, E.V., Alward, W.L.M., 2000. Rieger syndrome: a clinical, molecular, and biochemical analysis. CMLS, Cell. Mol. Life Sci. 57, 1652-1666.

Amendt, B.A., Sutherland, L.B., Russo, A.F., 1999. Multifunctional Role of the Pitx2 Homeodomain Protein C-Terminal Tail. Molecular and Cellular Biology 19, 7001-7010.

Amendt, B.A., Sutherland, L.B., Semina, E.V., Russo, A.F., 1998. The Molecular Basis of Rieger Syndrome: Analysis of Pitx2 Homeodomain Protein Activities. Journal of Biological Chemistry 273, 20066-20072.

Amrein, H., Hedley, M.L., Maniatis, T., 1994. The role of specific protein-RNA and protein-protein interactions in positive and negative control of pre-mRNA splicing by Transformer 2. Cell 76, 735-746.

Applegate, K.E., Goske, M.J., Pierce, G., Murphy, D., 1999. Situs Revisited: Imaging of the Heterotaxy Syndrome1. Radiographics 19, 837-852.

Arakawa, H., Nakamura, T., Zhadanov, A.B., Fidanza, V., Yano, T., Bullrich, F., Shimizu, M., Blechman, J., Mazo, A., Canaani, E., Croce, C.M., 1998. Identification and characterization of the ARP1 gene, a target for the human acute leukemia ALL1 gene. Proceedings of the National Academy of Sciences 95, 4573-4578.

Aw, S., Adams, D.S., Qiu, D., Levin, M., 2008. H,K-ATPase protein localization and Kir4.1 function reveal concordance of three axes during early determination of left,Äìright asymmetry. Mechanisms of Development 125, 353-372.

Aylsworth, A.S., 2001. Clinical aspects of defects in the determination of laterality. American Journal of Medical Genetics 101, 345-355.

Bajolle, F., Zaffran, S., Kelly, R.G., Hadchouel, J., Bonnet, D., Brown, N.A., Buckingham, M.E., 2006. Rotation of the Myocardial Wall of the Outflow Tract Is Implicated in the Normal Positioning of the Great Arteries. Circulation Research 98, 421-428.

Bangs, F., Antonio, N., Thongnuek, P., Welten, M., Davey, M.G., Briscoe, J., Tickle, C., 2011. Generation of mice with functional inactivation of talpid3, a gene first identified in chicken. Development 138, 3261-3272.

Baum, V.C., Duncan, P.N., 2011. When Right Is Right and When It's Not: Laterality in Cardiac Structures. Anesthesia & Analgesia 113, 1334-1336.

Beddington, R.S.P., Robertson, E.J., 1999. Axis Development and Early Asymmetry in Mammals. Cell 96, 195-209.

Bekir, N.A., Güngör, K., 2000. Atrial septal defect with interatrial aneurysm and Axenfeld-Rieger syndrome. Acta Ophthalmologica Scandinavica 78, 101-103.

Beyer, T., Danilchik, M., Thumberger, T., Vick, P., Tisler, M., Schneider, I., Bogusch, S., Andre, P., Ulmer, B.r., Walentek, P., Niesler, B., Blum, M., Schweickert, A., 2012. Serotonin Signaling Is Required for Wnt-Dependent GRP Specification and Leftward Flow in Xenopus. Current Biology 22, 33-39.

Bisgrove, B.W., Essner, J.J., Yost, H.J., 1999. Regulation of midline development by antagonism of lefty and nodal signaling. Development 126, 3253-3262.

Boettger, T., Wittler, L., Kessel, M., 1999. FGF8 functions in the specification of the right body side of the chick. Current Biology 9, 277-280.

Brennan, J., Norris, D.P., Robertson, E.J., 2002. Nodal activity in the node governs left-right asymmetry. Genes & Development 16, 2339-2344.

Briata, P., Ilengo, C., Corte, G., Moroni, C., Rosenfeld, M.G., Chen, C.Y., Gherzi, R., 2003. The Wnt/ β -catenin→Pitx2 pathway controls the turnover of Pitx2 and other unstable mRNAs. Molecular Cell 12, 1201-1211.

Burn, S.F., Hill, R.E., 2009. Left-right asymmetry in gut development: what happens next? BioEssays 31, 1026-1037.

Cáceres, J.F., Misteli, T., Screaton, G.R., Spector, D.L., Krainer, A.R., 1997. Role of the Modular Domains of SR Proteins in Subnuclear Localization and Alternative Splicing Specificity. The Journal of Cell Biology 138, 225-238.

Campione, M., Steinbeisser, H., Schweickert, A., Deissler, K., van Bebber, F., Lowe, L.A., Nowotschin, S., Viebahn, C., Haffter, P., Kuehn, M.R., Blum, M., 1999. The homeobox gene Pitx2: mediator of asymmetric left-right signaling in vertebrate heart and gut looping. Development 126, 1225-1234.

Casey, B., Hackett, B.P., 2000. Left-right axis malformations in man and mouse. Current Opinion in Genetics & Development 10, 257-261.

Cazalla, D., Zhu, J., Manche, L., Huber, E., Krainer, A.R., Cáceres, J.F., 2002. Nuclear Export and Retention Signals in the RS Domain of SR Proteins. Molecular and Cellular Biology 22, 6871-6882.

Chan, S.-K., Struhl, G., 1997. Sequence-specific RNA binding by Bicoid. Nature 388, 634-634.

Chang, T.C., Summers, C.G., Schimmenti, L.A., Grajewski, A.L., 2012. Axenfeld-Rieger syndrome: new perspectives. British Journal of Ophthalmology 96, 318-322.

Cho, P.F., Poulin, F., Cho-Park, Y.A., Cho-Park, I.B., Chicoine, J.D., Lasko, P., Sonenberg, N., 2005. A New Paradigm for Translational Control: Inhibition via 52-32 mRNA Tethering by Bicoid and the eIF4E Cognate 4EHP. Cell 121, 411-423.

Collignon, J., Varlet, I., Robertson, E.J., 1996. Relationship between asymmetric nodal expression and the direction of embryonic turning. Nature 381, 155-158.

Cox, C.J., Espinoza, H.M., McWilliams, B., Chappell, K., Morton, L., Hjalt, T.A., Semina, E.V., Amendt, B.A., 2002. Differential Regulation of Gene Expression by PITX2 Isoforms. Journal of Biological Chemistry 277, 25001-25010.

Cui, C., Little, C.D., Rongish, B.J., 2009. Rotation of Organizer Tissue Contributes to Left–Right Asymmetry. The Anatomical Record: Advances in Integrative Anatomy and Evolutionary Biology 292, 557-561.

Cunningham, E.T., Jr, Eliott, D., Miller, N.R., Maumenee, I.H., Green, W., 1998. Familial axenfeld-rieger anomaly, atrial septal defect, and sensorineural hearing loss: A possible new genetic syndrome. Archives of Ophthalmology 116, 78-82.

D'haene, B., Meire, F.ß., Claerhout, I., Kroes, H.Y., Plomp, A., Arens, Y.H., de Ravel, T., Casteels, I., De Jaegere, S., Hooghe, S., Wuyts, W., van den Ende, J., Roulez, F.ß., Veenstra-Knol, H.E., Oldenburg, R.A., Giltay, J., Verheij, J.B.G.M., de Faber, J.-T., Menten, B.r., De Paepe, A., Kestelyn, P., Leroy, B.P., De Baere, E., 2011. Expanding the Spectrum of FOXC1 and PITX2 Mutations and Copy Number Changes in Patients with Anterior Segment Malformations. Investigative Ophthalmology & Visual Science 52, 324-333.

Damoc, E., Fraser, C.S., Zhou, M., Videler, H., Mayeur, G.L., Hershey, J.W.B., Doudna, J.A., Robinson, C.V., Leary, J.A., 2007. Structural Characterization of the Human Eukaryotic Initiation Factor 3 Protein Complex by Mass Spectrometry. Molecular & Cellular Proteomics 6, 1135-1146.

Dathe, V., Gamel, A., Männer, J., Brand-Saberi, B., Christ, B., 2002. Morphological left-right asymmetry of Hensen's node precedes the asymmetric expression of Shh and Fgf8 in the chick embryo. Anat Embryol 205, 343-354.

Ding, J.-H., Xu, X., Yang, D., Chu, P.-H., Dalton, N.D., Ye, Z., Yeakley, J.M., Cheng, H., Xiao, R.-P., Ross, J., Chen, J., Fu, X.-D., 2004. Dilated cardiomyopathy caused by tissue-specific ablation of SC35 in the heart. EMBO J 23, 885-896.

Dong, Z., Zhang, J.-T., 2006. Initiation factor eIF3 and regulation of mRNA translation, cell growth, and cancer. Critical Reviews in Oncology/Hematology 59, 169-180.

Dubnau, J., Struhl, G., 1996. RNA recognition and translational regulation by a homeodomain protein. Nature 379, 694-699.

Ede, D.A., Kelly, W.A., 1964. Developmental abnormalities in the trunk and limbs of the talpid3 mutant of the fowl. Journal of Embryology and Experimental Morphology 12, 339-356.

Eronen, M.P., Aittomäki, K.A.U., Kajantie, E.O., Sairanen, H.I., Pesonen, E.J., 2013. The Outcome of Patients With Right Atrial Isomerism is Poor. Pediatr Cardiol 34, 302-307.

Espinoza, H.M., Ganga, M., Vadlamudi, U., Martin, D.M., Brooks, B.P., Semina, E.V., Murray, J.C., Amendt, B.A., 2005. Protein Kinase C Phosphorylation Modulates N- and C-Terminal Regulatory Activities of the PITX2 Homeodomain Protein. Biochemistry 44, 3942-3954.

Essner, J.J., Branford, W.W., Zhang, J., Yost, H.J., 2000. Mesendoderm and left-right brain, heart and gut development are differentially regulated by pitx2 isoforms. Development 127, 1081-1093.

Essner, J.J., Vogan, K.J., Wagner, M.K., Tabin, C.J., Yost, H.J., Brueckner, M., 2002. Left-right development: Conserved function for embryonic nodal cilia. Nature 418, 37-38.

Esteban, C.R., Capdevila, J., Economides, A.N., Pascual, J., Ortiz, A., Belmonte, J.C.I., 1999. The novel Cer-like protein Caronte mediates the establishment of embryonic left-right asymmetry. Nature 401, 243-251.

Fischer, A., Viebahn, C., Blum, M., 2002. FGF8 Acts as a Right Determinant during Establishment of the Left-Right Axis in the Rabbit. Current Biology 12, 1807-1816.

Flomen, R.H., Gorman, P.A., Vatcheva, R., Groet, J., Barisić, I., Ligutić, I., Sheer, D., Nizetić, D., 1997. Rieger syndrome locus: a new reciprocal translocation t(4;12)(q25;q15) and a deletion del(4)(q25q27) both break between markers D4S2945 and D4S193. Journal of Medical Genetics 34, 191-195.

Fu, X.D., Mayeda, A., Maniatis, T., Krainer, A.R., 1992. General splicing factors SF2 and SC35 have equivalent activities in vitro, and both affect alternative 5' and 3' splice site selection. Proceedings of the National Academy of Sciences 89, 11224-11228.

Fukumoto, T., Kema, I.P., Levin, M., 2005. Serotonin Signaling Is a Very Early Step in Patterning of the Left-Right Axis in Chick and Frog Embryos. Current Biology 15, 794-803.

Gage, P.J., Camper, S.A., 1997. Pituitary homeobox 2, a novel member of the bicoid-related family of homeobox genes, is a potential regulator of anterior structure formation. Human Molecular Genetics 6, 457-464.

Gage, P.J., Suh, H., Camper, S.A., 1999. Dosage requirement of Pitx2 for development of multiple organs. Development 126, 4643-4651.

Gaio, U., Schweickert, A., Fischer, A., Garratt, A.N., Müller, T., Ozcelik, C., Lankes, W., Strehle, M., Britsch, S., Blum, M., Birchmeier, C., 1999. A role of

the cryptic gene in the correct establishment of the left,Äîright axis. Current Biology 9, 1339-1342.

Ganga, M., Espinoza, H.M., Cox, C.J., Morton, L., Hjalt, T.A., Lee, Y., Amendt, B.A., 2003. PITX2 Isoform-specific Regulation of Atrial Natriuretic Factor Expression. Journal of Biological Chemistry 278, 22437-22445.

Gritsman, K., Zhang, J., Cheng, S., Heckscher, E., Talbot, W.S., Schier, A.F., 1999. The EGF-CFC Protein One-Eyed Pinhead Is Essential for Nodal Signaling. Cell 97, 121-132.

Gros, J., Feistel, K., Viebahn, C., Blum, M., Tabin, C.J., 2009. Cell Movements at Hensen's Node Establish Left/Right Asymmetric Gene Expression in the Chick. Science 324, 941-944.

Hanes, S.D., Brent, R., 1989. DNA specificity of the bicoid activator protein is determined by homeodomain recognition helix residue 9. Cell 57, 1275-1283.

Henikoff, S., 2008. Nucleosome destabilization in the epigenetic regulation of gene expression. Nat Rev Genet 9, 15-26.

Hildreth, V., Webb, S., Chaudhry, B., Peat, J.D., Phillips, H.M., Brown, N., Anderson, R.H., Henderson, D.J., 2009. Left cardiac isomerism in the Sonic hedgehog null mouse. Journal of Anatomy 214, 894-904.

Hjalt, T.A., Semina, E.V., 2005. Current molecular understanding of Axenfeld-Rieger syndrome. Expert Reviews in Molecular Medicine 7, 1-17.

Hjalt, T.A., Semina, E.V., Amendt, B.A., Murray, J.C., 2000. The Pitx2 protein in mouse development. Developmental Dynamics 218, 195-200.

Holmberg, J., Liu, C.-Y., Hjalt, T.A., 2004. PITX2 Gain-of-Function in Rieger Syndrome Eye Model. The American Journal of Pathology 165, 1633-1641.

Hong, S.-K., Dawid, I.B., 2009. FGF-dependent left-right asymmetry patterning in zebrafish is mediated by Ier2 and Fibp1. Proceedings of the National Academy of Sciences 106, 2230-2235.

Huang, Y., Huang, K., Boskovic, G., Dementieva, Y., Denvir, J., Primerano, D.A., Zhu, G.-Z., 2009. Proteomic and genomic analysis of PITX2 interacting and regulating networks. FEBS Letters 583, 638-642.

Hyatt, B.A., Yost, H.J., 1998. The Left-Right Coordinator: The Role of Vg1 in Organizing Left-Right Axis Formation. Cell 93, 37-46.

Ibañez-Tallon, I., Gorokhova, S., Heintz, N., 2002. Loss of function of axonemal dynein Mdnah5 causes primary ciliary dyskinesia and hydrocephalus. Human Molecular Genetics 11, 715-721.

Isaac, A., Sargent, M.G., Cooke, J., 1997. Control of Vertebrate Left-Right Asymmetry by a Snail-Related Zinc Finger Gene. Science 275, 1301-1304.

Jorgenson, R.L., Levin, L.S., Cross, H.E., Yoder, F., Kelly, T.E., 1978. The Rieger syndrome. American Journal of Medical Genetics 2, 307-318.

Jumaa, H., Wei, G., Nielsen, P.J., 1999. Blastocyst formation is blocked in mouse embryos lacking the splicing factor SRp20. Current Biology 9, 899-902.

Katsu, K., Tokumori, D., Tatsumi, N., Suzuki, A., Yokouchi, Y., 2012. BMP inhibition by DAN in Hensen's node is a critical step for the establishment of left-right asymmetry in the chick embryo. Developmental Biology 363, 15-26.

Kioussi, C., Briata, P., Baek, S.H., Rose, D.W., Hamblet, N.S., Herman, T., Ohgi, K.A., Lin, C., Gleiberman, A., Wang, J., Brault, V., Ruiz-Lozano, P., Nguyen, H.D., Kemler, R., Glass, C.K., Wynshaw-Boris, A., Rosenfeld, M.G., 2002. Identification of a Wnt/Dvl/ β -Catenin → Pitx2 Pathway Mediating Cell-Type-Specific Proliferation during Development. Cell 111, 673-685.

Kitajima, K., Oki, S., Ohkawa, Y., Sumi, T., Meno, C., 2013. Wnt signaling regulates left-right axis formation in the node of mouse embryos. Developmental Biology 380, 222-232.

Kitamura, K., Miura, H., Miyagawa-Tomita, S., Yanazawa, M., Katoh-Fukui, Y., Suzuki, R., Ohuchi, H., Suehiro, A., Motegi, Y., Nakahara, Y., Kondo, S., Yokoyama, M., 1999. Mouse Pitx2 deficiency leads to anomalies of the ventral body wall, heart, extra- and periocular mesoderm and right pulmonary isomerism. Development 126, 5749-5758.

Kitamura, K., Miura, H., Yanazawa, M., Miyashita, T., Kato, K., 1997. Expression patterns of Brx1 (Rieg gene), Sonic hedgehog, Nkx2.2, Dlx1 and Arx during zona limitans intrathalamica and embryonic ventral lateral geniculate nuclear formation. Mechanisms of Development 67, 83-96.

Klezovitch, O., Vasioukhin, V., 2013. Your Gut Is Right to Turn Left. Developmental Cell 26, 553-554.

Komatsu, Y., Mishina, Y., 2013. Establishment of left-right asymmetry in vertebrate development: the node in mouse embryos. Cellular and Molecular Life Sciences, 1-8.

Kosaki, K., Casey, B., 1998. Genetics of human left-right axis malformations. Seminars in Cell & Developmental Biology 9, 89-99.

Kouba, T., Dányi, I., Gunišová, S., Munzarová, V., Vlčková, V., Cuchalová, L., Neueder, A., Milkereit, P., Valášek, L.S., 2012. Small Ribosomal Protein RPS0 Stimulates Translation Initiation by Mediating 40S-Binding of eIF3 via Its Direct Contact with the eIF3a/TIF32 Subunit. PLOS One 7, e40464.

Krebs, L.T., Iwai, N., Nonaka, S., Welsh, I.C., Lan, Y., Jiang, R., Saijoh, Y., O'Brien, T.P., Hamada, H., Gridley, T., 2003. Notch signaling regulates left-right asymmetry determination by inducing Nodal expression. Genes & Development 17, 1207-1212.

Kurpios, N.A., Ibañes, M., Davis, N.M., Lui, W., Katz, T., Martin, J.F., Belmonte, J.C.I., Tabin, C.J., 2008. The direction of gut looping is established by changes in the extracellular matrix and in cell:cell adhesion. Proceedings of the National Academy of Sciences 105, 8499-8506.

Lai, H.K., Borden, K.L.B., 2000. The promyelocytic leukemia (PML) protein suppresses cyclin D1 protein production by altering the nuclear cytoplasmic distribution of cyclin D1 mRNA. Oncogene 19, 1623-1634.

Lee, S.E., Kim, H.Y., Jung, S.E., Lee, S.C., Park, K.W., Kim, W.K., 2006. Situs anomalies and gastrointestinal abnormalities. Journal of Pediatric Surgery 41, 1237-1242.

Lenhart, K.F., Lin, S.-Y., Titus, T.A., Postlethwait, J.H., Burdine, R.D., 2011. Two additional midline barriers function with midline lefty1 expression to maintain asymmetric Nodal signaling during left-right axis specification in zebrafish. Development 138, 4405-4410.

Levin, M., 2005. Left-right asymmetry in embryonic development: a comprehensive review. Mechanisms of Development 122, 3-25.

Levin, M., Johnson, R.L., Sterna, C.D., Kuehn, M., Tabin, C., 1995. A molecular pathway determining left-right asymmetry in chick embryogenesis. Cell 82, 803-814.

Levin, M., Mercola, M., 1999. Gap junction-mediated transfer of left-right patterning signals in the early chick blastoderm is upstream of Shh asymmetry in the node. Development 126, 4703-4714.

Levin, M., Pagan, S., Roberts, D.J., Cooke, J., Kuehn, M.R., Tabin, C.J., 1997. Left/Right Patterning Signals and the Independent Regulation of Different Aspects of Situs in the Chick Embryo. Developmental Biology 189, 57-67.

Levin, M., Palmer, A.R., 2007. Left–right patterning from the inside out: Widespread evidence for intracellular control. BioEssays 29, 271-287.

Levin, M., Thorlin, T., Robinson, K.R., Nogi, T., Mercola, M., 2002. Asymmetries in H+/K+-ATPase and Cell Membrane Potentials Comprise a Very Early Step in Left-Right Patterning. Cell 111, 77-89.

Lin, A.E., Ticho, B.S., Houde, K., Westgate, M.-N., Holmes, L.B., 2000. Heterotaxy: Associated conditions and hospital-based prevalence in newborns. Genet Med 2, 157-172.

Lin, C.-J., Lin, C.-Y., Chen, C.-H., Zhou, B., Chang, C.-P., 2012. Partitioning the heart: mechanisms of cardiac septation and valve development. Development 139, 3277-3299.

Lin, C.R., Kioussi, C., O'Connell, S., Briata, P., Szeto, D., Liu, F., Izpisua-Belmonte, J.C., Rosenfeld, M.G., 1999. Pitx2 regulates lung asymmetry, cardiac positioning and pituitary and tooth morphogenesis. Nature 401, 279-282.

Lin, L., Holbro, T., Alonso, G., Gerosa, D., Burger, M.M., 2001. Molecular interaction between human tumor marker protein p150, the largest subunit of eIF3, and intermediate filament protein K7. Journal of Cellular Biochemistry 80, 483-490.

Lines, M.A., Kozlowski, K., Walter, M.A., 2002. Molecular genetics of Axenfeld-Rieger malformations. Human Molecular Genetics 11, 1177-1184.

Liu, C., Liu, W., Lu, M.-F., Brown, N.A., Martin, J.F., 2001. Regulation of left-right asymmetry by thresholds of Pitx2c activity. Development 128, 2039-2048.

Liu, Z., Dong, Z., Yang, Z., Chen, Q., Pan, Y., Yang, Y., Cui, P., Zhang, X., Zhang, J.-T., 2007. Role of eIF3a (eIF3 p170) in intestinal cell differentiation and its association with early development. Differentiation 75, 652-661.

Logan, M., Pagan-Westphal, S.M., Smith, D.M., Paganessi, L., Tabin, C.J., 1998. The Transcription Factor Pitx2 Mediates Situs-Specific Morphogenesis in Response to Left-Right Asymmetric Signals. Cell 94, 307-317.

Lowe, L.A., Supp, D.M., Sampath, K., Yokoyama, T., Wright, C.V.E., Potter, S.S., Overbeek, P., Kuehn, M.R., 1996. Conserved left-right asymmetry of nodal expression and alterations in murine situs inversus. Nature 381, 158-161.

Loyola, A., Almouzni, G., 2004. Histone chaperones, a supporting role in the limelight. Biochimica et Biophysica Acta (BBA) - Gene Structure and Expression 1677, 3-11.

Lu, M.-F., Pressman, C., Dyer, R., Johnson, R.L., Martin, J.F., 1999. Function of Rieger syndrome gene in left-right asymmetry and craniofacial development. Nature 401, 276-278.

Ma, H.-Y., Xu, J., Eng, D., Gross, M.K., Kioussi, C., 2013. Pitx2-mediated cardiac outflow tract remodeling. Developmental Dynamics 242, 456-468.

MacDonald, J.S., Verdi, J., Meakin, S., 1999. Activity-dependent interaction of the intracellular domain of rat TrkA with intermediate filament proteins, the β-6 proteasomal subunit, Ras-GRF1, and the p162 subunit of eIF3. J Mol Neurosci 13, 141-158.

Macdonald, P.M., 2005. Translational Repression by Bicoid: Competition for the Cap. Cell 121, 321-322.

Maciolek, N.L., Alward, W.L.M., Murray, J.C., Semina, E.V., McNally, M.T., 2006. Analysis of RNA splicing defects in PITX2 mutants supports a gene dosage model of Axenfeld-Rieger syndrome. BMC Medical Genetics 7, Online.

Makita, Y., Masno, M., Imaizumi, K., Yamashita, S., Ohba, S., Ito, D., Kuroki, Y., 1995. Rieger syndrome with de novo reciprocal translocation t(1;4) (q23.1;q25). American Journal of Medical Genetics 57, 19-21.

Männer, J., 2001. Does an equivalent of the ”ventral node” exist in chick embryos? A scanning electron microscopic study. Anat Embryol 203, 481-490.

Marchler-Bauer, A., Anderson, J.B., DeWeese-Scott, C., Fedorova, N.D., Geer, L.Y., He, S., Hurwitz, D.I., Jackson, J.D., Jacobs, A.R., Lanczycki, C.J., Liebert, C.A., Liu, C., Madej, T., Marchler, G.H., Mazumder, R., Nikolskaya, A.N., Panchenko, A.R., Rao, B.S., Shoemaker, B.A., Simonyan, V., Song, J.S., Thiessen, P.A., Vasudevan, S., Wang, Y., Yamashita, R.A., Yin, J.J., Bryant, S.H., 2003. CDD: a curated Entrez database of conserved domain alignments. Nucleic Acids Research 31, 383-387.

Meggendorfer, M., Roller, A., Haferlach, T., Eder, C., Dicker, F., Grossmann, V., Kohlmann, A., Alpermann, T., Yoshida, K., Ogawa, S., Koeffler, H.P., Kern, W.,

Haferlach, C., Schnittger, S., 2012. SRSF2 mutations in 275 cases with chronic myelomonocytic leukemia (CMML). Blood 120, 3080-3088.

Meno, C., Gritsman, K., Ohishi, S., Ohfuji, Y., Heckscher, E., Mochida, K., Shimono, A., Kondoh, H., Talbot, W.S., Robertson, E.J., Schier, A.F., Hamada, H., 1999. Mouse Lefty2 and Zebrafish Antivin Are Feedback Inhibitors of Nodal Signaling during Vertebrate Gastrulation. Molecular Cell 4, 287-298.

Meno, C., Shimono, A., Saijoh, Y., Yashiro, K., Mochida, K., Ohishi, S., Noji, S., Kondoh, H., Hamada, H., 1998. Lefty-1 Is Required for Left-Right Determination as a Regulator of Lefty-2 and Nodal. Cell 94, 287-297.

Meno, C., Takeuchi, J., Sakuma, R., Koshiba-Takeuchi, K., Ohishi, S., Saijoh, Y., Miyazaki, J.-I., ten Dijke, P., Ogura, T., Hamada, H., 2001. Diffusion of Nodal Signaling Activity in the Absence of the Feedback Inhibitor Lefty2. Developmental Cell 1, 127-138.

Meyers, E.N., Martin, G.R., 1999. Differences in Left-Right Axis Pathways in Mouse and Chick: Functions of FGF8 and SHH. Science 285, 403-406.

Mine, N., Anderson, R.M., Klingensmith, J., 2008. BMP antagonism is required in both the node and lateral plate mesoderm for mammalian left-right axis establishment. Development 135, 2425-2434.

Miquerol, L., Kelly, R.G., 2013. Organogenesis of the vertebrate heart. Wiley Interdisciplinary Reviews: Developmental Biology 2, 17-29.

Monsoro-Burq, A.-H., Le Douarin, N.M., 2001. BMP4 Plays a Key Role in Left-Right Patterning in Chick Embryos by Maintaining Sonic Hedgehog Asymmetry. Molecular Cell 7, 789-799.

Mucchielli, M.-L., Mitsiadis, T.A., Raffo, S., Brunet, J.-F., Proust, J.-P., Goridis, C., 1997. Mouse Otlx2/RIEG Expression in the Odontogenic Epithelium Precedes Tooth Initiation and Requires Mesenchyme-Derived Signals for Its Maintenance. Developmental Biology 189, 275-284.

Munakata, T., Adachi, N., Yokoyama, N., Kuzuhara, T., Horikoshi, M., 2000. A human homologue of yeast anti-silencing factor has histone chaperone activity. Genes to Cells 5, 221-233.

Murcia, N.S., Richards, W.G., Yoder, B.K., Mucenski, M.L., Dunlap, J.R., Woychik, R.P., 2000. The Oak Ridge Polycystic Kidney (orpk) disease gene is required for left-right axis determination. Development 127, 2347-2355.

Murray, S.A., Gridley, T., 2006. Snail family genes are required for left-right asymmetry determination, but not neural crest formation, in mice. Proceedings of the National Academy of Sciences 103, 10300-10304.

Nakamura, T., Hamada, H., 2012. Left-right patterning: conserved and divergent mechanisms. Development 139, 3257-3262.

Nakamura, T., Mine, N., Nakaguchi, E., Mochizuki, A., Yamamoto, M., Yashiro, K., Meno, C., Hamada, H., 2006. Generation of Robust Left-Right Asymmetry in the Mouse Embryo Requires a Self-Enhancement and Lateral-Inhibition System. Developmental Cell 11, 495-504.

Nonaka, S., Shiratori, H., Saijoh, Y., Hamada, H., 2002. Determination of left-right patterning of the mouse embryo by artificial nodal flow. Nature 418, 96-99.

Nonaka, S., Tanaka, Y., Okada, Y., Takeda, S., Harada, A., Kanai, Y., Kido, M., Hirokawa, N., 1998. Randomization of Left Right Asymmetry due to Loss of Nodal Cilia Generating Leftward Flow of Extraembryonic Fluid in Mice Lacking KIF3B Motor Protein. Cell 95, 829-837.

Nonaka, S., Yoshiba, S., Watanabe, D., Ikeuchi, S., Goto, T., Marshall, W.F., Hamada, H., 2005. De Novo Formation of Left-Right Asymmetry by Posterior Tilt of Nodal Cilia. PloS Biology 3, e268.

Norris, D.P., Robertson, E.J., 1999. Asymmetric and node-specific nodal expression patterns are controlled by two distinct cis-acting regulatory elements. Genes & Development 13, 1575-1588.

Okada, Y., Nonaka, S., Tanaka, Y., Saijoh, Y., Hamada, H., Hirokawa, N., 1999. Abnormal Nodal Flow Precedes Situs Inversus in iv and inv mice. Molecular Cell 4, 459-468.

Patel, K., Isaac, A., Cooke, J., 1999. Nodal signalling and the roles of the transcription factors SnR and Pitx2 in vertebrate left-right asymmetry. Current Biology 9, 609-S601.

Peterson, A.G., Wang, X., Joseph Yost, H., 2013. Dvr1 transfers left-right asymmetric signals from Kupffer's vesicle to lateral plate mesoderm in zebrafish. Developmental Biology 382, 198-208.

Phoon, C.K., Neill, C.A., 1994. Asplenia syndrome: Insight into embryology through an analysis of cardiac and extracardiac anomalies. The American Journal of Cardiology 73, 581-587.

Pick, E., Hofmann, K., Glickman, M.H., 2009. PCI Complexes: Beyond the Proteasome, CSN, and eIF3 Troika. Molecular Cell 35, 260-264.

Piedra, M.E., Icardo, J.M., Albajar, M., Rodriguez-Rey, J.C., Ros, M.A., 1998. Pitx2 Participates in the Late Phase of the Pathway Controlling Left-Right Asymmetry. Cell 94, 319-324.

Pincheira, R., Chen, Q., Zhang, J.T., 2001. Identification of a 170-kDa protein over-expressed in lung cancers. Br J Cancer 84, 1520-1527.

Plageman Jr, T.F., Zacharias, A.L., Gage, P.J., Lang, R.A., 2011. Shroom3 and a Pitx2-N-cadherin pathway function cooperatively to generate asymmetric cell shape changes during gut morphogenesis. Developmental Biology 357, 227-234.

Prendiville, T., Barton, L., Thompson, W., Fink, D., Holmes, K., 2010. Heterotaxy Syndrome: Defining Contemporary Disease Trends. Pediatr Cardiol 31, 1052-1058.

Proshkin, S.A., Shematorova, E.K., Souslova, E.A., Proshkina, G.M., Shpakovski, G.V., 2011. A minor isoform of the human RNA polymerase II subunit hRPB11 (POLR2J) interacts with several components of the translation initiation factor eIF3. Biochemistry Moscow 76, 976-980.

Ramsdell, A.F., Yost, H.J., 1999. Cardiac looping and the vertebrate left-right axis: antagonism of left-sided Vg1 activity by a right-sided ALK2-dependent BMP pathway. Development 126, 5195-5205.

Raya, A., Belmonte, J.C.I., 2006. Left-right asymmetry in the vertebrate embryo: from early information to higher-level integration. Nat Rev Genet 7, 283-293.

Raya, A., Kawakami, Y., Rodríguez-Esteban, C., Büscher, D., Koth, C.M., Itoh, T., Morita, M., Raya, R.M., Dubova, I., Bessa, J.n.G., de la Pompa, J.L., Belmonte, J.C.I., 2003. Notch activity induces Nodal expression and mediates the establishment of left-right asymmetry in vertebrate embryos. Genes & Development 17, 1213-1218.

Raya, A., Kawakami, Y., Rodriguez-Esteban, C., Ibanes, M., Rasskin-Gutman, D., Rodriguez-Leon, J., Buscher, D., Feijo, J.A., Izpisua Belmonte, J.C., 2004. Notch

activity acts as a sensor for extracellular calcium during vertebrate left-right determination. Nature 427, 121-128.

Reis, L.M., Tyler, R.C., Volkmann Kloss, B.A., Schilter, K.F., Levin, A.V., Lowry, R.B., Zwijnenburg, P.J.G., Stroh, E., Broeckel, U., Murray, J.C., Semina, E.V., 2012. PITX2 and FOXC1 spectrum of mutations in ocular syndromes. Eur J Hum Genet 20, 1224-1233.

Rivera-Pomar, R., Niessing, D., Schmidt-Ott, U., Gehring, W.J., Jackle, H., 1996. RNA binding and translational suppression by bicoid. Nature 379, 746-749.

Rousseau, D., Kaspar, R., Rosenwald, I., Gehrke, L., Sonenberg, N., 1996. Translation initiation of ornithine decarboxylase and nucleocytoplasmic transport of cyclin D1 mRNA are increased in cells overexpressing eukaryotic initiation factor 4E. Proceedings of the National Academy of Sciences 93, 1065-1070.

Ruben, G.D., Templeton Jr, J.M., Ziegler, M.M., 1983. Situs inversus: The complex inducing neonatal intestinal obstruction. Journal of Pediatric Surgery 18, 751-756.

Ryan, A.K., Blumberg, B., Rodriguez-Esteban, C., Yonei-Tamura, S., Tamura, K., Tsukui, T., de la Pena, J., Sabbagh, W., Greenwald, J., Choe, S., Norris, D.P., Robertson, E.J., Evans, R.M., Rosenfeld, M.G., Belmonte, J.C.I., 1998. Pitx2 determines left-right asymmetry of internal organs in vertebrates. Nature 394, 545-551.

Saadi, I., Toro, R., Kuburas, A., Semina, E., Murray, J.C., Russo, A.F., 2006. An unusual class of PITX2 mutations in Axenfeld-Rieger syndrome. Birth Defects Research Part A: Clinical and Molecular Teratology 76, 175-181.

Saijoh, Y., Adachi, H., Sakuma, R., Yeo, C.-Y., Yashiro, K., Watanabe, M., Hashiguchi, H., Mochida, K., Ohishi, S., Kawabata, M., Miyazono, K., Whitman,

M., Hamada, H., 2000. Left-Right Asymmetric Expression of Lefty2 and Nodal Is Induced by a Signaling Pathway that Includes the Transcription Factor FAST2. Molecular Cell 5, 35-47.

Saijoh, Y., Oki, S., Ohishi, S., Hamada, H., 2003. Left-right patterning of the mouse lateral plate requires nodal produced in the node. Developmental Biology 256, 161-173.

Sakuma, R., Ohnishi, Y., Meno, C., Fujii, H., Juan, H., Takeuchi, J., Ogura, T., Li, E., Miyazono, K., Hamada, H., 2002. Inhibition of Nodal signalling by Lefty mediated through interaction with common receptors and efficient diffusion. Genes to Cells 7, 401-412.

Saletta, F., Rahmanto, Y.S., Richardson, D.R., 2010. The translational regulator eIF3a: The tricky eIF3 subunit! Biochimica et Biophysica Acta (BBA) - Reviews on Cancer 1806, 275-286.

Schweickert, A., Campione, M., Steinbeisser, H., Blum, M., 2000. Pitx2 isoforms: involvement of Pitx2c but not Pitx2a or Pitx2b in vertebrate left-right asymmetry. Mechanisms of Development 90, 41-51.

Semina, E.V., Reiter, R., Leysens, N.J., Alward, W.L.M., Small, K.W., Datson, N.A., Siegel-Bartelt, J., Bierke-Nelson, D., Bitoun, P., Zabel, B.U., Carey, J.C., Murray, J.C., 1996. Cloning and characterization of a novel bicoid-related homeobox transcription factor gene, RIEG, involved in Rieger syndrome. Nat Genet 14, 392-399.

Serraf, A., Bensari, N., Houyel, L., Capderou, A., Roussin, R.g., Lebret, E., Ly, M., Belli, E., 2010. Surgical management of congenital heart defects associated with heterotaxy syndrome. European Journal of Cardio-Thoracic Surgery 38, 721-727.

Severin, F.F., Shanina, N.A., Shevchenko, A., Solovyanova, O.B., Koretsky, V.V., Nadezhdina, E.S., 1997. A major 170 kDa protein associated with bovine adrenal medulla microtubules: a member of the centrosomin family? FEBS Letters 420, 125-128.

Shinohara, K., Kawasumi, A., Takamatsu, A., Yoshiba, S., Botilde, Y., Motoyama, N., Reith, W., Durand, B., Shiratori, H., Hamada, H., 2012. Two rotating cilia in the node cavity are sufficient to break left-right symmetry in the mouse embryo. Nat Commun 3, 622.

Shiraishi, I., Ichikawa, H., 2012. Human Heterotaxy Syndrome, From Molecular Genetics to Clinical Features, Management, and Prognosis. Circulation Journal 76, 2066-2075.

Shiratori, H., Hamada, H., 2006. The left-right axis in the mouse: from origin to morphology. Development 133, 2095-2104.

Shiratori, H., Sakuma, R., Watanabe, M., Hashiguchi, H., Mochida, K., Sakai, Y., Nishino, J., Saijoh, Y., Whitman, M., Hamada, H., 2001. Two-Step Regulation of Left-Right Asymmetric Expression of Pitx2: Initiation by Nodal Signaling and Maintenance by Nkx2. Molecular Cell 7, 137-149.

Simard, A., Di Giorgio, L., Amen, M., Westwood, A., Amendt, B.A., Ryan, A.K., 2009. The Pitx2c N-terminal domain is a critical interaction domain required for asymmetric morphogenesis. Developmental Dynamics 238, 2459-2470.

Sleat, D.E., Wiseman, J.A., El-Banna, M., Price, S.M., Verot, L., Shen, M.M., Tint, G.S., Vanier, M.T., Walkley, S.U., Lobel, P., 2004. Genetic evidence for nonredundant functional cooperativity between NPC1 and NPC2 in lipid transport. Proceedings of the National Academy of Sciences of the United States of America 101, 5886-5891.

Smidt, M.P., Cox, J.J., van Schaick, H.S.A., Coolen, M., Schepers, J., van der Kleij, A.M., Burbach, J.P.H., 2000. Analysis of Three Ptx2 Splice Variants on Transcriptional Activity and Differential Expression Pattern in the Brain. Journal of Neurochemistry 75, 1818-1825.

St. Amand, T.R., Ra, J., Zhang, Y., Hu, Y., Baber, S.I., Qiu, M., Chen, Y., 1998. Cloning and Expression Pattern of Chicken Pitx2: A New Component in the SHH Signaling Pathway Controlling Embryonic Heart Looping. Biochemical and Biophysical Research Communications 247, 100-105.

Storch, J., Xu, Z., 2009. Niemann-Pick C2 (NPC2) and intracellular cholesterol trafficking. Biochimica et Biophysica Acta (BBA) - Molecular and Cell Biology of Lipids 1791, 671-678.

Strife, J.L., Bisset, G.S., Burrows, P.E., 1998. Cardiovascular system, 3 ed. Lippincott-Raven, Philadelphia.

Strudwick, S., Borden, K.L.B., 2002. The emerging roles of translation factor eIF4E in the nucleus. Differentiation 70, 10-22.

Tabin, C.J., Vogan, K.J., 2003. A two-cilia model for vertebrate left-right axis specification. Genes & Development 17, 1-6.

Takeda, S., Yonekawa, Y., Tanaka, Y., Okada, Y., Nonaka, S., Hirokawa, N., 1999. Left-Right Asymmetry and Kinesin Superfamily Protein KIF3A: New Insights in Determination of Laterality and Mesoderm Induction by kif3A−/− Mice Analysis. Journal of Cell Biology 145, 825-836.

Tanaka, C., Sakuma, R., Nakamura, T., Hamada, H., Saijoh, Y., 2007. Long-range action of Nodal requires interaction with GDF1. Genes & Development 21, 3272-3282.

Ticho, B.S., Goldstein, A.M., Van Praagh, R., 2000. Extracardiac anomalies in the heterotaxy syndromes with focus on anomalies of midline-associated structures. The American Journal of Cardiology 85, 729-734.

Trembath, D.G., Semina, E.V., Jones, D.H., Patil, S.R., Qian, Q., Amendt, B.A., Russo, A.F., Murray, J.C., 2004. Analysis of two translocation breakpoints and identification of a negative regulatory element in patients with Rieger's syndrome. Birth Defects Research Part A: Clinical and Molecular Teratology 70, 82-91.

Tsikolia, N., Schröder, S., Schwartz, P., Viebahn, C., 2012. Paraxial left-sided nodal expression and the start of left–right patterning in the early chick embryo. Differentiation 84, 380-391.

Tsukui, T., Capdevila, J., Tamura, K., Ruiz-Lozano, P., Rodriguez-Esteban, C., Yonei-Tamura, S., Magallon, J., Chandraratna, R.A.S., Chien, K., Blumberg, B., Evans, R.M., Belmonte, J.C.I., 1999. Multiple left-right asymmetry defects in Shh(-/-) mutant mice unveil a convergence of the Shh and retinoic acid pathways in the control of Lefty-1. Proceedings of the National Academy of Sciences 96, 11376-11381.

Tumer, Z., Bach-Holm, D., 2009. Axenfeld-Rieger syndrome and spectrum of PITX2 and FOXC1 mutations. Eur J Hum Genet 17, 1527-1539.

Umehara, T., Horikoshi, M., 2003. Transcription Initiation Factor IID-interactive Histone Chaperone CIA-II Implicated in Mammalian Spermatogenesis. Journal of Biological Chemistry 278, 35660-35667.

Vandenberg, L.N., Levin, M., 2013. A unified model for left-right asymmetry? Comparison and synthesis of molecular models of embryonic laterality. Developmental Biology 379, 1-15.

Verot, L., Chikh, K., Freydière, E., Honoré, R., Vanier, M.T., Millat, G., 2007. Niemann–Pick C disease: functional characterization of three NPC2 mutations and clinical and molecular update on patients with NPC2. Clinical Genetics 71, 320-330.

Volkmann, B.A., Zinkevich, N.S., Mustonen, A., Schilter, K.F., Bosenko, D.V., Reis, L.M., Broeckel, U., Link, B.A., Semina, E.V., 2011. Potential Novel Mechanism for Axenfeld-Rieger Syndrome: Deletion of a Distant Region Containing Regulatory Elements of PITX2. Investigative Ophthalmology & Visual Science 52, 1450-1459.

Waldman, J.D., Rosenthal, A., Smith, A.L., Shurin, S., Nadas, A.S., 1977. Sepsis and congenital asplenia. The Journal of Pediatrics 90, 555-559.

Walentek, P., Beyer, T., Thumberger, T., Schweickert, A., Blum, M., 2012. ATP4a Is Required for Wnt-Dependent Foxj1 Expression and Leftward Flow in Xenopus Left-Right Development. Cell Reports 1, 516-527.

Wang, H.-Y., Xu, X., Ding, J.-H., Bermingham Jr, J.R., Fu, X.-D., 2001. SC35 Plays a Role in T Cell Development and Alternative Splicing of CD45. Molecular Cell 7, 331-342.

Wang, J., Takagaki, Y., Manley, J.L., 1996. Targeted disruption of an essential vertebrate gene: ASF/SF2 is required for cell viability. Genes & Development 10, 2588-2599.

Watanabe, D., Saijoh, Y., Nonaka, S., Sasaki, G., Ikawa, Y., Yokoyama, T., Hamada, H., 2003. The left-right determinant Inversin is a component of node monocilia and other 9+0 cilia. Development 130, 1725-1734.

Welsh, I.C., Thomsen, M., Gludish, D.W., Alfonso-Parra, C., Bai, Y., Martin, J.F., Kurpios, N.A., 2013. Integration of Left-Right Pitx2 Transcription and Wnt

Signaling Drives Asymmetric Gut Morphogenesis via Daam2. Developmental Cell 26, 629-644.

Wilson, D.S., Sheng, G., Jun, S., Desplan, C., 1996. Conservation and diversification in homeodomain-DNA interactions: a comparative genetic analysis. Proceedings of the National Academy of Sciences 93, 6886-6891.

Wu, M.-H., Wang, J.-K., Lue, H.-C., 2002. Sudden death in patients with right isomerism (asplenism) after palliation. The Journal of Pediatrics 140, 93-96.

Xiao, R., Sun, Y., Ding, J.-H., Lin, S., Rose, D.W., Rosenfeld, M.G., Fu, X.-D., Li, X., 2007. Splicing Regulator SC35 Is Essential for Genomic Stability and Cell Proliferation during Mammalian Organogenesis. Molecular and Cellular Biology 27, 5393-5402.

Yamamoto, M., Mine, N., Mochida, K., Sakai, Y., Saijoh, Y., Meno, C., Hamada, H., 2003. Nodal signaling induces the midline barrier by activating Nodal expression in the lateral plate. Development 130, 1795-1804.

Yan, Y.-T., Gritsman, K., Ding, J., Burdine, R.D., Corrales, J.D., Price, S.M., Talbot, W.S., Schier, A.F., Shen, M.M., 1999. Conserved requirement for EGF-CFC genes in vertebrate left-right axis formation. Genes & Development 13, 2527-2537.

Yokouchi, Y., Vogan, K.J., Pearse Ii, R.V., Tabin, C.J., 1999. Antagonistic Signaling by Caronte, a Novel Cerberus-Related Gene, Establishes Left-Right Asymmetric Gene Expression. Cell 98, 573-583.

Yoshioka, H., Meno, C., Koshiba, K., Sugihara, M., Itoh, H., Ishimaru, Y., Inoue, T., Ohuchi, H., Semina, E.V., Murray, J.C., Hamada, H., Noji, S., 1998. Pitx2, a Bicoid-Type Homeobox Gene, Is Involved in a Lefty-Signaling Pathway in Determination of Left-Right Asymmetry. Cell 94, 299-305.

Yu, X., St. Amand, T.R., Wang, S., Li, G., Zhang, Y., Hu, Y.P., Nguyen, L., Qiu, M.S., Chen, Y.P., 2001. Differential expression and functional analysis of Pitx2 isoforms in regulation of heart looping in the chick. Development 128, 1005-1013.

Zeng, L., Wan, Y., Li, D., Wu, J., Shao, M., Chen, J., Hui, L., Ji, H., Zhu, X., 2013. The m-subunit of murine translation initiation factor eIF3 maintains the integrity of the eIF3 complex and is required for embryonic development, homeostasis, and organ size control. Journal of Biological Chemistry.

Zhou, C., Arslan, F., Wee, S., Krishnan, S., Ivanov, A.R., Oliva, A., Leatherwood, J., Wolf, D.A., 2005. PCI proteins eIF3e and eIF3m define distinct translation initiation factor 3 complexes. BMC Biology 3, Online.

Zhou, W., Lin, L., Majumdar, A., Li, X., Zhang, X., Liu, W., Etheridge, L., Shi, Y., Martin, J., Van de Ven, W., Kaartinen, V., Wynshaw-Boris, A., McMahon, A.P., Rosenfeld, M.G., Evans, S.M., 2007. Modulation of morphogenesis by noncanonical Wnt signaling requires ATF/CREB family-mediated transcriptional activation of TGFβ2. Nat Genet 39, 1225-1234.

Zhu, L., Marvin, M.J., Gardiner, A., Lassar, A.B., Mercola, M., Stern, C.D., Levin, M., 1999. Cerberus regulates left-right asymmetry of the embryonic head and heart. Current Biology 9, 931-938.